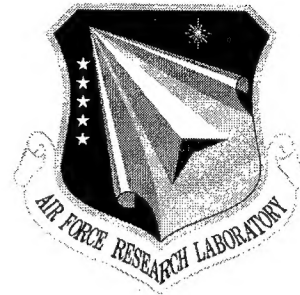AFRL-IF-RS-TR-2001-187
Final Technical Report
September 2001

FAST ELECTRO-OPTIC DEVICES FOR NEXT GENERATION OPTICAL CROSS-CONNECTS

Pennsylvania State University

Sponsored by
Defense Advanced Research Projects Agency
DARPA Order No. J163/01

20020117 031

**AIR FORCE RESEARCH LABORATORY
INFORMATION DIRECTORATE
ROME RESEARCH SITE
ROME, NEW YORK**

This report has been reviewed by the Air Force Research Laboratory, Information Directorate, Public Affairs Office (IFOIPA) and is releasable to the National Technical Information Service (NTIS). At NTIS it will be releasable to the general public, including foreign nations.

AFRL-TR-RS-TR-2001-187 has been reviewed and is approved for publication.

APPROVED: *Paul Sierak*

PAUL F. SIERAK
Project Engineer

FOR THE DIRECTOR: *Warren*

WARREN H. DEBANY, JR.
Technical Advisor
Information Grid Division
Information Directorate

FAST ELECTRO-OPTIC DEVICES FOR NEXT GENERATION OPTICAL CROSS-CONNECTS

Jay S. Patel

Contractor: Pennsylvania State University
Contract Number: F30602-98-1-0191
Effective Date of Contract: 20 April 1998
Contract Expiration Date: 20 April 2001
Program Code Number: 5L10
Short Title of Work: Fast Electro-Optic Devices for Next Generation Optical Cross-Connects

Period of Work Covered: Apr 98 – Apr 01

Principal Investigator: Jay S. Patel
            Phone: (814) 863-5345
AFRL Project Engineer: Paul F. Sierak
            Phone: (315) 330-7346

Distribution Unlimited: Approved for Public Release.

REPORT DOCUMENTATION PAGE	Form Approved OMB No. 0704-0188

Public reporting burden for this collection of information is estimated to average 1 hour per response, including the time for reviewing instructions, searching existing data sources, gathering and maintaining the data needed, and completing and reviewing the collection of information. Send comments regarding this burden estimate or any other aspect of this collection of information, including suggestions for reducing this burden, to Washington Headquarters Services, Directorate for Information Operations and Reports, 1215 Jefferson Davis Highway, Suite 1204, Arlington, VA 22202-4302, and to the Office of Management and Budget, Paperwork Reduction Project (0704-0188), Washington, DC 20503.

1. AGENCY USE ONLY *(Leave blank)*	2. REPORT DATE	3. REPORT TYPE AND DATES COVERED	
	September 2001	Final	Apr 98 - Apr 01

4. TITLE AND SUBTITLE

FAST ELECTRO-OPTIC DEVICES FOR NEXT GENERATION OPTICAL CROSS-CONNECTS

6. AUTHOR(S)

Jay S. Patel

5. FUNDING NUMBERS

C   - F30602-98-1-0191
PE - 62110E
PR - G146
TA - 00
WU - 01

7. PERFORMING ORGANIZATION NAME(S) AND ADDRESS(ES)

Pennsylvania State University
110 Technology Park
University Park PA 16802

8. PERFORMING ORGANIZATION REPORT NUMBER

N/A

9. SPONSORING/MONITORING AGENCY NAME(S) AND ADDRESS(ES)

Defense Advanced Research Projects Agency   AFRL/IFGA
3701 North Fairfax Drive   525 Brooks Road
Arlington VA 22203-1714   Rome NY 13441-4505

10. SPONSORING/MONITORING AGENCY REPORT NUMBER

AFRL-IF-RS-TR-2001-187

11. SUPPLEMENTARY NOTES

AFRL Project Engineer: Paul F. Sierak/IFGA/(315) 330-7346
DARPA Program Manager: Mari Maeda/ITO/(703) 696-2255

12a. DISTRIBUTION AVAILABILITY STATEMENT

Distribution unlimited: Approved for public release

12b. DISTRIBUTION CODE

13. ABSTRACT *(Maximum 200 words)*

The project was undertaken to construct fast liquid crystal based devices, which would increase the reconfiguration speeds by two or more orders of magnitude. We explored the use of a new class of materials based on smectic liquid crystals, which have been demonstrated to have switching speeds as fast as 15 ns. In our prior work, we had used liquid crystals as switching elements in WDM optical interconnects using the slower nematic liquid crystals with outstanding performance but much slower speeds. The goal of this project was to explore other technologies that could be used to increase the performance of these devices. We found that while ferroelectric liquid crystal provide superior switching speeds, these materials exhibited a stronger temperature dependence which prevented us from using this technology with the desired level of performance in the optical cross-connects. Alternate technologies based on bistable nematic liquid crystals were explored and while these performed better, the fabrication of these devices proved to be more difficult.

14. SUBJECT TERMS

Ferroelectric Liquid Crystals, Optical Switching, Optical Devices

15. NUMBER OF PAGES

108

16. PRICE CODE

17. SECURITY CLASSIFICATION OF REPORT	18. SECURITY CLASSIFICATION OF THIS PAGE	19. SECURITY CLASSIFICATION OF ABSTRACT	20. LIMITATION OF ABSTRACT
UNCLASSIFIED	UNCLASSIFIED	UNCLASSIFIED	UL

Standard Form 298 (Rev. 2-89) (EG)
Prescribed by ANSI Std. 239.18
Designed using Perform Pro, WHS/DIOR, Oct 94

TABLE OF CONTENTS

i

I. Summary

The project was undertaken to construct fast liquid crystal based devices, which would increase the reconfiguration speeds by two or more orders of magnitude. We explored the use of a new class of materials based on smectic liquid crystals, which have been demonstrated to have switching speeds as fast as 15 ns. In our prior work, we had used liquid crystals as switching elements in WDM optical interconnects using the slower nematic liquid crystals with outstanding performance but much slower speeds. The goal of this project was to explore other technologies that could be used to increase the performance of these devices. We found that while ferroelectric liquid crystal provide superior switching speeds, these, materials exhibited a stronger temperature dependence which prevented us from using this technology with the desired level of performance in the optical cross-connects. Alternate technologies based on bistable nematic liquid crystals were explored and while these performed better, the fabrication of these devices proved to be more difficult.

II. Overall Objectives

The primary goal of the program was to replace the slower switching nematic liquid-crystal-devices currently in use in wavelength-selective cross-connect (WS-XC) switches with the faster ferroelectric liquid crystal technology. Liquid crystal and grating-based WS-XC are capable of independently switching WDM channels with a channel spacing of less than 1.6nm, and with a cross-talk and channel rejection ratio of better than 35 dB. These configurations are currently being explored both by JDS Uniphase as well as Corning.

III. Goals and Objectives for the First Year:

In the first year, the proposed activity was to investigate the fast switching ferroelectric liquid crystals to be used as switching elements in optical cross connects. In the early phase of the program the activity was primarily limited to investigating ferroelectric materials, with focus on procuring liquid crystal materials from commercial sources and making test devices through process development. Additionally we will focus on developing modeling capabilities to investigate the performance of these devices.

IV. Goals and Objectives for the Second Year:

The goal was the successful construction of a 2x2 switch using the fast ferroelectric liquid crystal technology. This goal was used to optimize the materials and the processing steps necessary to construct an optimized liquid crystal based switching element, first for a 2x2 wavelength independent cross connect switch then followed up in the following year with a final 32 channel optimized array module to be incorporated into the 2x2 wavelength selective cross-connect switch.

This goal was accomplished by first constructing a free space nematic liquid crystal based device, and then substituting the nematic liquid crystal cells with the ferroelectric liquid crystal cells.

While the effort was successful it was found that the temperature dependence of the electro-optic materials, ferroelectric liquid crystals in this case, was not satisfactory. This was due to the temperature dependence of the tilt angle, which was the source of the problem. Effort was made to change the

2

technology by reverting back to the nematic liquid crystals but operated in the bistable mode.

V. Goals and Objectives for the Third Year:

While the approach of using nematic liquid crystals operated in the bistable mode was successful, with respect to the contrast ratio and performance levels proved to be a difficult technology to master because of the tight tolerances required during the cell fabrication process. The work however delayed the task of constructing the arrays based on the ferroelectric liquid crystal technology, which was abandoned.

VI. Summary of Results

The project was undertaken to construct fast liquid crystal based devices, which would increase the reconfiguration speeds by two or more orders of magnitude. We explored the use of a new class of materials based on smectic liquid crystals, which have been demonstrated to have switching speeds as fast as 15 ns. In our prior work, we had used liquid crystals as switching elements in WDM optical interconnects using the slower nematic liquid crystals with outstanding performance but much slower speeds. The goal of this project was to explore other technologies that could be used to increase the performance of these devices. We found that while ferroelectric liquid crystal provide superior switching speeds, these, materials exhibited a stronger temperature dependence which prevented us from using this technology with the desired level of performance in the optical cross-connects. Alternate technologies based on bistable nematic liquid crystals were explored and while these performed better, the fabrication of these devices proved to be more difficult.

The detailed results of the work are contained in the attached reports and the complete description contained in the associated published papers that are also attached.

VII. List of Technical Publications (copies attached)

1. Y. J. Kim, Z. Zhuang and J. S. Patel, "Reflective single-polarizer bistable nematic liquid crystal display with optimum twist," SID **99** Digest, 866 (1999).

2. Z. Zhuang, S. Suh and J. S. Patel, "Polarization controller using nematic liquid crystals," Optics Letter, **24**, 694 (1999).

3. Z. Zhuang, Y. J. Kim and J. S. Patel, "Parameters optimization for a reflective bistable twisted nematic display using the Poincare sphere method," Optics Letter, **24**, 1166 (1999)..

4. Z. Zhuang, Y. J. Kim and J. S. Patel, "Optimized configuration for reflective bistable twisted nematic displays," Applied Physics Letter, **75**, 1225 (1999).

5. Z. Zhuang, S. Suh and J. S. Patel "Arbitrary to arbitrary polarization controller using nematic liquid crystals," August 1999. Proc. SPIE99.

6. Z. Zhuang, Y. J. Kim and J. S. Patel, "Bistable twisted nematic liquid-crystal optical switch" Applied Physics Letters, vol. **75**, number 19, pp 3008 to 3010, November 1999.

7. Z. Zhuang, and J. S. Patel, "Behavior of cholesteric liquid crystals in a Fabry-Perot cavity" Optics Letters, vol. **24**, number 23, pp 1759 to 1761, December 1999.

8. Z. Zhuang, Y. J. Kim and J. S. Patel, " Liquid crystal devices for light limiting applications," December 1999. Proc. MRS99

9. Z. Zhuang, Y. J. Kim and J. S. Patel, " Behavior of cholesteric liquid crystals in a Fabry-Perot cavity in the Bragg Reflection Band," Physical Review Letter, vol. **84**, number 6, pp 1168 to 1171, February 2000.

10. Z. Zhuang, Y. J. Kim and J. S. Patel, " Electrically controllable azimuth optical rotator," Applied Physics Letter, vol. **76**, number 17, pp 2334 to 2336, April 2000

11. Z. Zhuang, S. Suh, Y. J. Kim and J. S. Patel, " Defect in the circular-circularity rubbed liquid crystal cell with off-center alignment," Applied Physics Letter, vol. **76**, number 21, pp 3005 to 3007, May 2000.

12. Z. Zhuang, Y. J. Kim and J. S. Patel, " Achromatic linear polarization rotator using twisted nematic liquid crystals," Applied Physics Letter, vol. **75**, number 26, pp 3995 to 3997, June 2000.

13. Z. Zhuang, Y. J. Kim and J. S. Patel, "Effect of multidirectional rubbing on the alignment of nematic liquid crystals," Applied Physics Letter, vol. **77**, number 4, pp 513 to 515, July 2000.

14. Z. Zhuang, Y. J. Kim and J. S. Patel, "Polarization states of Ferroelectric Liquid-crystal in a twisted structure," Jpn. J. Appl. Phys. Vol. 39, pp. 5927 to 5930, October 2000.

FAST ELECTRO-OPTIC DEVICES FOR NEXT GENERATION OPTICAL CROSS-CONNECTS
Penn State University

Principal Investigator

Prof. Jay. S. Patel

Report Date: 11-Aug-98

Overall Objectives

Our goal is to construct fast liquid-crystal-based devices that will increase the reconfiguration speeds of optical links by more than one order of magnitude. These switches are the building blocks of various optical networks and offer a wide-ranging utility, from simple by-pass protection switches to more complex wavelength-dependent cross- connect switches used in WDM architectures.

A primary goal of the following program is replacing the slower switching nematic liquid-crystal-devices currently in use in wavelength-selective cross-connect (WS-XC) switches. Liquid crystal and grating-based WS-XC are capable of independently switching WDM channels with a channel spacing of less than 1.6nm, and with a cross-talk and channel rejection ratio of better than 35 dB.

This is a technical report summarizing the accomplishments since the conception of the program in mid April.

Goals and Objectives for the First Year:

In the first year, the proposed activity was to investigate the fast switching ferroelectric liquid crystals to be used as switching elements in optical cross connects. In the early phase of the program the activity will be primarily limited to investigating these materials, with focus on procuring liquid crystal materials from commercial sources and making test devices through process development. Additionally we will focus on developing modeling capabilities to investigate the performance of these devices.

Accomplishments in this quarter:

We have established a web site for the program located at: http://thor.phys.psu.edu/ngi. This site outlines the aim of the project and major accomplishments will be posted at this site form time to time to gain visibility for the program.

Personal associated with the project

Since the beginning of the project in mid-April, we have hired two additional post-doctoral personnel. Dr. Barad has been recruited for his work in optics, and Dr. Kim for his expertise in the modeling and construction of liquid crystal devices. They join the pre-existing team of Dr. Suh, a third post-doc, a graduate student Mr. Zhuang, and Prof. Jay Patel, the PI.

Technical Progress:

The team has already developed preliminary modeling capabilities for the rapid evaluation of new structures of liquid crystals. This includes numerical simulations of liquid crystal structures and their optical properties. Additionally, we have begun the construction of a new process in an effort to make defect-free structures of ferroelectric liquid crystals. We have also begun the construction of an automated, computer-based polarization measurement system, which will be used to characterize the performance of the fabricated liquid crystal devices and to compare the results with simulations. This measurement system is currently being tested using conventional nematic liquid crystal devices. And in foresight of the challenges of FY-99, we have also begun the

6

construction of a 2x2 free space optical system using nematic liquid crystals, which will allow us to better assess our progress toward achieving our scheduled goals.

Publications:
No papers on work supported by this program were published in this quarter

Consultative and Advisory Functions:
None

Significant discoveries
Although much progress has been made, the program is in its very early stages for major significant discoveries.

**FAST ELECTRO-OPTIC DEVICES FOR NEXT GENERATION OPTICAL
CROSS-CONNECTS**
Penn State University

Technical Report Provided to:

Rome Air Force
Technical Contact: Larry Sues

Agreement Number:
F30602-98-1-0191

Principal Investigator
Prof. Jay. S. Patel

Report Date: December 14, 1998

This is a technical report summarizing the accomplishments since the first quarterly
report submitted in August 1998

The web site for the program located at:
http://thor.phys.psu.edu/ngi, it has been updated to include the material recently presented
at the DARPA PI meeting.

Comparison of the goals and achievements:
The goal for the first six months of the projects was to explore ferroelectric liquid crystal
technology to make control elements for optical cross connects. The strategy in achieving
this goal was to identify potential roadblocks, and examine possible solutions to
overcome these roadblocks.

The first problem was to obtain a well aligned sample of ferroelectric liquid crystal,
before any attempt is made to optimize the speed. Although this is a well know problem
in the liquid crystal field, the solution has been lacking. Our approach has been to use a
commercially available liquid crystal material to investigate the problem. It was
confirmed that using standard techniques for cell construction, leads to the formation of
the zigzag defects which result in optical losses through the device. Although this
problem is not serious for common display applications, the use of this technology for
optical cross-connects requires achieving demanding performance targets, and therefore
these defects needs to be eliminated or controlled.

The defects arise from the changes in the layer thickness of the smectic layers, which
causes layer buckling giving rise to the characteristic zigzag defects. An alignment
method in which these defects can be removed would represent a significant
breakthrough.

Our strategy has been to surround the active region with a more easily deformed region,
using lithographic techniques, with the idea that the strain will migrate to the area where
the deformations are easy. Our early results suggests that this strategy has indeed been
successful and that in the samples processed in this was there is no evidence of zigzag
defects.

We believe this represents a significant achievement, but one which has to be evaluated
further to better understand the limits of its applicability. For example the size and the
nature of the strain relief area it is not yet be evaluated in a systematic manner. This is
expected to be completed in the next quarter.

We have also evaluated the switching characteristic of the aligned sample, and although
much faster switching speeds have been achieved compared to the nematic liquid crystal
based technology, we believe that by using different materials we should be able to
further improve the switching speeds. We are currently in the process of procuring faster
switching materials.

9

The task of making a 2X2 liquid crystal based cross connect switch is also under way, initially using a nematic liquid crystal cells to optimize the optics. Once the ferroelectric liquid crystals have been constructed, these will be substituted in the switch.
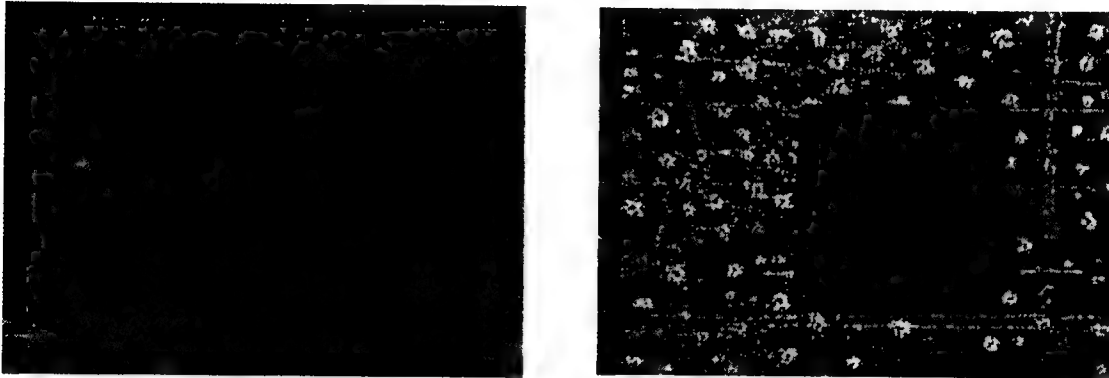
Figure 1. Photographs of the ferroelectric liquid crystal cells taken between cross polarizers. The characteristic defects are clearly visible in the left photograph, whereas on the right the defects are eliminated (center dark region) using a surrounding relief region formed by lithography.

Third Quarterly Report

Fast Electro-optic Devices For Next Generation Optical Cross-Connects

Technical Report

Performance Period :
1st Dec 1998 to 28th Feb 1999

Agreement Number:
F30602-98-1-0191

Professor Jay S. Patel,

Liquid Crystal Materials and Device Research Lab.

The Pennsylvania State University

Date: March 31, 1999

I. Comparison of the project's goals and achievements

The goal for this project in 1999 is to construct a 2x2 switch using the fast ferroelectric liquid crystal technology. This goal will allow us to optimize the materials and the processing steps necessary to construct an optimized liquid crystal based switching element, which will first be used in a 2x2 wavelength independent cross connect switch. Once completed, our work will serve as the basis for the construction of the final 32 channel optimized array module to be incorporated into the 2x2 wavelength selective cross-connect switch.

Based on the presentations and the vendor exhibits at the recent Optical Fiber Optic Communications Conference, it is clear that there is a demand for optical switches that operate with microsecond response time. Thus, our study of the ferroelectric liquid crystals and other faster switching liquid crystal technologies is both timely and important.

The work has begun on two fronts:

(1) Constructing the optical systems necessary to evaluate the cross-connect switch and other devices and

(2) Developing the necessary theoretical modeling capabilities, based on Stokes parameters calculations, for the optimization of the liquid crystal devices.

In last quarter, we began constructing the 2x2 switches using polarization beam splitters. Using nematic liquid technology, we have obtained very encouraging results. Also, we have obtained preliminary results using ferroelectric liquid crystals and have demonstrated switching speeds of less than 100 microseconds. However, we need to complete additional work to improve the cross-talk and rejection.

In developing the modeling capabilities, we have chosen to first model the nematic liquid crystals whose electro-optic behavior is better understood. This part of our project has been successful. We have been able to apply these tools to explore new bistable nematic liquid crystal structures, which could lead to high performance fiber-optic switches capable of latching. This work has resulted in several publications and provisional patents, which have been filed. At this point, we feel confident with our modeling capabilities to tackle the more challenging task of understanding and optimizing the electro-optical properties of the faster switching ferroelectric liquid crystals.

The following figure (Figure 1) shows an example of comparison between the experimentally obtain data, represented by points, and the theoretically calculated curve. Using Stokes vector, the figure shows the output polarization of the light passing through a ferroelectric liquid crystal in presence of an applied electric field. The field is varied linearly from 0 to 5 volts and applied across a five-micrometer thick ferroelectric liquid crystal sample.

The solid curve represents the output Polarization State of a fixed waveplate, which is rotated through 180 degrees. The match between theory and experiment suggests that the application of the electric field essentially rotates the optic axis without much change in the optical thickness.
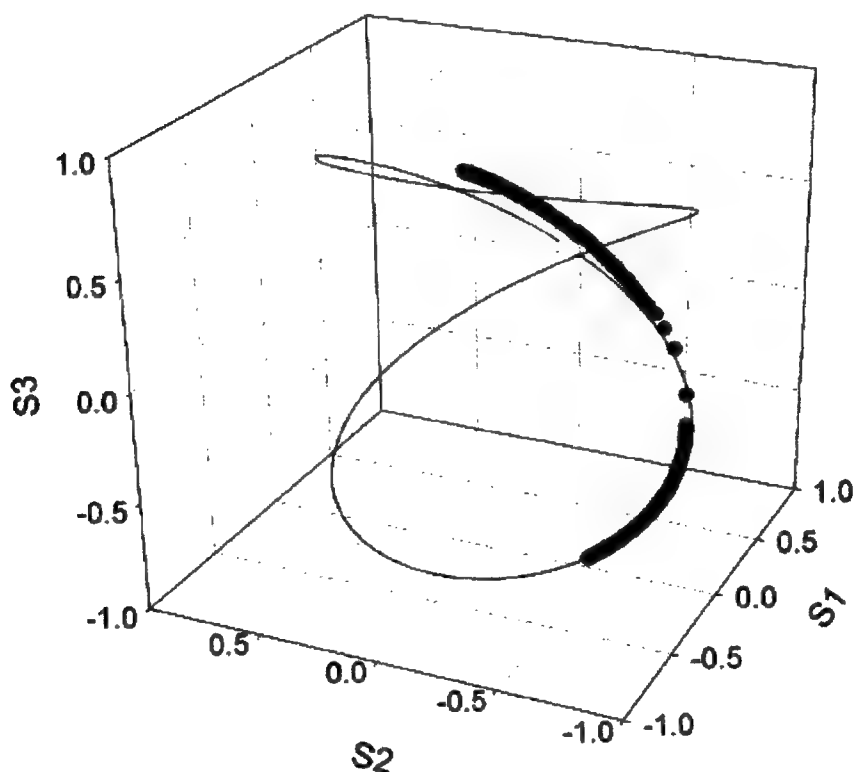

Figure 1. Output polarization of light passing through ferroelectric liquid crystal. Comparison between theory and experiments is shown.

13

II. Publications and Manuscripts in Preparation

1. Y. J. Kim, Z. Zhuang and J. S. Patel, "Reflective single-polarizer bistable nematic liquid crystal display with optimum twist," to be published in Proc. SID**99**.

2. Z. Zhuang, S. Suh and J. S. Patel, "Polarization controller using nematic liquid crystals," to be published in Optics Letters, May 15, 1999.

3. Z. Zhuang, Y. J. Kim and J. S. Patel, "Poincare sphere representation for twisted nematic liquid crystals: application to reflective BTN display," In Preparation for Appl. Phys. Letts.

4. Z. Zhuang, Y. J. Kim and J. S. Patel, "Optimization of single-polarizer reflective BTN display," In Preparation for Optics. Letts.

III. Professional Personal

Z. Zhuang   - Graduate Student

Y. J. Kim   - Post Doctoral Fellow

Yaniv Barad   - Post Doctoral Fellow

Jay Patel   - Principal Investigator

IV. Inventions and Patent Disclosures

During the course of the work, in the process of developing modeling capabilities we have discovered new optimized bistable nematic structures. While these structures will have uses for bistable switches, we believe that it may also have uses as displays. We have filed two provisional patents, which cover these discoveries.

1. "Reflective Mode of a bistable twisted nematic with a single polarizer in an optimized transition for twist," PSU Invention disclosure No. 98-2050.

2. "Polarization controller using nematic liquid crystals," PSU Invention disclosure No. 98-2072.

PENNSTATE

Fourth Quarterly Report

*Fast Electro-optic Devices For Next
Generation Optical Cross-Connects*

Technical Report

Performance Period :
01/03/1999 to 30/06/1999

Professor Jay S. Patel,

Liquid Crystal Materials and Device Research Lab.,

The Pennsylvania State University   Date: 30/06/1999

Technical Status Report

I. Comparison of the project's goals and achievements

The goal for his project in 1999 is to construct a 2x2 switch using the fast ferroelectric liquid crystal technology. This goal will allow us to optimize the materials and the processing steps necessary to construct an optimized liquid crystal based switching element, which will first be used in a 2x2 wavelength independent cross connect switch. Once completed, our work will serve as the basis for the construction of the final 32 channel optimized array module to be incorporated into the 2x2 wavelength selective cross-connect switch.

Based on the presentations and the vendor exhibits at the recent Optical Fiber Optic Communications Conference, it is clear that there is a demand for optical switches that operate with microsecond response time. Thus, our study of the ferroelectric liquid crystals and other fast switching liquid crystal technologies is both timely and important.

The work has begun on two fronts:

(1) Constructing the optical systems necessary to evaluate the cross-connect switch and other devices and

(2) Developing the necessary theoretical modeling capabilities, based on Stokes parameters calculations, for the optimization of the liquid crystal devices.

In the last quarter, we used Stokes vector and the Poincare sphere representation to model the evolution of the state of polarization (SOP) of light as a function of applied voltage for ferroelectric liquid crystals. In this report, we successfully optimized the ferroelectric liquid crystal cell and obtained well-aligned samples.

To achieve cell optimization, we have investigated several liquid crystal materials in cell with various thickness, and measured the output SOP using Stokes parameters in the Poincare sphere representation. Figure 1 shows the ferroelectric liquid crystal sample, which is optimized for the wavelength of 1550nm. The material used is CS-1026 (Chisso Corp.), and the cell thickness is 4.9 μm. The output polarization through this cell is measured using Stokes parameters. The results are shown in Figure 2. The output polarizations of the two stable states are substantially linear and orthogonal to each other. The transmission of the cell between the cross-polarizer is measured to be -42dB at one state and -1.3dB at the other state for 1550nm wavelength,

The switching property of this sample is shown in Figure 3. Square waveform voltage is applied to the sample and the rising and falling times are
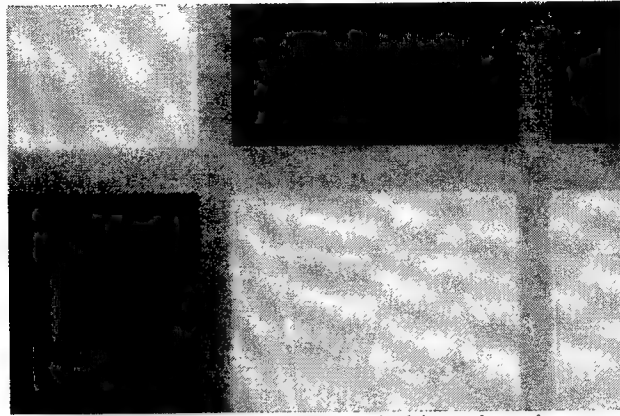
measured using an oscilloscope. The switching time is measure to be 200 μsec.
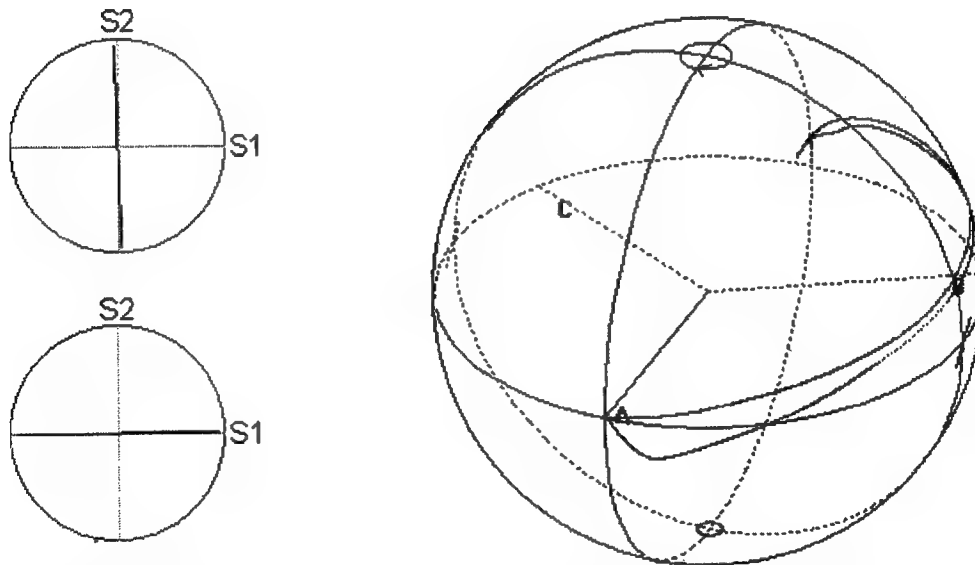
Figure 1.   Photo of the optimized ferroelectric liquid crystal sample.

Figure 2.   Output SOP for two stable states.
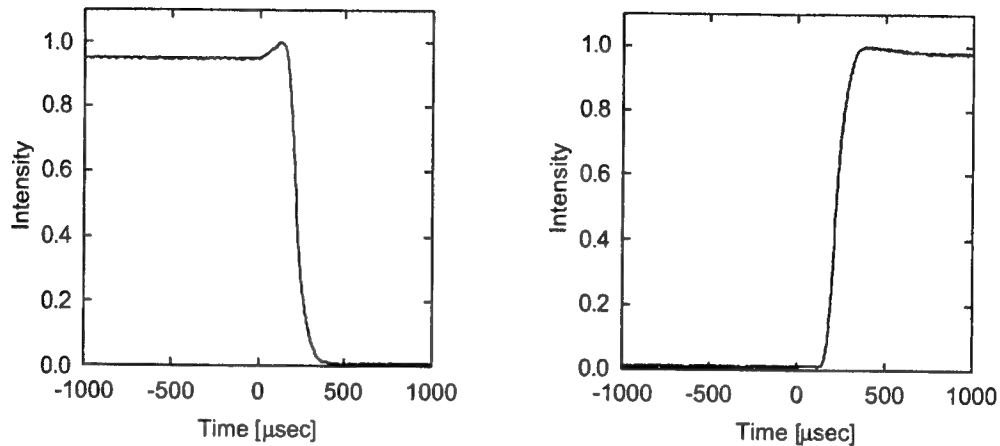
Figure 3. The switching property of the ferroelectric liquid crystal sample.

II. Publications

1. Y. J. Kim, Z. Zhuang and J. S. Patel, "Reflective single-polarizer bistable nematic liquid crystal display with optimum twist," SID **99** Digest, 866 (1999). Previously reported as to be published.

2. Z. Zhuang, S. Suh and J. S. Patel, "Polarization controller using nematic liquid crystals," Optics Letter, **24**, 694 (1999). Previously reported as to be published.

3. Z. Zhuang, Y. J. Kim and J. S. Patel, "Parameters optimization for a reflective bistable twisted nematic display using the Poincare sphere method," to be published in Optics Letter, Aug. 15, 1999. Previously reported as in preparation.

4. Z. Zhuang, Y. J. Kim and J. S. Patel, "Optimized configuration for reflective bistable twisted nematic displays," to be published in Applied Physics Letter. Previously reported as in preparation.

III. Professional Personal

Z. Zhuang   - Graduate Student

Y. J. Kim   - Post Doctoral Fellow

Jay Patel   - Principal Investigator

IV. Inventions and Patent Disclosures

During the course of the work, while developing modeling capabilities, we discovered new optimized bistable nematic structures. These structures will have uses in bistable switches, but we believe that they may also have uses as displays. We have filed four provisional patents.

1. "Reflective Mode of a bistable twisted nematic with a single polarizer in an optimized transition for twist," PSU Invention disclosure No. 98-2050.

2. "Parameters optimization for reflective BTN display using the Poincare sphere method," PSU Invention disclosure No. 98-2050/2.

3. "Optimized configuration for reflective bistable twisted nematic displays," PSU Invention disclosure No. 98-2050/3.

4. "Polarization controller using nematic liquid crystals," PSU Invention disclosure No. 98-2072.

Technical Status

Fast Electro-optic Devices For Next Generation Optical Cross-Connects

Technical Report

Professor Jay S. Patel,

Liquid Crystal Materials and Device Research Lab.,

The Pennsylvania State University

Date: 31/08/1999

I. Comparison of the project's goals and achievements

The goal for this project in 1999 is to construct a 2x2 switch using the fast ferroelectric liquid crystal technology. This goal will allow us to optimize the materials and the processing steps necessary to construct an optimized liquid crystal based switching element, which will first be used in a 2x2 wavelength independent cross connect switch. Once completed, our work will serve as the basis for the construction of the final 32 channel optimized array module to be incorporated into the 2x2 wavelength selective cross-connect switch.

Based on the presentations and the vendor exhibits at the recent Optical Fiber Optic Communications Conference, it is clear that there is a demand for optical switches that operate with microsecond response time. Thus, our study of the ferroelectric liquid crystals and other fast switching liquid crystal technologies is both timely and important.

The work has begun on two fronts:

(1) Constructing the optical systems necessary to evaluate the cross-connect switch and other devices and

(2) Developing the necessary theoretical modeling capabilities, based on Stokes parameters calculations, for the optimization of the liquid crystal devices.

In the last quarter, we successfully optimized the ferroelectric liquid crystal cell and obtained well-aligned samples by investigating several liquid crystal materials with various thickness. In this report, we explored the new structures of the bistable twisted nematic (BTN) liquid crystal, which could lead to high performance fiber-optic switches capable of latching.

BTN structure is attractive because it can be switched between two bistable states using special electrical pulses. This property makes BTN ideal structure for latching switches. We have successfully developed a geometrical method to model BTN structure, which is based on the Poincaré sphere (PS) representation and Stokes parameters. We have already solved the optimization problems for the reflective BTN display using this geometrical method. The same method can be applied in optimizing BTN for optical switch.

For a BTN structure to be used in optical switches, the two bistable states need to produce orthogonal linear SOP in the absence of the field, to obtain complete transmission and complete extinction. Preliminary results have been obtained in the optimization of the BTN optical switched. As shown in Fig. 1., we assume the entrance director (C1) of the BTN cell is at 0°. The front polarizer (A) is at angle $\square$/2 ($\square$ on the PS), while the rear polarizer is at angle

φ/2. We note that the angle between the polarizer and the analyzer (φ+ψ) may not be integer multiplier of 90°, as is commonly assumed for display applications. The two twisted states have uniform twists of φ and φ+2α, respectively, so the rear director (C2) is at an angle 2α with respect to C1 on the PS. There are two cases (A1 and A2 in Fig. 1) when the output SOP are linear. The angle between these two output linear polarized states is 2α on the PS (α in the real space). As illustrated in Fig. 1(b), for optimized structure, the orthogonality of these two output linear SOP requires that α=π/2. Therefore the incident light should be linearly polarized at ±45° with respect to the entrance director.
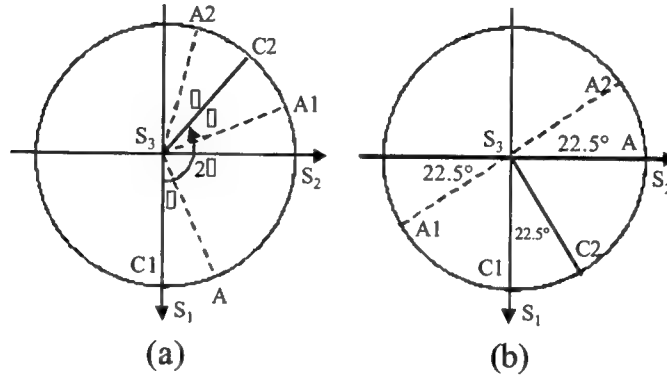
Fig. 1: S_1-S_2 projection plane of the Poincaré sphere for the linear SOP output. C1 and C2 are the directions of the entrance and rear directors, respectively. A is the orientation of the front polarizer. (a): general structure. (b): optimized structure.

Works are currently in progress in obtaining the specific configurations for the optimized geometry by the use of the Poincaré sphere method. Preliminary experiments are also in preparation.

II. Publications

1. Z. Zhuang, Y. J. Kim and J. S. Patel, "Parameters optimization for a reflective bistable twisted nematic display using the Poincare sphere method," Optics Letter, **24**, 1166 (1999). Previously reported as to be published.

2. Z. Zhuang, Y. J. Kim and J. S. Patel, "Optimized configuration for reflective bistable twisted nematic displays," Applied Physics Letter, **75**, 1225 (1999). Previously reported as to be published.

III. Professional Personal

Z. Zhuang   - Graduate Student

Y. J. Kim   - Post Doctoral Fellow

Jay Patel   - Principal Investigator

IV. Inventions and Patent Disclosures

During the course of the work, while developing modeling capabilities, we discovered new optimized bistable nematic structures. These structures will have uses in bistable switches, but we believe that they may also have uses as displays. We have filed five provisional patents.

1. "Reflective Mode of a bistable twisted nematic with a single polarizer in an optimized transition for twist," PSU Invention disclosure No. 98-2050.

2. "Parameters optimization for reflective BTN display using the Poincare sphere method," PSU Invention disclosure No. 98-2050/2.

3. "Optimized configuration for reflective bistable twisted nematic displays," PSU Invention disclosure No. 98-2050/3.

4. "Polarization controller using nematic liquid crystals," PSU Invention disclosure No. 98-2072.

Technical Status

Fast Electro-optic Devices For Next Generation Optical Cross-Connects

Technical Report

Performance Period :
01/08/1999 to 31/10/1999

Professor Jay S. Patel,

Liquid Crystal Materials and Device Research Lab.,

The Pennsylvania State University

Date: 31/10/1999

I. Comparison of the project's goals and achievements

One of the secondary goals of the project is to explore other liquid crystal technologies that could lead to breakthroughs. Towards this end we have begun the exploration of cholesteric liquid crystals which will become the focus of our activities over the next 6 to 9 months.

In beginning this project considerable amount of effort was devoted to the alignment of the cholesteric liquid crystals and making sure that there are very few defects in the sample. This is particularly important because the materials will be used in a Fabry-Perot resonator to allow a wavelength tunable device.

The goal is examine these structures in two pitch regimes:

(1) Pitch much larger that the optical wavelength

(2) Pitch comparable to the optical wavelength..

II. Achievements

In this quarter, we successfully examined the long wavelength regime. We investigate the behavior of cholesteric liquid crystal (CLC) inside a Fabry-Perot (FP) cavity. Although FP cavities filled with various liquid crystals have been extensively studied, the behavior of the CLC based FP has not been reported. For CLC, the twisted structure can be changed because the pitch is a function of temperature. In a parallel-rubbed CLC FP, the balance between the strong surface anchoring and the elastic energy yields a step-like resonance spectrum. This corresponds to the quantized effective pitch that the system assumes when both surface alignments are fixed. Experiment results for parallel-rubbed samples are presented and explained theoretically by the use of the Jones matrix calculations.

For the twisted nematic LC structure, the twisted director profile is a product of the surface anchoring effect. The pitch of the twisted structure is determined by the surface rubbing direction and the thickness of the cell. For CLC, the material has a natural pitch, which is determined, by the temperature of the material. In case where the CLC molecules at the surfaces are in the plane of the surface, the planar structure of the CLC is well defined, at least in principle. If we consider the surface to be parallel to the x-y plane, then the director can be represented by $(\sin kz, \cos kz, 0)$, where $k=2\pi/p$ and p is the helical pitch. The director is rotated linearly along the z-axis by an angle $k \cdot d$ from one surface to the other, where d is the thickness of the sample. In general k is temperature dependent. However, if the CLC is confined in a cell with fixed boundary conditions such that the directors at both surfaces are

forced to lie along a fixed direction, then the total amount of twist from one surface to the other is no longer $k \cdot d$ but rather $k' \cdot d$, where k' satisfies the relation $k' \cdot d = m\pi$. The integer m is chosen in such a way that k and k' differs as little as possible. Although k is a continuos function of temperature, k' is quantized. This suggests that a CLC FP subjected to temperature changes would produce cavity resonance spectrums that vary in a step-like fashion.

To demonstrate the above considerations, we used a material which is readily available from Aldrich and shows a rapid change in helical pitch with temperature: 4-[(S,S)-2,3-expoxyhexyloxy] phenyl4-(decyloxy)benzoate. The natural pitch of the materials is shown in Fig. 1 as dashed lines. In addition to the change of the helical structure, there exists a critical temperature ($T_c \approx 81°C$) at which the helical pitch becomes infinite and the twisting sense of the helix is opposite on either side of T_c. In our experiments, the cell surfaces are parallel rubbed. Because of the strong surface anchoring effect, the total twisted angle can only take interger numbers of π, i.e. $\phi = m\pi$, where m is an integer. This discrete twisted angle makes the effective pitch quantized ($P = d \cdot 2\pi/\phi = 2d/m$), although the natural pitch can change continuously. A simple model is to assume that the effective pitch takes the quantized value $2d/m$ when the natural twisted angle falls in the range $(m-1/2)\pi \sim (m+1/2)\pi$. The quantized effective pitch is observed. The results of the unpolarized (a) and polarized (b) spectra are shown in the folowing two graphs.

(a)

(b)
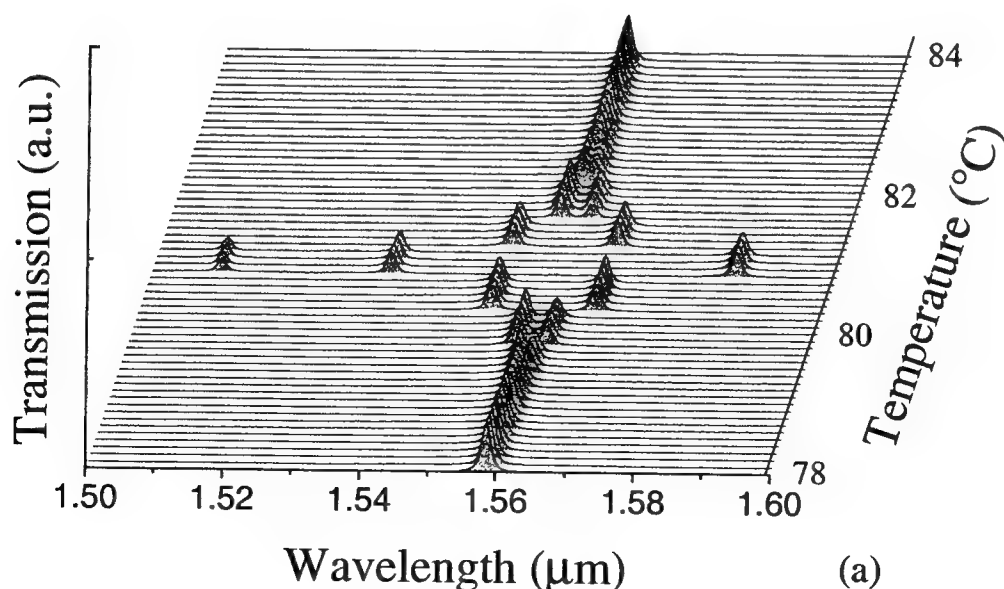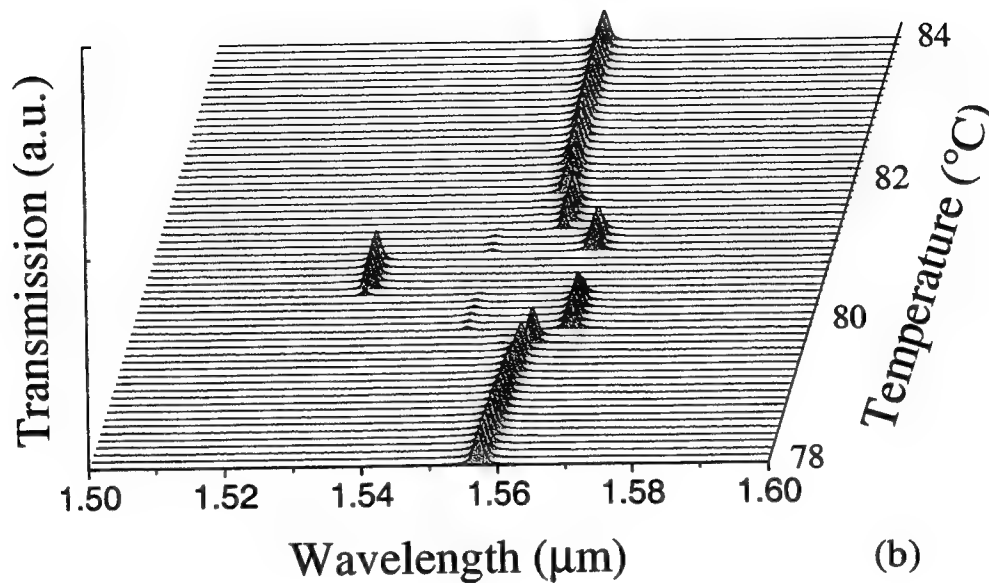
III. Publications

1. Z. Zhuang, Y. J. Kim and J. S. Patel, "Parameter optimization for a reflective bistable twisted nematic display by use of the Poincare sphere method" Optics Letters, vol. **24**, number 16, pp 1166 to 1168, August 1999.

2. Z. Zhuang, Y. J. Kim and J. S. Patel, "Optimized configuration for reflective bistable twisted nematic displays" Applied Physics Letters, vol. **75**, number 9, pp 1225 to 1227, August 1999.

3. Z. Zhuang, S. Suh and J. S. Patel "Arbitrary to arbitrary polarization controller using nematic liquid crystals," August 1999. Proc. SPIE99.

IV. Professional Personal

Z. Zhuang   - Graduate Student

Y. J. Kim   - Post Doctoral Fellow

Jay Patel   - Principal Investigator

27

V. Inventions and Patent Disclosures

None

PENNSTATE

Technical Status

Fast Electro-optic Devices For Next Generation Optical Cross-Connects

Technical Report

Performance Period :
01/11/1999 to 31/01/2000

Professor Jay S. Patel,

Liquid Crystal Materials and Device Research Lab.,

The Pennsylvania State University   Date: 31/01/2000

I. Comparison of the project's goals and achievements

One of the secondary goals of the project is to explore other liquid crystal technologies that could lead to breakthroughs. Towards this end we have begun the exploration of cholesteric liquid crystals which will become the focus of our activities over the next 6 to 9 months.

In beginning this project considerable amount of effort was devoted to the alignment of the cholesteric liquid crystals and making sure that there are very few defects in the sample. This is particularly important because the materials will be used in a Fabry-Perot resonator to allow a wavelength tunable device.

The goal is examine these structures in two pitch regimes:

(1) Pitch much larger that the optical wavelength

(2) Pitch comparable to the optical wavelength..

II. Achievements

In the last quarter we showed the results of the behavior of the chjoelsteric material outside of the reflection band. In this quarter, we successfully examined the short wavelength regime.

We investigate the behavior of the cholesteric liquid-crystal Fabry-Perot cavity in the spectral range of the Bragg reflection band. We show that in this region, the 2x2 Jones matrix calculation gives a false predication. However, by the use of the 4x4-matrix method, interesting features are revealed in the resonance spectra. The resonance spectra split when $\lambda \sim \bar{n}P$. Our experiments confirm this phenomenon. The experimental results show that the splitting occurs in a step-like fashion. This can be explained by the quantization of the pitch that occurs due to the fixed boundary conditions.

It is well known that a highly twisted cholesteric liquid-crystal (CLC) medium behaves just like an isotropic medium that has an average refractive index of the anisotropic material. Therefore, for a CLC medium inside a Fabry-Perot (FP) etalon, if the pitch is much larger compared to the wavelength, one expects to have two sets of resonance peaks, for the two refractive indices n_e and n_o, respectively. As the pitch of the medium gets shorter, the two sets of peaks converge into one set, which corresponds to the average refractive index. However, if the CLC medium is inside its Bragg reflection band, due to the selective Bragg reflection, one expects that new features will appear in the resonance spectrum.

In order to consider the selective Bragg reflection of the CLC medium, the 4x4-matrix calculation was performed. In doing so, we assumed that the entrance director was along the x-direction and the linearly polarized light was polarized along the y-direction. We also assumed that the CLC medium was in the so-called planar state, which means that the helical axis was perpendicular to the cell surface. From the Maxwell's equations, the following set of four linear differential equations for the tangential components of the electromagnetic field can be derived :

$$\partial\psi/\partial z = -ik_0\Delta\cdot\psi \ ,\tag{1}$$

$$\psi = \begin{pmatrix} E_x, & H_y, & E_y, & -H_x \end{pmatrix}^T ,\tag{2}$$

where $k_0 = \omega/c$, ω is the angular velocity and c is the velocity of light in vacuum. The matrix Δ depends on the dielectric constants, the wave vector, and the orientation of the optic axis. One can relate the electromagnetic field at $z=0$ to the field at $z=d$ by dividing the CLC medium into N layers, each layer has a thickness a:

$$\begin{aligned} \psi(0) &= M\cdot\psi(d) \\ &= M(0,a)\cdot M(a,2a)\cdots\cdots M((N-1)a, Na)\cdot\psi(d). \end{aligned}\tag{3}$$

In our calculation, N=500 is used. Other value of N yields the same results if N is chosen in such a way that there are more than 10 layers per pitch. M is the transfer matrix. For CLC FP, because the CLC medium is in the planar state, the matrix M can be written out explicitly.
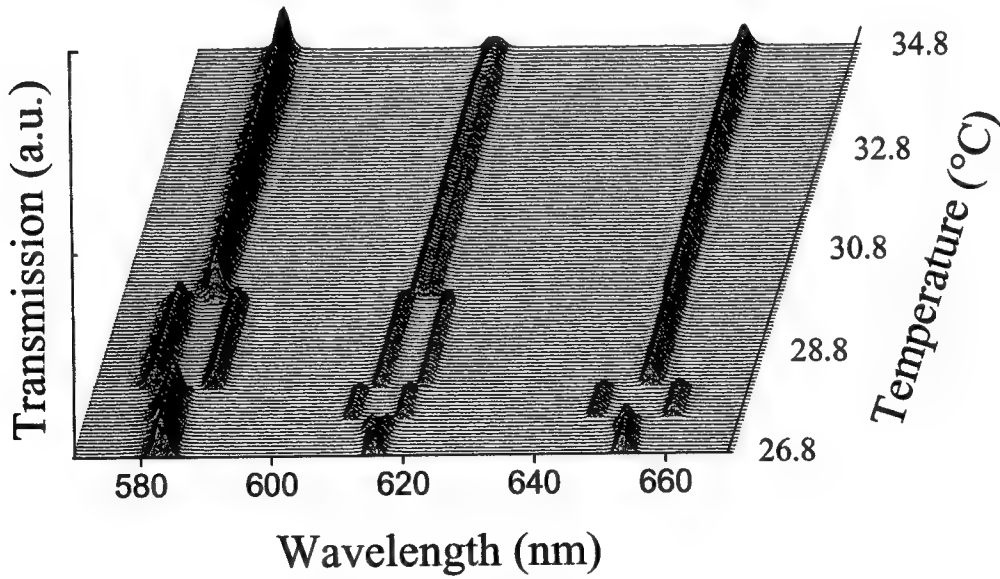
(a)

We have been able to obtain spectacular agreement between experiment (shown above) and the theory (shown below).
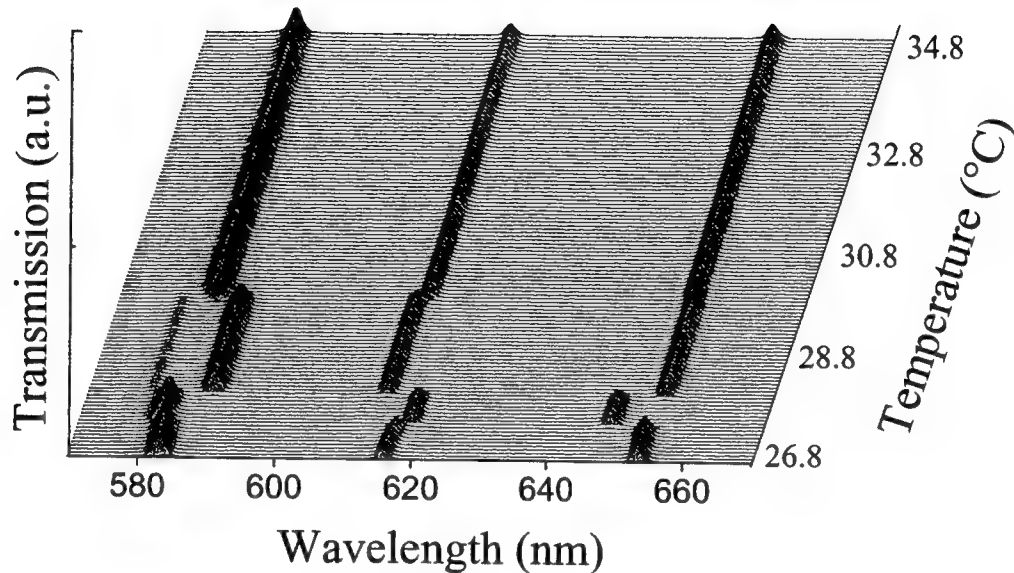
(b)

III. Publications

1. Z. Zhuang, Y. J. Kim and J. S. Patel, "Bistable twisted nematic liquid-crystal optical switch" Applied Physics Letters, vol. **75**, number 19, pp 3008 to 3010, November 1999.

2. Z. Zhuang, and J. S. Patel, "Behavior of cholesteric liquid crystals in a Fabry-Perot cavity" Optics Letters, vol. **24**, number 23, pp 1759 to 1761, December 1999.

3. Z. Zhuang, Y. J. Kim and J. S. Patel, " Liquid crystal devices for light limiting applications," December 1999. Proc. MRS99.

IV. Professional Personal

Z. Zhuang   - Graduate Student

Tejas Patel   - Graduate Student

Vikram Hegde - Graduate Student

Jay Patel   - Principal Investigator

V. Inventions and Patent Disclosures

None

Technical Status

Fast Electro-optic Devices For Next Generation Optical Cross-Connects

Technical Report

Performance Period :
01/02/2000 to 30/04/2000

Sponsored by
DARPA/ITO, ARPA Order G146-01
AFRL Agreement Number: F30602-98-1-0191

Professor Jay S. Patel,

Liquid Crystal Materials and Device Research Lab.,

The Pennsylvania State University   Date: 30/04/2000

I. Comparison of the project's goals and achievements

In the previous reports we have been focused our effort to make cholesteric liquid crystal devices and examined their optically properties in and outside of the reflection bands. Two different configurations have been examined:

(1) Pitch much larger that the optical wavelength

(2) Pitch comparable to the optical wavelength.

During the course of the work we have found that work is needed to better understand the alignment of alignment of liquid crystals. Thus we have undertaken work to examine the effect of circular rubbing of surfaces to controllably produce defects such as those observed in cholesteric liquid crystals.

II. Achievements

In the last two quarter we showed the results of the behavior of the cholesteric material inside and outside of the reflection band.

Here the behavior of the defects in a circular-circularly rubbed liquid crystal cell with an off-center alignment is reported. We show that the line defect forms a circle that passes through the rubbing centers of the two surfaces. The size and the position of the defect circle depend on the cell gap and the pitch of the materials. We propose a simple model, based on an analysis of the free energy, to explain this interesting phenomenon. This technique of defect making is useful to confine the defect to a particular position by controlling the cell parameters and the material properties. It can also be applied to the pitch measurement, the generation of the space-variant polarized light, and the study of the dynamic properties of the defect.

To study the defect formation in a circular-circularly rubbed cell, we chose a liquid crystal (ZLI-3488 from Merck) whose pitch continuously changes with the temperature. This material has a cholesteric phase when its temperature is between 66°C and 85°C. Figure 1 shows the nominal pitch of this material as a function of the temperature. The cell was made using indium-tin-oxide (ITO) glass substrates. To promote planar alignment, the ITO glass was coated with a thin layer of Polybutylene-terepthallate (PBT). PBT was chosen with no specific reason, and other alignment material, such as polyimide, yields the same results. Then, the PBT layers were rubbed circularly. To have a uniform rubbing pattern, the rubbing strength should be adjusted because of the variation in the linear speed as one moves away from the center of rubbing. The rubbed plates were assembled into a 10μm thick cell. When assembling the cell, the rubbing centers of the two surfaces were deliberately

separated by a small distance. Several cells were made, and the one with a suitable separation (about 1mm) between the two rubbing centers was chosen to be used in our experiment. The liquid-crystal material was inserted into the cell in its isotropic phase by the capillary action.

In order to obtain a better understanding of this phenomenon, we propose a simple model, which is based on an analysis of the free energy. We assume that the molecules are in the so-called planar state, which means that the molecules are parallel to the surfaces of the cell. By doing so, the small pretilt angle generated by rubbing was omitted. The influence of the pretilt angle is so small that no sensible effect was observed in our experiment. In this case, the elastic free energy has only one term, the twisted term[1]

$$f = \int_0^d K_2 \left(\frac{\partial \phi}{\partial z} - q \right)^2 dz, \tag{1}$$

where K_2 is the twist elastic constant, ϕ is the azimuth angle of twist for the director, z is the coordinate in the surface normal, d is the cell gap, $q = 2\pi/p$, and p is the pitch. If the temperature and the pitch are fixed, $(d\phi/dz)$ is a constant and there is no external field, then the free energy can be written in a simple form as

$$f = K_2 \left(\frac{\phi_T}{d} - q \right)^2 d, \tag{2}$$

where ϕ_T is the total twisted angle from one surface to the other.

The nature of the disclination line tells us that the molecules on either side of the disclination line should have the same free energy in equilibrium state. If this were not the case, the disclination line would move to reach a stable, equilibrium configuration. If one assumes that at the two sides of the disclination line, the total twisted angles are $\theta \pm \pi/2$, then, the equilibrium conditions yield the following equation:

$$\left(\frac{\theta + \pi/2}{d} - q \right)^2 = \left(\frac{\theta - \pi/2}{d} - q \right)^2. \tag{3}$$

Therefore, the deviation angle θ can be easily determined as

$$\theta = \frac{2\pi d}{p}. \tag{4}$$

The equilibrium between the two domains separated by the disclination line requires that the total twisted angle should be $\theta \pm \pi/2$ on the two sides of the defect. As illustrated in Fig. 3, C_1 and C_2 are the two rubbing centers of the

bottom and the upper surfaces, respectively. The two dashed circles (α and β) represent the rubbing direction at the two surfaces. According to the above analysis, if point C is on the defect curve, then the molecules at this point should have a total twisted angle $\theta \pm \pi/2$ on the two sides of the defect. Because, at the surface, the molecules are aligned as a circle that follows the rubbing pattern, the $\theta \pm \pi/2$ total twisted angle along the defect line requires the angle $\chi = \theta \pm \pi/2$. The handedness of the twist determines which sign (+ or –) should be used.

III. Publications

1. Z. Zhuang, Y. J. Kim and J. S. Patel, " Behavior of cholesteric liquid crystals in a Fabry-Perot cavity in the Bragg Reflection Band," Physical Review Letter, vol. **84**, number 6, pp 1168 to 1171, February 2000.

2. Z. Zhuang, Y. J. Kim and J. S. Patel, " Electrically controllable azimuth optical rotator," Applied Physics Letter, vol. **76**, number 17, pp 2334 to 2336, April 2000.

IV. Professional Personal

Z. Zhuang   - Graduate Student

Summet Suri   - Graduate Student

Tejas Patel   - Graduate Student

Vikram Hegde - Graduate Student

Jay Patel   - Principal Investigator

V. Inventions and Patent Disclosures

1. none

PENNSTATE

Technical Status

Fast Electro-optic Devices For Next Generation Optical Cross-Connects

Technical Report

Performance Period :
01/05/2000 to 31/07/2000

Professor Jay S. Patel,

Liquid Crystal Materials and Device Research Lab.,

The Pennsylvania State University   Date: 31/07/2000

I. Comparison of the project's goals and achievements

In the previous reports we have focused our effort to obtain an understanding of the behavior of the defects in a circular-circularly rubbed liquid crystal cell with an off-center alignment. This has been an interesting study, which led to a much better understanding of the interaction of the liquid crystals with surfaces. In the present report we continue along similar lines to examine a more practical system in which the surfaces are rubbed in two orthogonal directions, one after another. This is a process, which is critical to understand because of its potential to make high performance liquid crystal devices for optical communications.

II. Achievements

In the previous report we show that the line defect forms a circle that passes through the rubbing centers of the two surfaces. The size and the position of the defect circle depend on the cell gap and the pitch of the materials. We proposed a simple model, based on an analysis of the free energy, to explain this interesting phenomenon.

Here we have report the results of our investigation of the alignment properties of liquid crystals induced by multiple rubbing of the surfaces in different directions. Experiments were carried out using homeotropic and hybrid-aligned samples. It is experimentally found that the alignment of the liquid crystals is along neither of the rubbing directions, but instead lies along an axis intermediate between these two directions, and that the direction depended on the relative strength of rubbing along the two axes. A model that assumed the grooves along two rubbing directions is proposed, and the relation between the orientation of liquid-crystal and the relative rubbing strength is analyzed. We found that this model can explain the observed experimental results.

We first focus on the alignment of the LC on a rubbed homeotropic surface. Instead of a unidirectional rubbing, we attempted a multi-directional rubbing of the homeotropic surface. The homeotropic surface was sequentially rubbed in two different directions. The sample was examined by using a polarizing microscope. It is found that the alignment of the liquid crystals is not along either of the rubbing directions but instead lies along an axis intermediate between these two directions, and that the orientation of the LC depends on the ratio of the rubbing strengths of the two rubbing directions. A proposed atheoretical model that assumes sinusoidal grooves that are created along two rubbing directions was used to explain the reulsts. Using this analysis, we obtained a relation between the orientation of the LC and the strengths of the

two rubbing axes, which showed good agreement with the experimental results.

The results show that for a finite cumulative number of rubs, the aligning effect of the first rubbing direction can not be ignored. The results also show that in order to align the LC molecules along the last rubbing direction, one has to apply several rubs in the direction of the last rubbing. This fact can be critical to the alignment of the tilted homeotropic surface especially when it is used in domain dividing technology.

Our model assumes sinusoidal boundary conditions. This is a simple consequence of analysis of the surface using Fourier series. The grooves on the surface can be represented as series of sinusoidal functions. To the first approximation we have chosen only one term due to the reason of simplicity. Thus in the framework of this over-simplified model, although the degree of rubbing does not exactly correspond to the spatial frequency, this is a reasonable assumption indicative of the strength of rubbing. Therefore, we suppose that there exist micro-grooves along x and y-axes on the surface, which is described as,

$$z = A_x \sin q_x x + A_y \sin q_y y . \tag{1}$$

The director of LC is represented as $(\cos\theta\cos\phi, \cos\theta\sin\phi, \sin\theta)$, where θ is a tilt angle measured from xy-plane, and ϕ is an azimuth angle measured from x-axis. We assumed that θ is a function of x, y, and z, and ϕ a constant independent of the coordinates.

In an approximation of a one elastic constant, the free energy density of nematic LC is described as $f = K\{(\cos\phi\theta_x + \sin\phi\theta_y)^2 + \theta_z^2\}$, where K is an elastic constant. The subscripts denote the partial derivative with respect to the coordinates. Using Euler-Lagrange equation, the equation of motion is obtained as,

$$\cos^2\phi\theta_{xx} + \sin^2\phi\theta_{yy} + \sin 2\phi\theta_{xy} + \theta_{zz} = 0 \tag{2}$$

The LC molecules on the grating-like boundary align along the tangential or perpendicular direction of the surface in a planar or homeotropic alignment, respectively. A solution to this differential equation that matches the boundary condition Eqn. (1) is obtained as $\theta(x, y, z) = A\sin(q_x x + q_y y)\exp(-\beta z)$, where $\beta = q_x\cos\phi + q_y\sin\phi$ and A is a constant. Using the solution obtained above,

the total free energy per unit area was calculated as $F = \int_0^\infty f dz = KA^2\beta/2$. By

minimizing this free energy with respect to ϕ, the azimuth angle was obtained satisfying the relation, $1/\tan\phi = q_x/q_y$. This relation shows that the orientation of the LC on the surface that is rubbed in multiple direction

depends on the density of the grooves in different directions created by the rubbing process.

Based on this model, we attempted to numerically fit the experimental data using the relation, $\tan\phi = q_y/q_x$. By increasing the cumulative number of rubs, it is possible to make more scratches or grooves on the surface, which increases the density of grooves. The increase of grooves can be represented by adding more sinusoidal functions with different spatial frequencies to the Eqn. (1). In the first order approximation, we assumed that the density of groove is represented by a spatial frequency of a single sinusoidal boundary. As the inserts of Figure below the value of the $1/\tan\alpha$ is indeed linearly proportional to n/m. Thus, the simple model appears to be a fairly good representation of the multiple rubbing of the surface. From the experimental results, we can conclude that the effect of two rubbings depends on the order in which the rubbing was carried out. For $(m, n) = (1, 1)$, the direction is not along the bisector of the two rubbing direction, but is biased towards the second rubbing direction. The order of rubbing seems to introduce a bias of a factor of 3 in homeotropic sample and 5 in HAN sample shown in the inserts of Figure below. This is because some of the grooves created by the first rubbing are erased by the second rubbing.
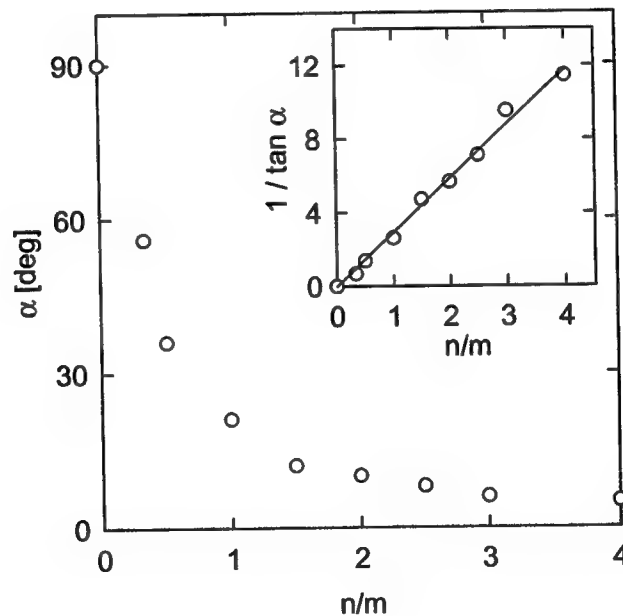
III. Publications

1. Z. Zhuang, S. Suh, Y. J. Kim and J. S. Patel, " Defect in the circular-circularity rubbed liquid crystal cell with off-center alignment," Applied Physics Letter, vol. **76**, number 21, pp 3005 to 3007, May 2000.

2. Z. Zhuang, Y. J. Kim and J. S. Patel, " Achromatic linear polarization rotator using twisted nematic liquid crystals," Applied Physics Letter, vol. **75**, number 26, pp 3995 to 3997, June 2000.

3. Z. Zhuang, Y. J. Kim and J. S. Patel, "Effect of multidirection rubbing on the alignment of nematic liquid crystals," Applied Physics Letter, vol. **77**, number 4, pp 513 to 515, July 2000.

IV. Professional Personal

Z. Zhuang   - Graduate Student

Summet Suri   - Graduate Student

Tejas Patel   - Graduate Student

Vikram Hegde - Graduate Student

Jay Patel   - Principal Investigator

V. Inventions and Patent Disclosures

1. none

Technical Status

Fast Electro-optic Devices For Next Generation Optical Cross-Connects

Technical Report

Performance Period :
01/08/2000 to 31/10/2000

Professor Jay S. Patel,

Liquid Crystal Materials and Device Research Lab.,

The Pennsylvania State University   Date: 31/10/2000

I. Project Goals for This Quarter

In the last quarter we investigated the effect of rubbing in producing oriented liquid crystals cells and found that when subsequent rubbing in different directions is used, the net orientation of the liquid crystal may not be along either of the two directions, but rather somewhere in-between. We found that the measured results can be explained well in the framework of a mathematical model.

In this quarter we examine a novel liquid crystal device based on nematic liquid crystals which can be used as an azimuthal optical rotator. We propose a simple configuration that is capable of rotating a linear polarization state of light by a certain angle for a wide range of wavelengths. The device consists of three liquid-crystal cells: two homogeneous cells and one twisted nematic (TN) cell. It is well known that a thick TN cell can rotate the linear polarization state of light by following the twisted structure. However, for a thin TN cell, achromatic polarization rotation is not possible. Using the Poincaré sphere model of the TN structure, we demonstrate that if one thin homogeneous cell is placed before and another one is placed after a thin TN structure, then a linear polarization state can be transformed close to the eigenmodes of TN. This structure can therefore be used to achieve achromatic polarization rotation. We have carried out detailed theoretical analysis and a demonstration of the achromatic linear polarization rotator by the use of a 1.9μm TN cell for the wavelength range 450-700nm.

II. Achievements

A twisted nematic liquid crystal has an intriguing structure. The optical properties of a TN LC are a combination of the linear birefringence and the optical rotation. Consider a structure, which has a total phase retardation that can be expressed as $2\pi d\Delta n/\lambda$, where d is the thickness of the cell and Δn is the optical anisotropy. The total twisted angle is ϕ. As it passes through the TN structure, the evolution of the initial SOP can be visualized by tracing the trajectory of a point on a cone, where the cone is rolled on the equatorial plane at a rate that is twice that of the twist of the directors. As Fig. 1 shows, the cone's axis is represented by OC, and the half-angle of the cone ω is defined as

$$\tan \omega = \frac{2\lambda}{\Delta np}, \qquad\qquad (1)$$

where $p=2\pi d/\phi$ is the pitch.

It is obvious from Fig. 1 that if the incident polarization is at point C, while it moves with the cone, the ellipticity does not change. The only effect of this movement is the azimuth rotation of the polarization direction. This

polarization state is called the "rotated eigenmode" of the TN structure. In the following discussion, we refer to this state as the eigenmode. It should be noted that, for the TN structure, there are two orthorgonal eigenmodes (points C and C' in Fig. 1). The azimuth angle of eigenmode (C) is parallel to the entrance director and the polar angle is defined by Eq. (1). The same results have been achieved with the use of the Jones matrix formalism.[i,ii]
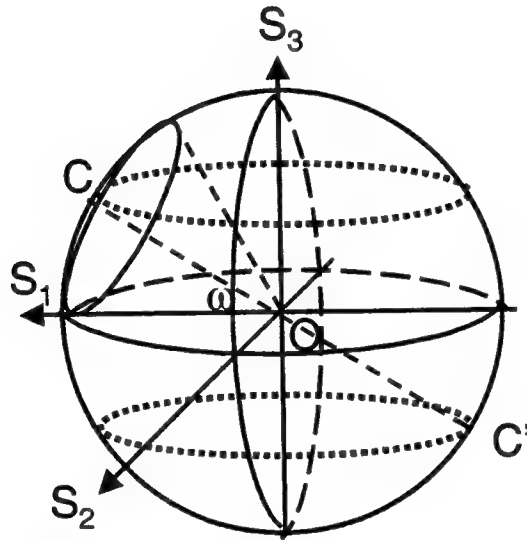

Figure 1. Poincaré sphere representation for a twisted nematic liquid crystal cell. ω is the half-angle of the cone; OC is the cone axis; C and C' are two orthogonal eigenmodes of the structure.

Based on the above discussion, one can easily conclude that if the incident polarization state is the eigenmode, then the only effect is the exact rotation of the polarization state by the total twisted angle without a change in its ellipticity. On the other hand, as described in Eq. (1), the eigenmode for the TN structure is wavelength dependent; therefore, this pure polarization azimuth rotation can only be achieved for a specific wavelength. There are two ways to accomplish the achromatic polarization azimuth rotation. The first method requires that the Mauguin limit ($\lambda << \Delta n \cdot d$) be satisfied. From Eq. (1), it is clear that, at the Mauguin limit, the cone will be reduced to a line that lies along the equatorial plane; therefore the wavelength dependence is eliminated. However, the Mauguin limit requires a thick sample, which is not practical in most applications and results in a slow response. The other method is to transform the incident polarization state of different wavelengths close to their corresponding eigenmodes. This method can be applied to a thin TN cell, and it is the method used in this Letter.

As Eq. (1) illustrates, the half-angle of the cone (ω) increases as the wavelength increases. In effect, this causes the polar angle of the eigenmode to increase as the wavelength increases. On the other hand, the phase retardation of a homogeneous nematic LC cell decreases as the wavelength increases. It is well known that the effect of a homogeneous waveplate on the incident polarization state of light is to rotate the polarization state by an angle equal to the phase retardation of the waveplate. Therefore, if one can design a suitable structure, which can transform the linear polarization state close to the eigenmodes of different wavelengths, the achromatic azimuth linear polarization rotation can be achieved.

The results of our effort are shown in the figure on the next page, where we show both the experimental and the theoretical results. The top portion of the figure shows the variation of the Stokes parameters for ordinary TN based rotator as well as the new achromatic rotator that we discuss here, clearly showing that the performance of the new device is far superior. This is more clearly evident in the bottom portion of the figure.
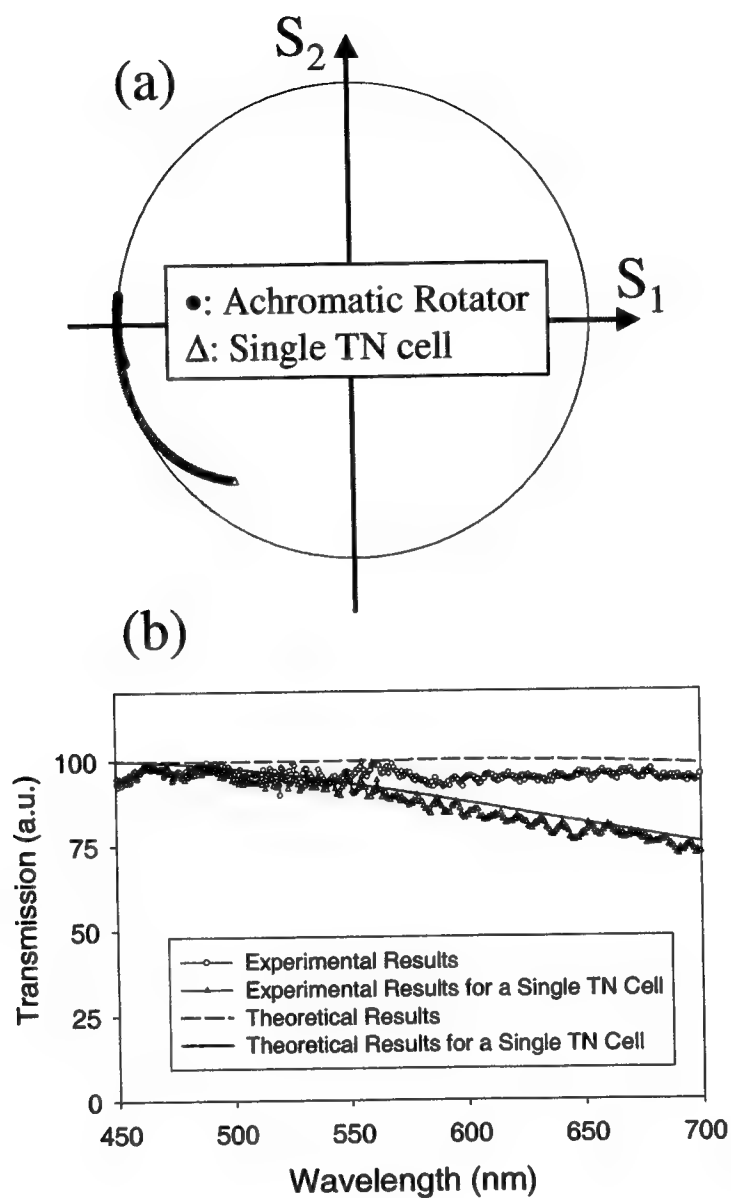
Theoretical and Experimental results for the achromatic polarization rotator and a single TN cell. (a) The calculated emergent polarization states in the S_1-S_2 projection plane. (b) The calculated and experimental results for transmission spectra between cross polarizers.

III. Publications

1. Z. Zhuang, Y. J. Kim and J. S. Patel, " Polarization states of Ferroelectric Liquid-crystal in a twisted structure," Jpn. J. Appl. Phys. Vol. 39, pp. 5927 to 5930, October 2000.

IV. Professional Personal

Z. Zhuang   - Graduate Student

Summet Suri   - Graduate Student

Tejas Patel   - Graduate Student

Vikram Hegde - Graduate Student

Jay Patel   - Principal Investigator

V. Inventions and Patent Disclosures

None

---

[i] J. A. Davis, I. Moreno, and P. Tsai, Appl. Opt. **37**, 937 (1998).
[ii] I. Moreno, J. A. Davis, K. G. D'Nelly, and D. B. Allison, Opt. Eng. **37**, 3048 (1998).

Technical Status

Fast Electro-optic Devices For Next
Generation Optical Cross-Connects

Technical Report

Performance Period :
01/11/2000 to 31/1/2001

Professor Jay S. Patel,

Liquid Crystal Materials and Device Research Lab.,

The Pennsylvania State University   Date: 31/1/2001

I. Comparison of the project's goals and achievements

In the last quarter we examine a novel liquid crystal device based on nematic liquid crystals which can be used as an azimuthal optical rotator. We proposed a simple configuration that is capable of rotating a linear polarization state of light by a certain angle for a wide range of wavelengths. We demonstrated the concept using detailed theoretical analysis and a demonstration of the achromatic linear polarization rotator by the use of a $1.9\mu m$ TN cell for the wavelength range 450-700nm.

In this report we extend our work to a generalized polarization rotator using nematic liquid crystals for arbitrary polarization transformation form one polarization state of the light to another.

II. Achievements

Here we demonstrate a polarization controller capable of changing any state of polarization of light from one arbitrary state to another. The controller consists of a stack of three homogeneous nematic liquid crystal cells. The polarization state is controlled by properly adjusting the voltages applied across each of the cells. The mathematical algorithm and principles of this polarization controller are developed in the framework of the Stokes parameters, allowing an easy visualization using Poincare sphere representation. The transformation functions are given for converting an arbitrary input state to any output state. Experiments are carried out to demonstrate the arbitrary polarization transformation.

We show that arbitrary polarization transformation can be achieved using three liquid crystal cells. The SOP is controlled by adjusting only the operating voltages of liquid crystal cells. It is obviously that in order to achieve this arbitrary SOP transformation, both the input and target SOP must be known; once the Stokes parameters[i] of these states are known, the transformation can be achieved by setting the operation voltages for the liquid crystal cells.

The configuration of the arbitrary to arbitrary polarization controller is shown in figure 1. It consists of three homogeneous nematic liquid crystal cells. The slow axes of each liquid crystal slab are at $0°$, $45°$ and $0°$, respectively. A series of linear birefringent elements (such as homogeneous nematic liquid crystals slab in our case) are described by a series of rotations on the Poincare sphere[ii] with respect to axes that lie on the equatorial plane[iii]. Thus, as shown in figure 2, the three cells in our device correspond to three axes, which are HV, PQ and HV respectively. By changing the applied voltages, the amount of rotations with respect to each axis can be controlled to achieve the arbitrary to arbitrary transformation.

Suppose the incident light field is represented by:

$$\begin{pmatrix} E_x^i \\ E_y^i \end{pmatrix} = \begin{pmatrix} \cos\alpha \\ \sin\alpha\exp(i\delta) \end{pmatrix} \tag{1}$$

This can also be represented by Stokes parameters as:

$$S_1^i = E_x^i E_x^{i*} - E_y^i E_y^{i*} = \cos 2\alpha$$

$$S_2^i = E_x^i E_y^{i*} + E_y^i E_x^{i*} = \sin 2\alpha\cos\delta \tag{2}$$

$$S_3^i = i\left(E_x^i E_y^{i*} - E_y^i E_x^{i*}\right) = \sin 2\alpha\sin\delta$$

The output light field emerging from a stack of three liquid crystal cells is given by:

$$\begin{pmatrix} E_x^o \\ E_y^o \end{pmatrix} = J(B_3)R(-\pi/4)J(B_2)R(\pi/4)J(B_1)\begin{pmatrix} E_x^i \\ E_y^i \end{pmatrix} \tag{3}$$

Where $J(B_j)$ is the Jones matrix for retarder with retardation B_j, $R(\theta)$ is the rotation matrix with rotating angle θ.

Then, the Stokes parameters of the output light can be calculated as following:

$$S_1^o = \cos B_2\cos 2\alpha + \sin B_2\sin(B_1-\delta)\sin 2\alpha$$

$$S_2^o = \sin B_3\sin B_2\cos 2\alpha + \cos B_3\sin 2\alpha\cos(B_1-\delta) - \sin B_3\cos B_2\sin(B_1-\delta)\sin 2\alpha$$

$$S_3^o = \cos B_3\sin B_2\cos 2\alpha - \sin B_3\sin 2\alpha\cos(B_1-\delta) - \cos B_3\cos B_2\sin(B_1-\delta)\sin 2\alpha$$

$$\tag{4}$$

If the voltage of the first cell is adjusted such that the retardation B_1 satisfy

$$B_1-\delta = \pi/2, \tag{5}$$

Equation (4) can be reduced as following:

$$S_1^o = \cos(B_2-2\alpha)$$

$$S_2^o = \sin B_3\sin(B_2-2\alpha) \tag{6}$$

$$S_3^o = \cos B_3\sin(B_2-2\alpha)$$

The above equation has the same form as the unit sphere co-ordinates with azimuth and polar angle ($B_2-2\alpha$) and B_3. Therefore, it can span the entire surface on Poincare sphere, if B_2 and B_3 are changed in a 2π range. This

proves that all points on the Poincare sphere are accessible by varying the birefringence, or equivalently, the voltages applied to each liquid crystal cells.

Device:	LC_1	LC_2	LC_3
Slow Axis:	$0°$	$45°$	$0°$
Retardation:	B_1	B_2	B_3
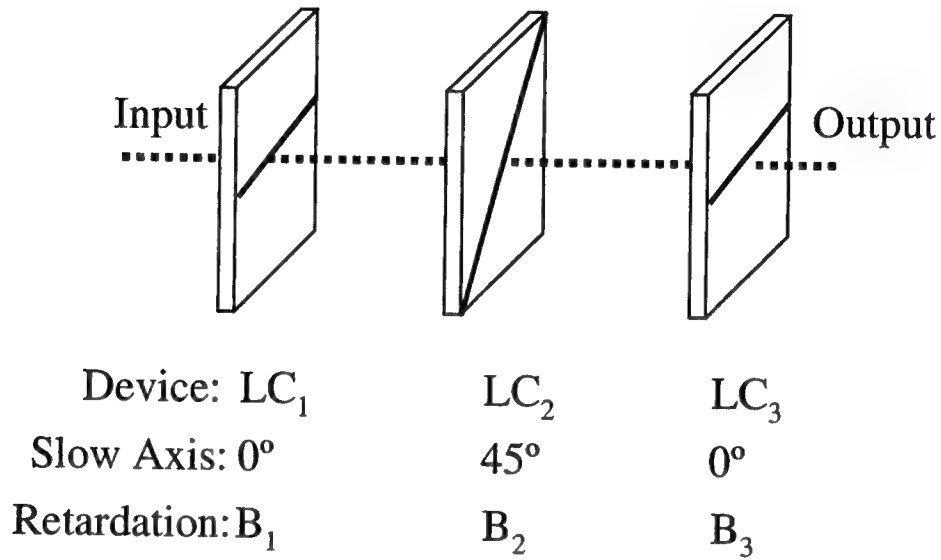
Figure.1: The configuration of arbitrary-arbitrary SOP controller.

Figure 2 Visualization of the arbitrary-arbitrary SOP mapping algorithms on Poincare sphere. V: vertical linear, H: horizontal linear, P: +45° linear, Q: -45° linear. L: left-handed circular, R: right-handed circular

III. Publications

None

IV. Professional Personal

Z. Zhuang   - Graduate Student

Sumeet Suri   - Graduate Student

Tejas Patel   - Graduate Student

Vikram Hegde - Graduate Student

Jay Patel   - Principal Investigator

V. Inventions and Patent Disclosures

1. None

[i] G. G. Stokes, Trans. Cambridge. Phil. Soc. **9**, 309 (1852).

[ii] H. Poincare, in *Theorie Mathematique de la Lumiere II*, George Carre ed. (Paris, 1892), p. 275

[iii] J. E. Bieglow and R. A. Kashnow, Appl. Opt. **16**, 2090 (1977).

Reflective Single-Polarizer Bistable Nematic Liquid Crystal Display with Optimum Twist

Young Jin Kim, Zhizhong Zhuang, and Jay. S. Patel
Department of Physics and Department of Electrical Engineering
The Pennsylvania State University, University Park, Pennsylvania

Abstract

A single polarizer reflective liquid crystal display in a bistable twisted nematic configuration is proposed and experimentally reported. In the two bistable states, the twist angles are 63.6° and 423.6° which produce the dark and bright states, respectively. Numerical optimization of the polarization states is performed by using Mueller matrix of the cell studied. Our results show that high contrast display is possible using this configuration without any use of an optical compensation film.

Introduction

Reflective liquid crystal displays (LCDs) are attractive for many display applications, particularly when opaque back substrate such as silicon are used for electrically addressing a pixel. In many reflective displays, two polarizers are used where the absorption losses reduce the overall efficiency of the devices. Single polarizer configurations are therefore preferred in reflective displays. A mixed-mode twisted nematic[1] and an optically compensated bend cell [2] have been investigated in a single polarizer structure to address the problems of low brightness and parallax observed in the two polarizer structures. Recently there has been much interest in bistable twisted nematic (BTN) LCDs. Transmissive mode device using two polarizers were first proposed by Berreman in the early 1980s [3], and electro-optic device has been recently demonstrated for the practical applications [4].

In this paper we propose a reflective BTN mode display with a single polarizer. In the following, we first outline some background of bistable nematic display, then the technique for optimization for the reflective displays, followed by the experimental results.

Optimization for the reflective mode

Since the BTN device has to be switched between two liquid crystal (LC) configurations, these configurations have to be topologically equivalent if they are to be driven from the same initial state. This requires that for a chosen boundary condition, the twist in these two states have to differ by integral multiple of 2π. The transmissive mode BTN display operated between two topologically equivalent states, which has a twist of 0 and 2π. The energy equivalence of these two states is achieved by using a chiral material, which at equilibrium produces a twist of π. This state is topologically different from the 0-twisted or the 2π-twisted state. When a high electric field is initially applied and then switched off, the field driven state relaxes into one of two possible states, 0-twisted or 2π-twisted state. For the application of reflective devices, additional cell optimization is necessary which means that the polarization transformation is such that for a linearly input polarization, the output polarization passed through the cell is also linear, but orthogonal to the input polarization. Therefore optimization requires a choice for the twist angle for the two states, and an appropriate choice of the birefringence of the cell.

We have recently showed that Stokes parameter optimization is a more convenient for this optimization [5,6]. The elements of Mueller matrix, $M = (m_{ij})$, (i,j=0..3) for the twisted nematic structure is represented as follows.

$$m_{00} = 1,$$

$$m_{01} = m_{02} = m_{03} = m_{10} = m_{20} = m_{30} = 0,$$

$$m_{11} = \cos 2\Phi_T (\cos^2 \beta + \frac{\Lambda^2 - \Phi_T^2}{\beta^2} \sin^2 \beta) + \frac{\Phi_T}{\beta} \sin 2\Phi_T \sin 2\beta,$$

$$m_{12} = -\sin 2\Phi_T \cos 2\beta + \frac{\Phi_T}{\beta} \cos 2\Phi_T \sin 2\beta,$$

$$m_{13} = \frac{2\Lambda\Phi_T}{\beta^2} \cos 2\Phi_T \sin^2 \beta - \frac{\Lambda}{\beta} \sin 2\Phi_T \sin 2\beta,$$

$$m_{21} = \sin 2\Phi_T \left(\cos^2 \beta + \frac{\Lambda^2 - \Phi_T^2}{\beta^2} \sin^2 \beta\right) - \frac{\Phi_T}{\beta} \cos 2\Phi_T \sin 2\beta,$$

$$m_{22} = \cos 2\Phi_T \cos 2\beta + \frac{\Phi_T}{\beta} \sin 2\Phi_T \sin 2\beta,$$

$$m_{23} = \frac{2\Lambda\Phi_T}{\beta^2} \sin 2\Phi_T \sin^2 \beta + \frac{\Lambda}{\beta} \cos 2\Phi_T \sin 2\beta,$$

$$m_{31} = \frac{2\Lambda\Phi_T}{\beta^2} \sin^2 \beta,$$

$$m_{32} = -\frac{\Lambda}{\beta} \sin 2\beta,$$

$$m_{33} = \cos^2 \beta - \frac{\Lambda^2 - \Phi_T^2}{\beta^2} \sin^2 \beta,$$

(1)

Where $\Lambda = \pi d \Delta n / \lambda$, $\beta = \sqrt{\Lambda^2 + \Phi_T^2}$, Φ_T a twist angle, Δn an optical anisotropy, d a cell gap, and λ a wavelength of an incident light. The Stokes vector of a linear polarization parallel to the rubbing axis of the cell is represented as $S_i = (1,1,0,0)$. The output polarization S passed through the cell is obtained by multiplying the incident Stokes vector by the Mueller matrix, thus $S = M \cdot S_i$.

The parameter optimization requires a change in polarization for one state and no change for the other state. For one state to satisfy the half-wave condition, the output polarization should be circularly polarized after the light passes through the cell once, and produce the required half-wave condition after reflection. With this condition, the polarization of the light reflected from a mirror is linear and orthogonal to the input polarization, and thus the dark state is readily obtained with a single polarizer. For the other state, the output polarization should be linearly polarized for the polarization reflected from a mirror not to be changed. This requires that $|S_3| = 1$ for the one state, and $S_3 = 0$ for the other state. Furthermore in absence of a field, the twist in these two states should differ by 2π. The optimization requires that these two conditions should be satisfied simultaneously. S_3 of the output polarization is calculated as $S_3 = (2\Lambda\Phi_T / \beta^2)\sin^2 \beta$. However, for the input polarization parallel to the rubbing direction, these conditions can't be satisfied simultaneously. Thus we chose the condition for the highest contrast by optimizing the cell parameters for the dark state. The optimized parameters for dark state are obtained as follows.

$$\Phi_T = \frac{(2N-1)\pi}{2\sqrt{2}} = \frac{\pi d \Delta n}{\lambda} ,$$

(2)

where N is an integer. This is the same result as previous studies for the reflective mode displays [6,7]. Using this optimization, $S_3 \neq 0$ for the $\phi_T + 2\pi$ twisted state, which means that the reflected light is not exactly linearly polarized. However, it can be expected that $S_3 \ll 1$ for the $\phi_T + 2\pi$ twisted state, because S_3 scales as $2\Lambda\phi_T / \beta^2$ indicating that the value of S_3 becomes smaller with increasing twist angle, since Λ is small and fixed. Thus for one of the twisted state, we choose using Eqn. (2) the twist to be 63.3° and the twist angle for the other state as 63.3°+2π.

Using this geometry, Stokes parameters were calculated for light passing through the cell for the two bistable states. The LC directors were assumed to be uniformly twisted and light was incident normal to the cell. The axis of a polarizer was chosen to be parallel to the rubbing direction. The wavelength of the light has assumed to be 550 nm, and Δnd of the cell is 194 nm.

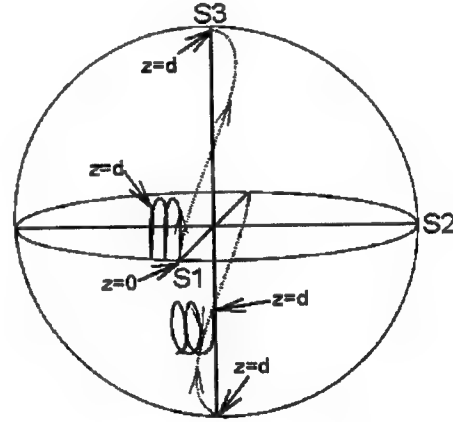**Fig. 1.** Numerical results for the polarization states of the light through the cell on the Poincare sphere. The solid and dashed lines stand for 423.6° and 63.6°-twisted states respectively. The input polarization is linear and the changes of the polarization states are shown in arrows for each twisted state.

The results are shown in Fig. 1, where the solid and dashed lines represent the larger and the

smaller twisted states, respectively. For the less twisted state, the linear polarization changes to the circular polarization along the path on the upper sphere, and back to the linear polarization along the path of lower sphere upon reflection from the mirror. The polarization state is orthogonal to the input polarization. For the higher twisted state, the polarization state rolls along the equator of the Poincare sphere, and reaches an elliptical polarization at $z=d$. Upon reflection from the mirror, the polarization state follows a different path and reaches at different state from the input polarization.

Experiment

We have attempted to experimentally demonstrate the electro-optical properties of the BTN in this reflective geometry. The BTN cell was made using indium-tin-oxide (ITO) glass substrates. The polyimide (PI) of AL-1051 (Japan Synthetic Rubber Co.) was coated on both substrates so as to promote planar alignment. The rubbing axes on the PI layers were given as the angle of 0° and 63.6° respectively to produce stable 63.6°-twisted and 423.6°-twisted states. The cell gap was maintained by glass spacers of 3.1 μm. A chiral dopant was added to the LC, and the doping concentration was adjusted to give d/p = 0.58. We have used ZLI-4119 (the optical anisotropy $\Delta n = 0.0603$) and S-811 as the LC and the chiral dopant respectively, and both were obtained from E. Merck. A polarizer was oriented parallel to the rubbing direction. The BTN cell was operated using the driving voltage waveform shown in Fig. 2, which consisted of a reset and a selection signal. With a proper selection voltage signal, the state can be transformed into the 63.6° twisted or the 423.6° twisted state. The reflected light intensity through the BTN cell was measured on a microscope.

Electro-optic characteristics

The photograph of the two bistable states are shown in Fig. 3. One pixel is switched on (63.6°) and the other switched off (423.6°). The selection voltages applied to the cell were 0 V (bright state) and 3 V (dark state). As shown in this figure, the BTN cell exhibits achromatic characteristics and high contrast with a single polarizer. The achromatic characteristic of the cell indicates that the wavelength dispersion is minimized at the first

minimum condition. The wavelength dependence of the electro-optic characteristics increases with higher order minimum condition. Several cells were made with different cell gaps in which the pitch of the LC was fixed to be 5.34 μm. Bistable switching was not observed when the cell gap was 3.0 and 3.2 μm, but it was observed when the cell gap was 3.1 μm. From the experimental results, the condition of d/p for bistable switching can be roughly estimated to be between 0.56 and 0.60.
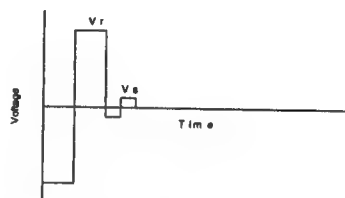
Fig. 2. The driving scheme for BTN.

Fig. 3. The photograph of the two bistable states of the BTN switching in a reflective geometry. A single polarizer is attached parallel to the rubbing direction and a mirror is placed on the back substrate of the cell. EO switching between dark and bright states is observed.

Fig. 4 shows the experimental results of reflected intensity of the BTN cell as a function of a selection voltage. A sharp transition between dark and bright states was observed. The dark and bright states correspond to the 63.6°-twisted and the 423.6°-twisted ones, respectively. The contrast was measured to be about 5 by using a white light source. This shows that this mode being studied is acceptable for the applications of reflective type display and gives better electro-optic characteristics with a single polarizer.

For the optimum electro-optic

characteristics, the two twisted states should be simultaneously optimized. We examined these conditions using geometrical transformation on a Poincare sphere. The details will be published elsewhere, but the results are shown in Fig. 5. For a single pass through the cell, the optimization for one of the states for which the output polarization through the cell is circularly polarized, the results are shown by the black lines.
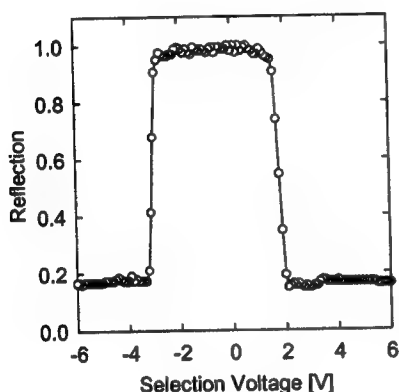

Fig. 4. Experimental results for the reflected light intensity as a function of a selection voltage in a reflective geometry.
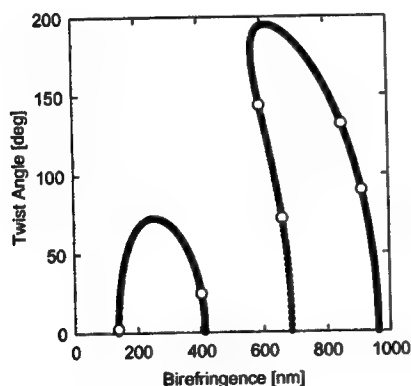

Fig. 5. Simultaneous optimization for the two bistable states, indicated by the open circles.

The optimum condition for the higher twisted state requires the polarization to be linear at $z = d$ for a single pass. The open circles represent the condition that two states are simultaneously optimized. The reflected output polarization is orthogonal to the input polarization for one state, and identical to the input polarization for the other state.

Conclusions

In conclusion, we have optimized the BTN mode for the applications of reflective type display with a single polarizer. The polarization states through the LC layers were studied using the Stokes parameters. For the experimental studies results are reported for the case where one of the two bistable states was optimized for the dark state. It was found that even if the other state is not exactly optimized, the results are very encouraging with achromatic characteristics. The electro-optical switching between dark and bright state was experimentally demonstrated in an optimized condition giving better contrast and brightness. The most recent results suggest that it is possible to further improve the contrast by simultaneous optimization of both the bistable states.

References

1. S.-T. Wu and C.-S. Wu, Appl. Phys. Lett. **68**, 1455 (1996).
2. T. Uchida, T. Nakayama, T. Miyashita, M. Suzuki, and T. Ishinabe, Proc. Asia Display **95**, 599 (1995).
3. D. W. Berreman and W. R. Heffner, Appl. Phys. Lett. **37**, 1 (1980).
4. T. Tanaka, Y. Sato, A. Inoue, Y. Momose, H. Nomura, and S. Iino, Proc. Asia Display **95**, 259 (1995).
5. G. N. Ramachandran and S. Ramaseshan, J. Opt. Soc. Am. **42**, 49 (1952).
6. S.-W. Suh, Z. Zhuang, and J. S. Patel, Proc. SID **98**, 997 (1998).
7. Y. Saitoh, Y. Yoshida, and H. Kamiya, Proc. SID **28**, 651 (1997).

Polarization controller using nematic liquid crystals

Zhizhong Zhuang, Seong-Woo Suh, and J. S. Patel

Departments of Physics and Electrical Engineering, Pennsylvania State University, University Park, Pennsylvania 16802

In this Letter we demonstrate a polarization controller capable of changing any state of polarization of light from one arbitrary state to another. The controller consists of a stack of three homogeneous nematic liquid-crystal cells. The polarization state is controlled by proper adjustment of the voltages applied across each of the cells. The mathematical algorithm and principles of this polarization controller are developed in the framework of the Stokes parameters, allowing easy visualization by use of a Poincaré sphere representation. The transformation functions are given for conversion of an arbitrary input state to any output state. Experiments are carried out to demonstrate arbitrary polarization transformation. © 1999 Optical Society of America

OCIS codes: 230.3720, 230.5440, 160.3710, 260.5430.

Polarization effects, although recognized as a fundamental property of light fields, have generally played a minor role in light-wave systems, because commercial optical receivers detect only optical power and are insensitive to polarization. In recent years, however, with the advance of optical amplifiers, the optical length of the light-wave systems has been dramatically increased, and as a result, small effects such as polarization-mode dispersion and polarization-dependent loss can accumulate and become an important consideration in a light-wave system.[1] Another obstacle to an optical coherent system is the unpredictable polarization change or drift that often comes from polarization-dependent components, including fibers, optical switches, and waveguides. In many systems, it is important to change or restore the altered state of polarization (SOP) to the desired SOP. Several studies have been reported on the use of traditional mechanical squeezing of fibers,[2] LiNbO$_3$ waveguides,[2,3] the Faraday effect,[4] rotating wave plates, and electro-optic crystals[5,6] to achieve polarization transformation. However, these methods are not convenient because of the high operating voltage and mechanical fatigue.

Since the birefringence of a liquid crystal can be changed by a relatively small electric field, a device based on this technology has many advantages. Previous studies on using liquid crystals to control the SOP (Ref. 7) have been limited to incident light with a specifically known linear polarization state. Because the intent was to use liquid crystals in a coherent communication system, the study reported in Ref. 7 was focused on how to compensate continuously for the SOP of the local oscillator to match that of the signal to prevent signal fading. The local oscillator is linearly polarized in a specific known direction. However, since the amount and direction of birefringence induced by thermal or mechanical fluctuations exhibit random changes, the input polarization state is generally arbitrary in a light-wave system. Therefore, a device capable of controlling arbitrary polarization states is desired.

In this Letter we show that arbitrary polarization transformation can be achieved with three liquid-crystal cells. The SOP is controlled by adjustment of only the operating voltages of the liquid-crystal cells. It is obvious that to achieve this arbitrary SOP transformation both the input and the target SOP's must be known; once the Stokes parameters[8] of these states are known, we can achieve this transformation by setting the operation voltages for the liquid-crystal cells.

We begin with a description of the configuration of the device, followed by calculation of the Stokes parameters of the input and the output light fields. We show mathematically that this arbitrary transformation can be done with three nematic liquid-crystal cells such that the relative orientations of these three cells are 45° with respect to one another. After that, we give experimental results to confirm the predictions of the theory.

The configuration of the arbitrary–arbitrary polarization controller is shown in Fig. 1. It consists of three homogeneous nematic liquid-crystal cells. The slow axes of each liquid-crystal slab are at 0°, 45°, and 0°. A series of linear birefringent elements (such as a homogeneous nematic liquid-crystal slab in our case) are described by a series of rotations on the Poincaré sphere[9] with respect to axes that lie on the equatorial plane.[10] Thus, as shown in Fig. 2, the three cells in our device, LC$_1$, LC$_2$, and LC$_3$, correspond to three axes, HV, PQ, and HV, respectively. By changing the applied voltages, we can control the amount of rotation with respect to each axis to achieve the arbitrary–arbitrary transformation.
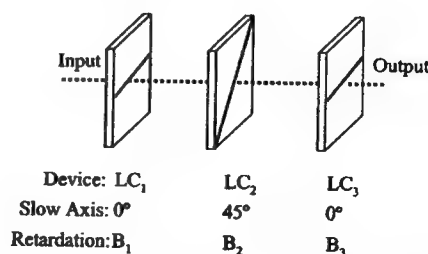

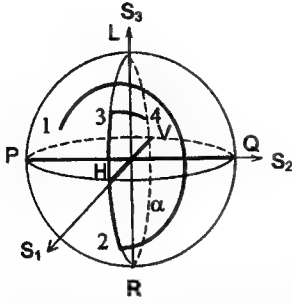Fig. 1. Configuration of the arbitrary SOP controller.

Fig. 2. Arbitrary–arbitrary SOP mapping algorithms on a Poincaré sphere. V, vertical linear; H, horizontal linear; P, +45° linear; Q, −45° linear; L, left-handed circular; R, right-handed circular.

Suppose that the incident light field is represented by

$$\begin{pmatrix} E_x{}^i \\ E_y{}^i \end{pmatrix} = \begin{bmatrix} \cos \alpha \\ \sin \alpha \, \exp(i\delta) \end{bmatrix}. \tag{1}$$

This field can also be represented by Stokes parameters as

$$S_1{}^i = E_x{}^i E_x{}^{i*} - E_y{}^i E_y{}^{i*} = \cos 2\alpha \,,$$

$$S_2{}^i = E_x{}^i E_y{}^{i*} + E_y{}^i E_x{}^{i*} = \sin 2\alpha \cos \delta \,,$$

$$S_3{}^i = i(E_x{}^i E_y{}^{i*} - E_y{}^i E_x{}^{i*}) = \sin 2\alpha \sin \delta \,. \tag{2}$$

The output light field emerging from a stack of three liquid-crystal cells is given by

$$\begin{pmatrix} E_x{}^o \\ E_y{}^o \end{pmatrix} = J(B_3)R(-\pi/4)J(B_2)R(\pi/4)J(B_1)\begin{pmatrix} E_x{}^i \\ E_y{}^i \end{pmatrix}, \tag{3}$$

where $J(B_j)$ is the Jones matrix for a retarder with retardation B_j and $R(\theta)$ is the rotation matrix with rotating angle θ.

Then, the Stokes parameters of the output light can be calculated as follows:

$$S_1{}^o = \cos B_2 \cos 2\alpha + \sin B_2 \sin(B_1 - \delta)\sin 2\alpha \,,$$

$$S_2{}^o = \sin B_3 \sin B_2 \cos 2\alpha + \cos B_3 \sin 2\alpha \cos(B_1 - \delta)$$

$$- \sin B_3 \cos B_2 \sin(B_1 - \delta) \sin 2\alpha \,,$$

$$S_3{}^o = \cos B_3 \sin B_2 \cos 2\alpha - \sin B_3 \sin 2\alpha \cos(B_1 - \delta)$$

$$- \cos B_3 \cos B_2 \sin(B_1 - \delta) \sin 2\alpha \,. \tag{4}$$

If the voltage of the first cell is adjusted such that the retardation B_1 satisfies

$$B_1 - \delta = \pi/2 \,, \tag{5}$$

then Eqs. (4) can be reduced as follows:

$$S_1{}^o = \cos(B_2 - 2\alpha) \,,$$

$$S_2{}^o = \sin B_3 \sin(B_2 - 2\alpha) \,,$$

$$S_3{}^o = \cos B_3 \sin(B_2 - 2\alpha) \,. \tag{6}$$

Equations (6) have the same form as the unit-sphere coordinates with azimuth and polar angle $(B_2 - 2\alpha)$ and B_3. Therefore, the Stokes vectors represented by Eqs. (6) can span the entire surface of a Poincaré sphere, if B_2 and B_3 are changed in a 2π range. Therefore all points on the Poincaré sphere are accessible if one varies the birefringence or, equivalently, the voltages that are applied to each liquid-crystal cell.

Although Eq. (5) is not a necessary condition, it simplifies the discussion for the following reason: For the configuration shown in Fig. 1 the rotation axes are fixed and orthogonal, so in general three rotations about these two axes are needed to map two arbitrary points on a sphere (Fig. 2). However, if the incident SOP is on the circle on which S_2 equals zero (α in Fig. 2), only two rotations around axes PQ and HV are needed. The condition for $S_2 = 0$ can be achieved by adjustment of B_1 to satisfy Eq. (5).

We can reduce the problem or arbitrary transformation from S^i to S^o to calculating the magnitude of the three angles required for rotation about the HV, PQ, and HV axes. According to Eqs. (2), (5), and (6), the birefringences of these three cells are

$$B_1 = \pi/2 + \tan^{-1}(S_3{}^i/S_2{}^i) + m\pi \,,$$

$$B_2 = \cos^{-1}S_1{}^i + \cos^{-1}S_1{}^o \,,$$

$$B_3 = \tan^{-1}(S_2{}^o/S_3{}^o) + n\pi \,, \tag{7}$$

The additional terms in B_1 and B_3 arise from the fact that the period of B is 2π, whereas the period of the tangent function is π; therefore we require additional information such as the sign of one of the Stokes parameters to determine the exact values of B_1 and B_3. As a result, m and n can be determined as follows: $m = 1$ when $S_3{}^i < 0$, and $n = 1$ when $S_2{}^o < 0$; otherwise, $m = n = 0$.

Since we applied voltages to control the birefringence, the relationship between the birefringence and the voltage needs to be determined. In our experiment this relationship was measured with a Hewlett-Packard HP8509B polarization analyzer. These data were interpolated by use of a cubic spline,[11] as shown in Fig. 3. Any 2π region of this curve can be used for determining the voltage–birefringence relationship. We chose the $\pi-3\pi$ region of the curve to avoid the high nonlinear region.

The validity of this analysis was tested experimentally in two experiments in which an arbitrary initial SOP was transferred to some preset target SOP. The experiments were done with a computer-based automatic polarization control and measurement system. The Stokes parameters were measured with a HP8509B polarization analyzer using an internal laser source at 1.3 μm. The applied voltages of the different liquid-crystal cells were controlled by a computer
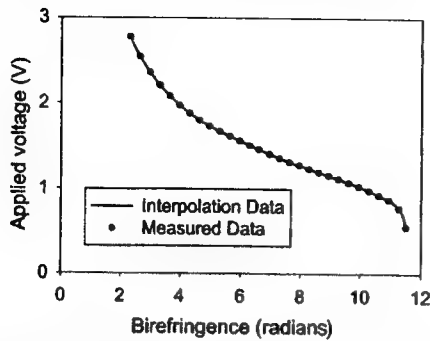
Fig. 3. Measured relationship between the applied voltages and the birefringence of the liquid-crystal cell. Filled circles, measured data; solid curve, result from the cubic spline interpolation. For clarity, only one tenth of the measured data are shown.
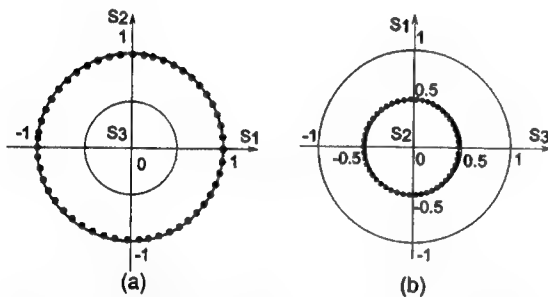

Fig. 4. Experimental results of arbitrary polarization transformation. The initial polarization state is arbitrarily chosen as $S^i = (-0.61, 0.11, -0.71)$. The final states are chosen to be two circles: (a) $S_3° = 0$, (b) $S_2° = 0.866$. The results are shown in (a) the $S_1 - S_2$ and (b) the $S_1 - S_3$ planes.

and three HP33120A function generators. The liquid-crystal cells were fabricated in our laboratory.

The initial states for both experiments were arbitrary chosen such that $S^i = (-0.61, 0.11, -0.71)$. The first experiment shows that this initial SOP was transferred to a SOP on the equatorial plane (i.e., $S_3° = 0$, $S_1°$, and $S_2°$ were continuously changed), as shown in Fig. 4(a). The second experiment shows that the initial SOP was transferred to the SOP on another circle with $S_2° = 0.866$, whereas $S_1°$ and $S_3°$ were changed continuously, as shown in Fig. 4(b). In this case the radius of the projection circle in the $S_1 - S_2$ plane should equal 0.5. The experimental results are shown in the $S_1 - S_2$ and the $S_1 - S_3$ projection planes.

During the experiment, the liquid-crystal cells were quite stable if the applied voltages were fixed. Fluctuations were less than 1% during a time period of several minutes. The fluctuations were determined to be the fluctuations of the reflective index of liquid crystal with temperature. No attempt was made to correct the drift for these experiments at room temperature although it can be reduced by temperature control or application of a feedback scheme. The additional source of error was in setting the suitable voltages according to the interpolation results, because the birefringence of liquid crystals is very sensitive to applied voltage. This change can be as large as a few degrees for a change of millivolts applied to the cell. The speed of the transformation is essentially limited by the electro-optic response of nematic liquid-crystal materials, which is typically of the order of 10 ms.

In conclusion, we have proposed a practical arbitrary polarization controller that uses nematic liquid crystals. The operating principles were addressed mathematically by use of Stokes parameters and Poincaré sphere representation. We showed the actual polarization transformation from one arbitrary state to another, using a computer-based polarization control and measurement system. This device is expected to play an important role in birefringence networks and may be useful in minimizing or controlling losses and other characteristics related to polarization-dependent devices in light-wave systems.

References

1. C. D. Poole and J. Nagel, in *Optical Fiber Telecommunications IIIA*, I. P. Kaminow and T. L. Koch, eds. (Academic, San Diego, Calif., 1997), pp. 114–162.
2. N. G. Walker and G. R. Walker, J. Lightwave Technol. **8**, 438 (1990).
3. J. Slaz, AT&T Tech. J. **64**, 2153 (1985).
4. T. Okoshi, Y. H. Cheng, and K. Kikuchi, Electron. Lett. **21**, 787 (1985).
5. T. Okoshi, J. Lightwave Technol. **3**, 1232 (1985).
6. T. Imai, K. Nosu, and H. Yamaguchi, Electron. Lett. **21**, 52 (1985).
7. S. H. Rumbaugh, M. D. Jones, and L. W. Casperson, J. Lightwave Technol. **8**, 459 (1990).
8. G. G. Stokes, Trans. Cambridge Philos. Soc. **9**, 309 (1852).
9. H. Poincaré, in *Theorie Mathematique de la Lumiere II*, G. Carré, ed. (Gauthier-Villars, Paris, 1892), p. 275.
10. J. E. Bieglow and R. A. Kashnow, Appl. Opt. **16**, 2090 (1977).
11. W. H. Press, B. P. Flannery, S. A. Teukolsky, and W. T. Vetterling, *Numerical Recipes in C* (Cambridge University, New York, 1988), p. 94.

Parameter optimization for a reflective bistable twisted nematic display by use of the Poincaré sphere method

Zhizhong Zhuang, Young Jin Kim, and J. S. Patel

Departments of Physics and Electrical Engineering, Pennsylvania State University, University Park, Pennsylvania 16802

Although reflective bistable twisted nematic (RBTN) displays have potential in low-power-consumption applications, to achieve the optimum conditions for both bistable states simultaneously remains a challenge. We use a geometrical method based on the Poincaré sphere representation to obtain the optimum conditions that can simultaneously satisfy both bistable states for a RBTN structure. With this method, the optimum conditions can be obtained analytically and the operation modes can be clearly visualized and better understood. © 1999 Optical Society of America

OCIS codes: 230.3720, 230.5440, 260.5430, 120.2040.

The bistable twisted nematic[1,2] (BTN) liquid-crystal display has become increasingly attractive, since it offers power-off memory, which is useful in matrix-addressed liquid-crystal displays with a large number of elements. Recently, practical application of the BTN display was demonstrated.[3] A BTN device displays bistability between two topologically equivalent ordered states; both states have a smooth configuration of the director and can be switched by use of a specially shaped electrical pulse. Most BTN displays are operated in the transmissive mode. To complete the display one needs a front and a rear polarizer. This two-polarizer configuration suffers from problems such as low brightness and parallax.

There have been a few efforts[4,5] to solve these problems by combining the advantages of the BTN and the reflective displays in a reflective bistable twisted nematic (RBTN) liquid-crystal display. A RBTN display contains only a front polarizer, a liquid-crystal cell, and a rear reflector, as was proposed by Xie and Kwok[4] and Kim et al.[5] In their studies parameter optimization was performed, but in both studies the authors failed to achieve the optimum conditions for both bistable states simultaneously. Xie and Kwok[4] used the parameter space method[6] to determine the optimum conditions for several incident polarization angles. Although the method that they employed provides the conditions for achieving a high contrast ratio, state-of-polarization (SOP) optimization was not considered. Kim et al.[5] performed optimization by assuming that the incident polarization was parallel to the entrance director. In this case the two states could not be simultaneously optimized, so the optimum conditions for the dark state were used. In this Letter we use a geometrical method to obtain the simultaneous optimum conditions for both bistable states.

From the reversibility theorem of Jones,[7] it can be shown[8] that, in a reflective structure, if the output SOP is required to be parallel (perpendicular) to the incident linear SOP, then the SOP at the mirror should be linear (circular). Therefore the problem of simultaneously optimizing both bistable states in a RBTN structure can be reduced to the following statement: The SOP at the mirror of a RBTN structure should be circular for one twisted state and linear for the other twisted state.

In Ref. 9 the use of a geometrical method to study the properties of a general twisted nematic (TN) structure in the static state was proposed. This method is based on the Poincaré sphere[10] (PS) representation of the SOP. The PS method represents the trajectory of the SOP's evolution as a geometrical curve on the PS when light passes through a TN cell. Compared with the commonly used parameter space method,[6] the PS method has several advantages. Because of its geometrical nature, the PS method provides a clear visualization of the evolution of the SOP and a better understanding of the operation modes; therefore optimization in terms of the SOP can be easily achieved. Equally important, in most cases optimization of the parameters can be reduced to a simple geometrical problem. This eliminates the need for complex numerical calculations.

A TN liquid crystal has an intriguing structure. Its optical properties are a combination of birefringence and optical rotation. Bigelow and Kashnow[11] used the PS representation to study the optical properties of a TN structure. They suggested that a TN structure can be represented on the PS by a cone that rolls without sliding along the equator. One can visualize the evolution of the initial SOP as it passes through a TN structure by tracing the trajectory of the initial point. This initial point is rigidly connected to the cone while the cone rolls on the equatorial plane at a rate that is twice the rate of the twist of the directors. The cone's axis (ON in Fig. 1) is defined by its half-angle ω:

$$\tan \omega = \lambda\varphi/\pi d\Delta n, \tag{1}$$

where λ is the wavelength, φ is the twisted angle, and $d\Delta n$ is the birefringence. The angle that the cone rolls about its axis ON is defined as

$$\Phi = [(2\pi d\Delta n/\lambda)^2 + (2\varphi)^2]^{1/2}. \tag{2}$$

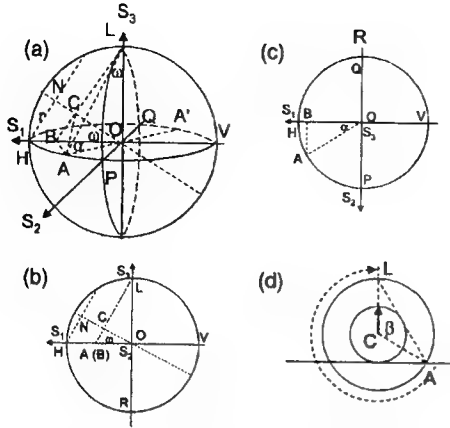The geometrical method outlined above has been used to study the SOP evolution of a TN structure when

61

Fig. 1. (a) Circular SOP output conditions. A is the incident SOP. ON is the cone's axis, and r is the radius of the cone's base. (b) S_1–S_3 projection plane, (c) S_1–S_2 projection plane. (d) Total rotation angle required for circular SOP output. The solid line represents the equator of the PS.

the incident light was linearly polarized and parallel to the entrance director.[9] Below, this geometrical method is used to obtain the simultaneous optimum conditions for both bistable states in a RBTN structure by consideration of a general incident polarization angle.

Suppose that the entrance director is at angle 0° and the rear director is at 2φ on the PS. The incident polarization angle with respect to the direction of the entrance director is α on the PS ($\alpha/2$ in real space).

First, the circular SOP output conditions for an arbitrary linear incident light for the first state (the twisted angle is φ) are deduced by use of the PS method. As shown in Fig. 1, the entrance director is along the S_1 axis. The incident SOP (point A) makes an angle α with respect to the S_1 axis. According to the rolling-cone model, as the cone's axis ON rotates about the polar axis by an angle 2φ, point A rotates about the ON axis by and angle Φ, as defined in Eq. (2). Two conditions are required for point A to reach the circular polarization state (point L in Fig. 1): First, the distance of points A and L from the ON axis must be the same; second, the cone must rotate by a specific angle along the equator.

The first requirement for the circular SOP output can be written as $LC = AC$. Figure 1 shows that $LC = \cos \omega$ and $AC = (AB^2 + BC^2)^{1/2}$, where $AB = \sin \alpha$, and $BC = OB \sin \omega = \cos \alpha \sin \omega$. Therefore the first requirement is that $\sin^2 \omega = \cos^2 \alpha / (1 + \cos^2 \alpha)$. The second requirement can be deduced by use of Fig. 1(d). The angle that the cone rotates is determined by $2\varphi/r = 2\varphi/\sin \omega$, where $r = \sin \omega$ is the radius of the cone's base. As Fig. 1(d) shows, this angle should be equal to $2n\pi - \beta$ when $0° < \alpha < 90°$. Therefore the second requirement is that $2\varphi = (2n\pi - \beta)\sin \omega$, where β can be defined from the triangle LCA, which is $\cos \beta = -\tan^2 \omega$. For the other range of α, one can obtain similar results by following the same procedures. In more-explicit form, the general

conditions for the circular SOP output can be written as follows:

For $0° < \alpha < 90°$ and $-180° < \alpha < -90°$,

$$\varphi = [(n + 1)\pi - \cos^{-1}(-\cos^2 \alpha)/2]\cos \alpha$$
$$/(1 + \cos^2 \alpha)^{1/2},$$

$$d\Delta n = \lambda \varphi / (\pi \cos \alpha), \qquad (3a)$$

and for $90° < \alpha < 180°$ and $-90° < \alpha < 0°$,

$$\varphi = [n\pi + \cos^{-1}(-\cos^2 \alpha)/2]\cos \alpha$$
$$/(1 + \cos^2 \alpha)^{1/2},$$

$$d\Delta n = \lambda \varphi / (\pi \cos \alpha), \qquad (3b)$$

where $n = 0, 1, 2, \ldots$

Equations (3) can be used to yield the incident polarization angle α, the optimum twist angle φ, and the birefringence $d\Delta n$.

The linear SOP output condition of the second state (the twisted angle is $\varphi' = \varphi \pm 2\pi$) can be deduced in a similar manner. As Fig. 2 illustrates, there are two instances in which the output SOP can be linear. The first instance, shown in Fig. 2(a), occurs when a cone rotates by an angle $2m\pi$. The other instance, shown in Fig. 2(b), occurs when the cone's total rotation angle is $2m\pi + 2\chi$. According to Eq. (2), we have

$$(\pi^2 d^2 \Delta n^2 / \lambda^2 + \varphi'^2)^{1/2} = m\pi \qquad (4)$$

or

$$(\pi^2 d^2 \Delta n^2 / \lambda^2 + \varphi'^2)^{1/2} = m\pi + \chi, \qquad (5)$$

where $\tan \chi = AB/BC = \tan \alpha / \sin \omega'$ and $\tan \omega' = \lambda \varphi' / \pi d \Delta n$; $\varphi' = \varphi \pm 2\pi$ is the twist angle for the second state. Equations (4) and (5) provide the linear SOP output conditions for the second state.

Equations (3)–(5) provide the optimum conditions that can simultaneously optimize both bistable states in a RBTN structure. These analytical solutions can be used to find the actual optimum conditions for α, φ, and $d\Delta n$. The results are shown in Table 1 and Fig. 3. In Fig. 3 the solid circles represent the conditions that satisfy Eqs. (3). Among these conditions, those that satisfy Eq. (4) or (5) are represented by squares. Each square
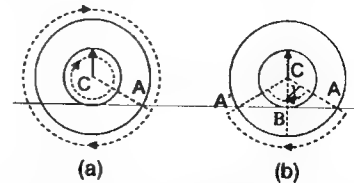

Fig. 2. Linear SOP output conditions: (a) Total rotation angle $2m\pi$; (b) total rotation angle $2m\pi + 2\chi$.

Table 1. Optimum Conditions for the RBTN Structure

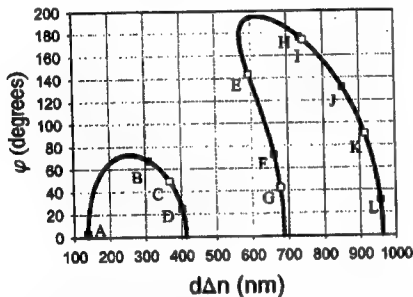|	Polarizer Angles $\alpha/2(°)$		φ 1st State (°)	φ 2nd State (°)	$d\Delta n$(nm)
A	46.65,	−43.35	2.59	−357.41	137.6
B	24.25,	−67.75	67.38	−292.62	310.69
C	32.95,	−57.05	49.22	409.22	368.31
D	39.6,	−50.4	24.68	−335.32	402.4
E	68.85,	−21.15	143.8	503.8	593
F	54.75,	−35.25	72.26	−287.74	661.4
G	50.55,	−39.45	42.74	402.74	678.29
H	21.45,	−68.55	176.56	−183.44	736.46
I	22.25,	−67.75	174.04	534.04	745.57
J	30.9,	−59.1	131.83	−228.17	852.4
K	36.3,	−53.7	90	450	914.6
L	42.15,	−47.85	31.1	−328.9	956.93

Fig. 3. Optimum conditions for the RBTN structure. The solid circles are the optimum conditions for perpendicular SOP output. The squares are the optimum conditions for both of the bistable states. The open squares indicate that the other state has a twisted angle $\varphi + 2\pi$; the filled squares indicate that the other state has a twisted angle $\varphi - 2\pi$.

in Fig. 3 corresponds to a unique condition specified by α, φ, and $d\Delta n$ that can simultaneously optimize both bistable states. These optimum conditions are summarized in Table 1. As Table 1 shows, there are two incident polarization angles for each mode, and in real space the difference between these two angles is 90°. This degeneracy arises because there are two orthogonal linear SOP [A and A′ in Fig. 1(a)] that have the same rotation properties with respect to the cone's axis.

According to Eqs. (3), the required twisted angle φ has no wavelength dependence, whereas the bire-

fringence $d\Delta n$ is proportional to the wavelength λ. Therefore, for those conditions with a higher $d\Delta n$, the wavelength dependence is stronger. Figure 3 shows the first two branches of the optimum conditions, which are the solutions for Eqs. (3) when n is set equal to 0 and 1. One can obtain the higher branches by setting n equal to higher values, but these solutions have high birefringence $d\Delta n$, and therefore they are not attractive owing to the large wavelength dependence. Those in the first branch (modes A, B, C, and D in Table 1) are preferred because of their low $d\Delta n$.

In conclusion, we have introduced a geometrical method, the Poincaré sphere method, to obtain the simultaneous optimum conditions for both bistable states for a RBTN structure. With this method, the optimum conditions can be obtained in analytical forms without a complex numerical calculation. The PS method also provides a clear visualization and a better understanding of these operation modes.

References

1. D. W. Berreman and W. R. Heffner, Appl. Phys. Lett. **37**, 1 (1980).
2. D. W. Berreman and W. R. Heffner, J. Appl. Phys. **52**, 3032 (1981).
3. T. Tanaka, Y. Sato, A. Inoue, Y. Momose, H. Nomura, and S. Iino, in *Proceedings of Asia Display '95* (Society for Information Display, San Jose, Calif., 1995), p. 259.
4. Z. L. Xie and H. S. Kwok, Jpn. J. Appl. Phys. **37**, 2572 (1998).
5. Y. J. Kim, Z. Zhuang, and J. S. Patel, in *Proceedings of SID '99* (Society for Information Display, San Jose, Calif., 1999), p. 866.
6. H. S. Kwok, J. Appl. Phys. **80**, 3687 (1996).
7. R. C. Jones, J. Opt. Soc. Am. **31**, 488 (1941).
8. N. Vansteenkiste, P. Vignolo, and A. Aspect, J. Opt. Soc. Am. A **10**, 2240 (1993).
9. S. W. Suh, Z. Zhuang, and J. S. Patel, in *Proceedings of SID '98* (Society for Information Display, San Jose, Calif., 1998).
10. H. Poincaré, in *Theorie Mathematique de la Lumiere II*, G. Carre, ed. (Gauthier-Villars, Paris, 1892), pp. 275–306.
11. J. E. Bigelow and R. A. Kashnow, Appl. Opt. **16**, 2090 (1977).

Optimized configuration for reflective bistable twisted nematic displays

Zhizhong Zhuang,[a] Young Jin Kim, and J. S. Patel
*Department of Physics and Department of Electrical Engineering, Pennsylvania State University,
University Park, Pennsylvania 16802*

In this letter, we experimentally verify the operation of a single-polarizer reflective bistable twisted nematic (BTN) liquid-crystal display using an optimized geometry. Based on the polarization optimization using the Poincaré sphere representation, several optimized operating modes, which can simultaneously optimize both bistable states, are possible. One of these optimized configurations, the 67.38° and −292.62° twisted bistable states with 310.69 nm birefringence and a 24.25° incident polarization angle, is studied in detail. The evolution of the state of polarization of light passing through this reflective BTN structure is numerically studied, and the electro-optic property of the reflective BTN structure is experimentally demonstrated. Our results show that, using these optimum configurations, a high-contrast display is possible. © *1999 American Institute of Physics.* [S0003-6951(99)02035-5]

Reflective liquid-crystal displays (LCDs) with a single polarizer are attractive for many display applications, particularly in those applications that require low-power consumption and high brightness. For reflective displays that use two polarizers, the overall efficiency is reduced by the low brightness that results from the color filter and the driving elements like thin-film transistors. Moreover, the parallax from the substrate further reduces the quality of the display, especially when it is used with a color filter. Therefore, single-polarizer configurations are preferred in reflective displays. To improve the contrast ratio and the switching time, various liquid-crystal (LC) modes that use a single-polarizer reflective configuration have been investigated.[1,2]

Recently, there has been considerable interest in the bistable twisted nematic (BTN) LCD since it offers power-off memory and makes the matrix-addressed liquid-crystal displays with a large number of elements possible. Since the BTN device has to be switched between two LC configurations, the two configurations have to be topologically equivalent if they are to be driven from the same initial state. This requires that, for a chosen boundary condition, the twists in the two bistable states have to differ by an integral multiple of 2π. When a high electric field is initially applied to a BTN structure and then switched off, the field-driven state relaxes into one of the two possible states: the φ-twisted state or the $(\varphi \pm 2\pi)$-twisted state, where φ is the twisted angle. Transmissive-mode BTN device using two polarizers were first proposed by Berreman in the early 1980s,[3,4] and recently a practical electro-optic device that shows a high contrast and fast switching characteristics has been demonstrated.[5]

There have been efforts to combine the advantages of the BTN and the reflective displays with a single polarizer.[6,7] In these works, the optimizations were numerically performed, and the conditions for the maximum contrast were suggested. Although higher contrast was obtained by these methods, the optimization principles were not clearly understood. In a recent paper,[8] we demonstrated that the optimum

conditions for a reflective BTN display can be obtained in analytical forms using the Poincaré sphere method. Several optimum conditions that can simultaneously optimize both bistable states are deduced using these analytical solutions.

Since the BTN cell is switching between two bistable twisted states, the optimization for the reflective mode should satisfy two requirements. We assume that the incident light is arbitrary linearly polarized. For one state (φ twisted), the state of polarization (SOP) of the reflected light should be linear and orthogonal to that of the incident light. For the other state [$(\varphi \pm 2\pi)$ twisted], the SOP of the reflected light should be identical to that of the incident light. We calculated the optimum conditions using the Poincaré sphere method. Three cell parameters, $d\Delta n$ (birefringence), φ (twisted angle), and α (incident polarization angle), were adjusted for the calculations. The optimized configurations are summarized in Table I. Among these conditions, those with larger $d\Delta n$ (modes E–L in Table I) are not attractive due to the large wavelength dependence. Therefore, for practical applications, we examined condition B stated in Table I, where the angle of the front polarizer is 24.25° and the birefringence of the cell is 310.69 nm. The twist angle is 67.38° for one state, and −292.62° for the other state. The wavelength of the incident light is assumed to be 550 nm. In this

TABLE I. Optimum conditions for the RBTN display.

Polarization angle $\alpha/2$ (°)	φ for the 1st state (°)	φ for the 2nd state (°)	$(d\Delta)$ (nm)
A	46.65, −43.35	2.59	−357.41	137.6
B	24.25, −67.75	67.38	−292.62	310.69
C	32.95, −57.05	49.22	409.22	368.31
D	39.6, −50.4	24.68	−335.32	402.4
E	68.85, −21.15	143.8	503.8	593
F	54.75, −35.25	72.26	−287.74	661.4
G	50.55, −39.45	42.74	402.74	678.29
H	21.45, −68.55	176.56	−183.44	736.46
I	22.25, −67.75	174.04	534.04	745.57
I	30.9, −59.1	131.83	−228.17	852.4
K	36.3, −53.7	90	450	914.6
L	42.15, −47.85	31.1	−328.9	956.93

[a] Electronic mail: zxz109@psu.edu

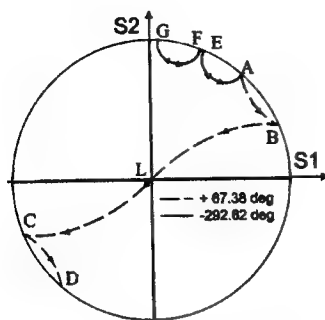Appl. Phys. Lett., Vol. 75, No. 9, 30 August 1999

Zhuang, Kim, and Patel

FIG. 1. Numerical results for the SOP evolutions inside the cell are shown on the Poincaré sphere. The solid and dashed lines represent the twist of 67.38° and −292.62°, respectively. The reflected output polarization is orthogonal to the input polarization for one state and identical for the other state.
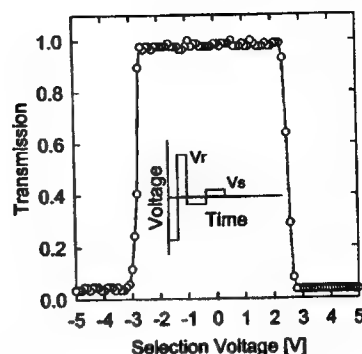

FIG. 2. Experimental results for the reflected light intensity as a function of a selection voltage in a reflective mode with a single polarizer. The driving voltage wave form consists of the reset and selection signals. The dark and bright states are obtained in the 67.38° and −292.62° twisted states, respectively.

letter, we provide a detailed study of this optimized configuration. The evolutions of the state of polarization of light are numerically studied, and the electrically switching between the dark and bright states are experimentally demonstrated.

In order to illustrate the operating principle for this optimized configuration (mode B in Table I), it is instructive to examine the evolutions of the SOP for both bistable states in the Poincaré sphere representation. For both bistable states, the LC directors are uniformly twisted. A perfect mirror was assumed to be placed on the back substrate of the cell. For numerically calculating the optical properties, the BTN cell is divided into 100 equally thick homogeneous plates. The Stokes parameter of light that emerges from each plate can be calculated using the Mueller matrix. The calculation principle has been described in our previous work.[7] The evolutions of the SOP for normal incident light are shown in the S_1-S_2 projection plane of the Poincaré sphere in Fig. 1. The dashed and solid lines represent the projection of SOP evolution for the states of the 67.38° twist and the −292.62° twist, respectively. For the less-twisted state, the SOP of light is launched at point A on the Poincaré sphere, which is at 48.5° (twice the incident polarization angle) with respect to the S_1 axis. During a single pass, it first reaches a linearly polarized state (point B) at the middle of the cell and then reaches the circular polarized state L at the mirror. When the light is reflected from the mirror and passes through the cell in the opposite direction, the SOP follows an orthogonal path. Each of the points on the reflective trajectory are orthogonal to the corresponding points on the incident trajectory. The SOP goes from point L (circularly polarized state) to point C (linearly polarized state), and it then emerges with polarization state D, which is orthogonal to the initial polarization state A. This configuration gives a dark state for the chosen wavelength. For the higher-twisted state, the incident SOP is launched at the same point A. For a single pass, the SOP first becomes linearly polarized (points E and F) inside the cell and then emerges with linearly polarized state G at the mirror. When reflected from the mirror, the SOP returns to the initial linearly polarized state A along the same path, but in the opposite direction. This configuration gives a bright state for the same given wavelength.

It is clearly shown in Fig. 1 that mode B in Table I is

optimized in terms of the SOP. For the two bistable states, the output SOP is perpendicular to the incident for the less-twisted state (dark state) and parallel for the higher-twisted state (bright state). These two states can be electrically switched by a specially shaped driving wave form, as shown in the inset of Fig. 2. The driving wave form consists of a reset signal and a selection signal. A reset voltage V_r was initially applied to the cell in order to orient the LC molecules perpendicular to the cell surface. At a high reset voltage, the LC directors are aligned perpendicular to the surface of the cell and reach a vertical state. Since the vertical state is topologically equivalent to the two bistable twisted planar states, it can be continuously transformed into one of the two bistable twisted states.[9] The two bistable states have the same energy and are equally probable to be transformed to the vertical state. When the reset pulse is suddenly switched off, the LC molecules relax to the planar state due to the elastic property. In the planar state, the LC directors lie in a plane parallel to the cell surface. The state selection is made possible due to the presence of the backflow,[10] a process that occurs during the switching process. The backflow effect can be controlled by the magnitude of the selection voltage for a fixed reset pulse. For a smaller value of the selection voltage, the backflow is larger, and the midplane director chooses the more-twisted state after the selection pulse ceases. On the other hand, the application of larger selection voltage results in a smaller backflow and the midplane director chooses the less-twisted state after the selection pulse ceases. With the proper combination of the reset and selection voltage, the vertical state can be transformed into the 67°-twisted or the −293°-twisted planar state.

In the following, we describe the sample fabrication procedure, followed by the experimental results. The BTN cell was made using indium–tin–oxide (ITO) glass substrates. To promote planar alignment, the polyamide (PI) of AL-1051 (Japan Synthetic Rubber Co.) was coated on both substrates. Several cells were made with different cell gaps, in which the pitch of the LC p was fixed at −14.8 μm. Bistable switching was not observed when the cell thickness d was 4.7 or 5.2 μm, but switching was observed when the cell thickness was between 4.9 and 5.0 μm. Based on these results, the required $|d/p|$ for bistable switching can be

Appl. Phys. Lett., Vol. 75, No. 9, 30 August 1999

Zhuang, Kim, and Patel

roughly estimated to be between 0.324 and 0.345. Ideally, the $|d/p|$ for mode B should be 0.313. At this $|d/p|$, the twist elastic energies of the two twisted states are the same. The shift of d/p from the ideal value has been observed previously.[11] One possible reason for this shift could be the presence of a surface pretilt angle. In the presence of a surface pretilt, there exist additional splay and bend deformations in the higher-twisted state, and the total elastic energy for the higher-twisted state is increased. For the two twisted states to be equivalent in energy, the elastic energy of the less-twisted state should be increased, which can be achieved by adding more twist energy to the less-twisted state. Therefore, $|d/p|$ could be larger than the ideal value.

To demonstrate the bistable switching of mode B in Table I, we chose a cell which has the closest configuration to that specified in Table I for mode B. The cell gap was maintained by glass spacers of 5.0 μm. Chiral dopant was introduced into the LC with the doping concentration adjusted to give $d/p = -0.338$ (left handed). The LC and the chiral dopant used were ZLI-4119 ($\Delta n = 0.0603$) and S-811 from E. Merck, respectively. The widths of the reset and the selection signals are 10 and 20 ms, respectively. The magnitude of the reset voltage was fixed at 30 V. This high voltage ensures that the LC directors are in the vertical state after the reset voltage. The frame frequency of the driving wave form was 1 Hz. A mirror was place under the cell and the reflected light intensity through the BTN cell was measured using a microscope. The wavelength of the incident light was at about 550 nm, obtained by a narrow-band filter and a broad-band light source. Figure 2 shows the experimental results of reflected intensity as a function of the selection voltage. The 67°-twisted (dark) and 294°-twisted (bright) states are produced under relatively high- and low-selection voltages, respectively. A sharp transition between dark and bright states was observed at about ±3 V. The contrast was measured to be around 29. The BTN cell exhibits achromatic characteristics, fast switching (<10 ms). Because of the planar switching, it also has a wider viewing angle. These properties show that mode B is sufficient for the applications of reflective-type displays and gives better electro-optic characteristics than any other mode in a single-polarizer configuration.

In this study, we have experimentally examined an optimized geometry for a bistable twisted nematic configuration which we suggested theoretically in a previous paper. While only the on-axis transmission were measured in these experiments, our preliminary measurements show that these devices have better viewing angle properties compared to the ordinary twisted nematic liquid-crystal displays. This is an expected result because of the lack of out-of-plane tilting in both bistable states. The experiment results show that it is indeed possible to obtain a high-contrast device using a single polarizer operating in a bistable configuration.

[1] S.-T. Wu and C.-S. Wu, Appl. Phys. Lett. **68**, 1455 (1996).
[2] T. Uchida, T. Nakayama, T. Miyashita, M. Suzuki, and T. Ishinabe, Proc. Asia Display **95**, 599 (1995).
[3] D. W. Berreman and W. R. Heffner, Appl. Phys. Lett. **37**, 1 (1980).
[4] D. W. Berreman and W. R. Heffner, J. Appl. Phys. **52**, 3032 (1981).
[5] T. Tanaka, Y. Sato, A. Inoue, Y. Momose, H. Nomura, and S. Iino, Proc. Asia Display **95**, 259 (1995).
[6] Z. L. Xie and H. S. Kwok, Jpn. J. Appl. Phys., Part 1 **37**, 2572 (1998).
[7] Y. J. Kim, Z. Zhuang, and J. S. Patel, SID **99**, 866 (1999).
[8] Z. Zhuang, Y. J. Kim, and J. S. Patel, Opt. Lett. **24**, 1166 (1999).
[9] J. Cheng, R. N. Thurston, and D. W. Berreman, J. Appl. Phys. **52**, 2756 (1981).
[10] D. W. Berreman, J. Appl. Phys. **46**, 3746 (1975).
[11] Y. J. Kim, S.-M. Park, I. Lee, S.-W. Suh, and S.-D. Lee, Proc. Euro Display **96**, 337 (1996).

Arbitrary to arbitrary polarization controller using nematic liquid crystals

Zhizhong Zhuang*, Seong-Woo Suh and J. S. Patel

Departments of Physics and Electrical Engineering

The Pennsylvania State University, University Park, PA 16802

ABSTRACT

In the study of lightwave systems, polarization related effects have become important considerations. This has led many researchers to focus on developing practical means of controlling the state of polarization of light. This paper demonstrates a polarization controller, consisting of a stack of three homogeneous nematic liquid crystal cells, that is capable of changing any state of polarization of light from one arbitrary state to another. By adjusting the voltages applied across each cell, the state of polarization can be controlled. The mathematical algorithm and the principles of this polarization controller are developed in the framework of the Stokes parameters, allowing an easy visualization and better understandings using Poincare sphere representation. In addition to providing the transformation functions for converting an arbitrary input polarization state to any output state, this paper describes the experiments that were carried out to illustrate and confirm the arbitrary polarization transformations.

Keywords: Polarization controller, Nematic liquid crystals, Stokes parameters and Poincare Sphere.

1. INTRODUCTION

Commercial optical receivers only detect optical power; they are not sensitive to polarization. For the most part this has relegated polarization effects, although recognized as an essential feature of the light field, to a minor role in lightwave systems. With the advance of optical amplifier technology in recent years, however, optical length has increased dramatically. As a result, polarization dependent loss (PDL) and polarization mode dispersion (PMD) can accumulate. PDL, PMD and other small effects are now regarded as important considerations in lightwave systems.[1] Another and equally significant obstacle to optical coherent systems is the polarization change, sometimes referred to as polarization drift, which is often produced by polarization dependent components, including fibers, optical switches and waveguides. It is essential, in many systems, to change or restore the resulting state of polarization (SOP) to the desired SOP.

A number of researchers have attempted to develop a viable method of achieving polarization transformations. For the most part, their studies have focused on the use of traditional mechanical squeezing of fibers[2], LiNbO$_3$ waveguides,[Error! Reference source not found.,3] Farraday effect,[4] rotating wave plates and electro-optic crystals.[5,6] However, since these methods require a high operating voltage and often suffer from mechanical fatigue, each has proved inconvenient.

A device based on liquid crystal technology has many advantages. Even a relatively small electric field can change the birefringence of the liquid crystal significantly. One study, completed by Rumbaugh, Jones and Casperson,[7] explored the use of liquid crystals to control the SOP. Similar to other studies, their work was limited to the incident light with a specific linearly polarization state. Rumbaugh *et, al* intended to use the liquid crystal device in a coherent communication system. To prevent signal fading, they focused on developing a means to compensate the SOP of the local oscillator to match that of the signal. The local oscillator is linearly polarized at a specific direction. However, the input polarization state is usually arbitrary in a lightwave system, since the amount and direction of birefringence induced by the thermal or mechanical fluctuations exhibit in random fashion. Therefore, there is a need to develop a device that has the capacity to control arbitrary polarization states.

This paper describes a three liquid crystal cell structure that can achieve an arbitrary polarization transformation. By adjusting the operating voltages of the liquid crystal cells, the SOP is controlled. Clearly, the input and target SOP must be

---

* Author to whom correspondence should be addressed; Email: zxz109@psu.edu

known to achieve this SOP transformation. Once the Stokes parameters[8] of these states are determined, the operation voltage for each liquid crystal cells can be set , and the desired SOP transformation can be achieved.

In the following, we begin with the description of the configuration of the device, followed by calculation of the Stokes parameters of the input and the output light fields. We show mathematically, that this arbitrary transformation can be done using three nematic liquid crystal cells such that the relative orientations of these three cells are 45⁰ with respect to one another. After that, the predication of the theory is confirmed by experimental results.
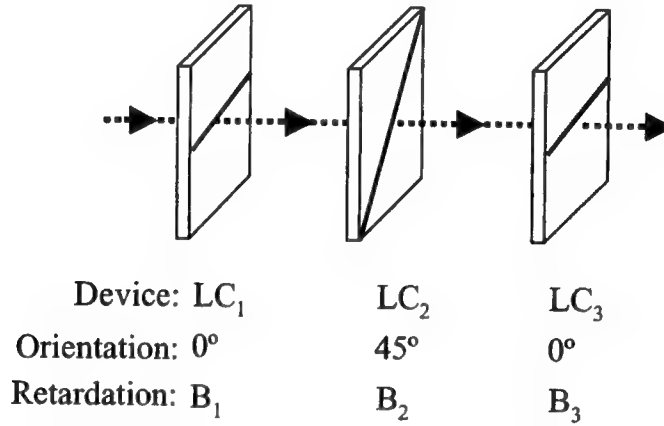

Device: LC_1 LC_2 LC_3

Orientation: 0°   45°   0°

Retardation: B_1 B_2 B_3

Figure.1: The configuration of arbitrary-arbitrary SOP controller.

2. STOKES PARAMETERS CALCULATION

Figure 1 shows the configuration of the arbitrary to arbitrary polarization controller. This polarization controller is made up of three homogenous nematic liquid crystal cells. Each liquid crystal slab has a slow axes that are at 0, 45⁰ and 0⁰ respectively. A series of linear birefringent elements (such as homogeneous nematic liquid crystals slab in our case) are described by a series of rotations on the Poincare sphere[9] with respect to axes that lie on the equatorial plane[10]. Thus, as shown in figure 2, the three cells in our device correspond to three axes, which are HV, PQ and HV respectively. By changing the applied voltages, the amount of rotations with respect to each axis can be controlled to achieve the arbitrary to
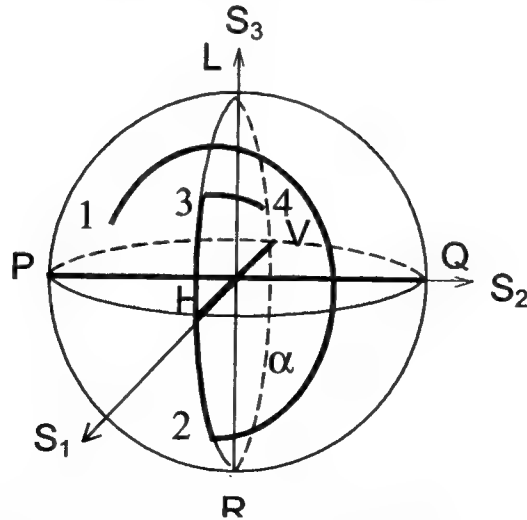

Figure.2: Visualization of the arbitrary-arbitrary SOP mapping algorithms on Poincare sphere. V: vertical linear, H: horizontal linear, P: +45° linear, Q: -45° linear. L: left-handed circular, R: right-handed circular

68

arbitrary transformation.

Suppose the incident light field is represented by:

$$\begin{pmatrix} E_x^i \\ E_y^i \end{pmatrix} = \begin{pmatrix} \cos\alpha \\ \sin\alpha\,\exp(i\delta) \end{pmatrix}. \tag{1}$$

This can also be represented by Stokes parameters as:

$$\begin{aligned}
S_1^i &= E_x^i E_x^{i*} - E_y^i E_y^{i*} = \cos 2\alpha \\
S_2^i &= E_x^i E_y^{i*} + E_y^i E_x^{i*} = \sin 2\alpha \cos\delta \\
S_3^i &= i\left(E_x^i E_y^{i*} - E_y^i E_x^{i*} \right) = \sin 2\alpha \sin\delta
\end{aligned} \qquad . \tag{2}$$

The output light field emerging from a stack of three liquid crystal cells is given by:

$$\begin{pmatrix} E_x^o \\ E_y^o \end{pmatrix} = J(B_3)R(-\pi/4)J(B_2)R(\pi/4)J(B_1)\begin{pmatrix} E_x^i \\ E_y^i \end{pmatrix}, \tag{3}$$

were $J(B_j)$ is the Jones matrix for retarder with retardation B_j, $R(\theta)$ is the rotation matrix with rotating angle θ.

Then, the Stokes parameters of the output light can be calculated as follows,

$$\begin{aligned}
S_1^o &= \cos B_2 \cos 2\alpha + \sin B_2 \sin(B_1 - \delta)\sin 2\alpha \\
S_2^o &= \sin B_3 \sin B_2 \cos 2\alpha + \cos B_3 \sin 2\alpha \cos(B_1 - \delta) - \sin B_3 \cos B_2 \sin(B_1 - \delta)\sin 2\alpha \\
S_3^o &= \cos B_3 \sin B_2 \cos 2\alpha - \sin B_3 \sin 2\alpha \cos(B_1 - \delta) - \cos B_3 \cos B_2 \sin(B_1 - \delta)\sin 2\alpha
\end{aligned} \qquad . \tag{4}$$

The final SOP of the light that emerges from the stack structure is given byEq. (4). By using this equation, several different applications can be developed by requiring the birefringence for each cell to satisfy one or a number of specific conditions. Discussed below are the conditions required for arbitrary polarization.

3. OPERATION PRINCIPLES

If the voltage applied to the first cell is adjusted such that the retardation B_1 satisfy

$$B_1 - \delta = \pi/2, \tag{5}$$

then Eq. (4) can be reduced as following:

$$\begin{aligned}
S_1^o &= \cos(B_2 - 2\alpha) \\
S_2^o &= \sin B_3 \sin(B_2 - 2\alpha) \\
S_3^o &= \cos B_3 \sin(B_2 - 2\alpha)
\end{aligned} \qquad . \tag{6}$$

The above equation has the same form as the unit sphere co-ordinates with azimuth and polar angle $(B_2-2\alpha)$ and B_3. Therefore, the Stokes vector defined by Eq. (6) can span the entire surface on Poincare sphere, if B_2 and B_3 are changed in a 2π range. This confirms that all points on the Poincare sphere are accessible by varying the birefringence, or equivalently, the voltages applied to each liquid crystal cells.

Equation 5, although not a necessary condition, simplifies the discussion for the following reason. For the configuration showed in figure 1, the rotation axes are fixed and they are orthogonal, so in general, it needs three rotations about these two axes to map two arbitrary points on a sphere (figure. 2). However, only two rotations around the axes PQ and HV are needed if the incident SOP is on the circle where S_2 is equal to zero (α in Fig. 2). This can be achieved if B_1 is adjusted to satisfy Eq. (5). If we suppose that Eq. (5) is not satisfied, as shown in Fig. 3, the SOP of light emerge from the first LC cell is not at point 2 where S_2 is equal to zero. Instead of being at point 2, it is at a point off circle α, for example at point 2'. The next cell,

according to Fig. 1, is oriented at 45☐ The SOP will be rotated about the PQ axis as it passes through the second cell, and it therefore can only reach points on the circle γ in Fig. 3. The last cell is oriented at 0 degrees, allowing the SOP to rotate about the HV axis. Figure 3 shows this operation, and demonstrates that it can only reach the SOP between plane aa' and bb'. Those in the shaded area cannot be reached.
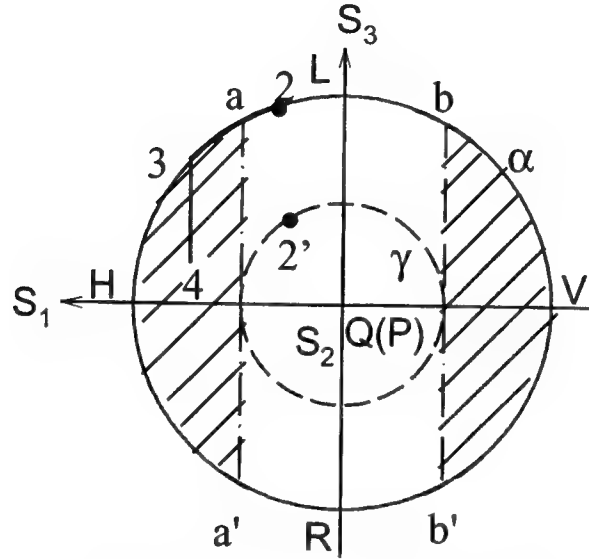

Figure 3: S_1-S_3 projection plane of the rotating operation.

From Fig. 3, for the stack structure of Fig. 1, the only way to ensure the capability that the device can reach an arbitrary SOP is to let point 2' on circle α. In other words, to satisfy Eq. (5), so that the S_2 of the SOP emerges from the first cell is zero.

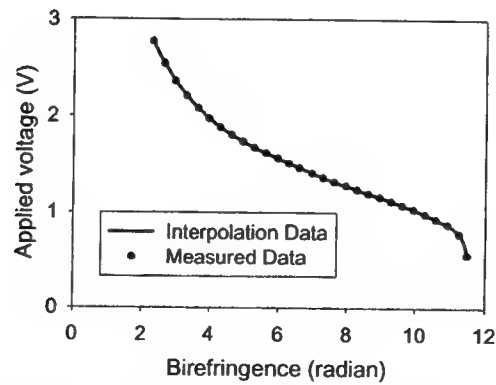
Figure.4: The measured relationship between the applied voltages and the birefringence of liquid crystal cell. The dots represen the measured data; the solid line represents the result from cubicspline interpolation. For clarity, only one tenth of the measured data are shown.

4. TRANSFORMATION FUNCTIONS

The problem of arbitrary transformation from S^i to S^o reduces to calculating the magnitude of the three angles required to rotate about HV, PQ and HV axes. According to equations (2, 5 and 6), the birefringence of these three cells are:

$$B_1 = \pi/2 + \tan^{-1}\left(S_3^i/S_2^i\right) + m\pi$$
$$B_2 = \cos^{-1} S_1^i + \cos^{-1} S_1^o \tag{7}$$
$$B_3 = \tan^{-1}\left(S_2^o/S_3^o\right) + n\pi$$

The additional terms in B_1 and B_3 arise from the fact that the period of B is 2π while the period of the tangent function is π, therefore additional information is required in order to determine the exact value of B_1 and B_3, such as the sign of one of the Stokes parameters. As a result, m and n can be determined as follows: m=1 when $S^i<0$, n=1 when $S_2^o<0$, otherwise, m=n=0.

To control the birefringence, voltages were applied to the cells. It is therefore necessary to accurately determine the relationship between the birefringence and the voltage. In our experiment, this relationship was measured using a HP8509B polarization analyzer. These data were interpolated using cubicspline[11] as shown in figure 4. Any 2□ region of this curve can be used for determining the voltage to birefringence relationship. The □ to 3□ region of the curve was chosen in the experiment described bellow to avoid the high non-linear region.

5. EXPERIMENTAL RESULTS

The validity of this analysis was tested experimentally. In two experiments, an arbitrary initial SOP was transferred to some preset target SOP. The experiments were done using a computer based automatic polarization controlling and measuring system. The Stokes parameters were measured using a HP8509B polarization analyzer using an internal laser source at 1.3□m. The applied voltages of different liquid crystal cells were controlled by a computer and three HP33120A function generators. The liquid crystal cells used in the experiment were fabricated in our laboratory.
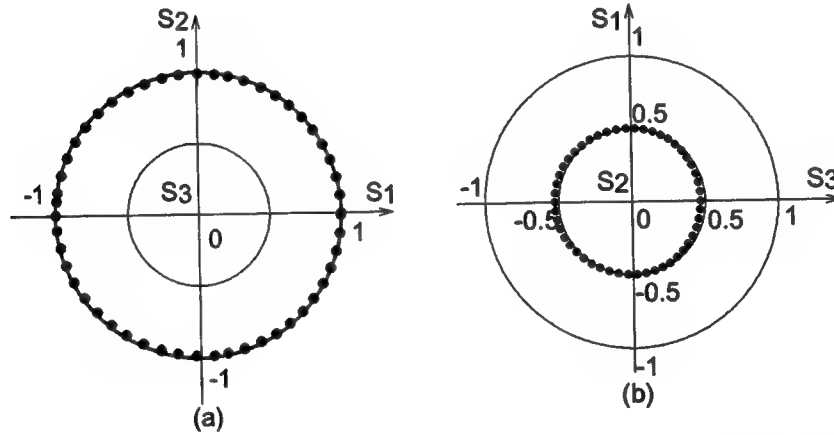

Figure. 5: The experimental results of arbitrary polarization transformation. The initial polarization state is arbitrary chosen as S^i=(-0.61, 0.11,-0.71). The final states are chosen to be two circles: (a): S_3^o=0, (b): S_2^o=0.866. The results are shown in the S_1-S_2 and the S_1-S_3 planes, respectively.

The initial state for both experiments were arbitrary chosen such that S^i =(-0.61, 0.11, -0.71). The first experiment shows that this initial SOP was transferred to SOP on the equatorial plane (i.e. S_3^o=0, S_1^o and S_2^o were continuously changed), as shown in figure 5(a). The second experiment shows that the initial SOP was transferred to SOP on another circle with S_2^o=0.866, while S_1^o and S_3^o were changed continuously, as shown in figure 5(b). In this case, the radius of the projection

circle in the S_1-S_3 plane should equal to 0.5. The experimental results are shown in the S_1-S_2 and the S_1-S_3 projection plane, respectively.

During the experiment, the liquid crystal cells were quite stable if the applied voltages were fixed. The fluctuations were less than one percent for a time period of several minutes. The fluctuation was determined to be the fluctuation of the reflective index of liquid crystal with temperature. No attempt was made to correct the drift for these experiments at room temperature, although it can be reduced by temperature control or applying feedback scheme The birefringence of liquid crystal is very sensitive to the applied voltage, and it appears that the source of any additional error was a product of setting the suitable voltages according to the interpolation results. It is possible that the resulting change can be as large as a few degrees on the Poincare sphere for a change of millivolts applied to the cell. The speed of the transformation is essentially limited by the electro-optical response of nematic liquid crystal materials, which is typically in the order of 10msec.

6. CONCLUSIONS

This paper has proposed using a stack structure of nematic liquid crystal cells as an arbitrary polarization controller. The operating principles of an arbitrary polarization controller have been addressed mathematically by the use of Stokes parameters and visually by the use of a Poincare sphere representation. A computer-based polarization controlling and measuring system has been used to demonstrate the polarization transformation from one arbitrary state to another arbitrary state. Such a device may prove useful in birefringence networks and may be useful in minimizing or controlling the losses and other characteristics commonly encountered with polarization dependent devices in lightwave systems.

ACKNOWLEDGEMENTS

REFERENCES

[1] C. D. Poole and J. Nagel, in *Optical Fiber Telecommunications IIIA*, I. P. Kaminow and T. L. Koch ed. (Academic Press, 1997), pp.114-162.
[2] N. G. Walker and G. R. Walker, J. Lightwave Technol. **8**, 438 (1990).
[3] J. Slaz, At&T Tech. J. **64**, 2153 (1985).
[4] T. Okoshi, Y. H. Cheng and K. Kikuchi, Electron Lett. **21**, 787 (1985).
[5] T. Okoshi, J. Lightwave Technol. **3**, 1232 (1985).
[6] T. Imai, K. Nosu and H. Yamaguchi, Electron Lett. **21**, 52 (1985).
[7] S. H. Rumbaugh, M. D. Jones and L. W. casperson, J. LightwaveTechnol. **8**, 459 (1990)
[8] G. G. Stokes, Trans. Cambridge. Phil. Soc. **9**, 309 (1852).
[9] H. Poincare, in *Theorie Mathematique de la Lumiere II*, George Carre ed. (Paris, 1892), p. 275
[10] J. E. Bieglow and R. A. Kashnow, Appl. Opt. **16**, 2090 (1977).
[11] William H. Press, Brain P.Flannery, Saul A. Teukolsky and Wiliam T. Vetterling, *Numerical Recipes in C*, (Cambridge, 1988), p.94

Bistable twisted nematic liquid-crystal optical switch

Zhizhong Zhuang,[a] Young Jin Kim, and J. S. Patel
Departments of Physics and Electrical Engineering, Pennsylvania State University, University Park, Pennsylvania 16802

In this letter, we describe a bistable twisted nematic (BTN) liquid-crystal device optimized for use in a fiber optical system. The device configuration is optimized so that the states of polarization for the two bistable states are linear and orthogonal to each other for a linearly polarized input light. This optimization is accomplished by the use of the Poincaré sphere method. Using this method, we obtained the analytical forms of the optimization conditions. Several different optimized conditions are obtained. In order to experimentally explore the use of the BTN structure in optical latching switches, one optimized structure (11.25° and −348.75° twists, $d\Delta n/\lambda = 0.496$) is studied in the infrared region by the measurement of the output state of polarization. The experimental results agree well with our theoretical predictions. This study also suggests that transmissive BTN displays with high contrast are possible by the use of these optimized conditions with nonparallel and noncross polarizer configurations. © *1999 American Institute of Physics.*
[S0003-6951(99)01145-6]

In the past, a variety of electro-optic and mechanical devices have been used to make fiber optical switches. Liquid-crystal materials have been used in fiber optical devices, but most have been attempts to make simple attenuators. If the state of polarization (SOP) is used to produce optical switching, then the SOP output of the two states has to be orthogonal. Although a simple nematic liquid-crystal structure can be used by control of the two voltages to produce the two SOP states, the bistable twisted nematic[1] (BTN) structure is preferred because of the fast response and the bistability that can be used in latching switches. However, for a BTN structure to be used in optical switched, the two bistable states with orthogonal SOP are required in the absence of the field; this is discussed in great detail in this letter.

Since first described by Berreman and Heffner[1] about two decades ago, the BTN liquid-crystal mode has been extensively studied and increasingly used in liquid-crystal displays (LCDs). Low power consumption due to the power-off memory makes the use of the BTN structure very attractive in a matrix-addressed LCD with a large number of elements. Recently, single-polarizer reflective BTN displays have been proposed,[2–4] and experimentally demonstrated.[5] However, utilization of the BTN structure in other areas has been neglected. In this letter, we explore the use of the BTN structure in optical latching switches in the infrared (IR) region by optimizing the output SOP of light.

For the most part, the study of BTN devices has been limited to the 0 and 2π twists and the cross-polarizer structure. There have been a few attempts[6] to obtain the optimized configuration for the transmissive BTN LCD. However, in these efforts optimization was not complete because the structure was optimized for a high contrast ratio. SOP optimization was not considered. To be used in an optical switch, one needs the two field-off bistable states to produce

orthogonal SOP output. In the following, we deduce the exact optimized configurations for the BTN optical switch using the Poincaré sphere[7] (PS) method and experimentally confirm the performance.

The PS method has been used to study the optical properties of a general twisted nematic structure[8,9] and to examine the optimization of the reflective BTN LCD.[4,5] In this letter, the PS method is applied to obtain the optimized conditions for BTN optical switches.

Optimization requires that the output SOP is both linear and perpendicular to each other for the two bistable states. As shown in Fig. 1(a), we assume the entrance director (C1) of the BTN cell is at 0°. The front polarizer (A) is at angle $\alpha/2$ (α on the PS), while the rear polarizer is at angle $\beta/2$. We note that the angle between the polarizer and the analyzer $(\alpha+\beta)$ may not be an integer multiplier of 90°, as is commonly assumed for display applications. The two twisted states have uniform twists of φ and $\varphi\pm2\pi$, respectively, so the rear director (C2) is at an angle 2φ with respect to C1 on the PS. There are two cases[4] (A1 and A2 in Fig. 1) when the output SOP is linear. The angle between these two output linear polarized states is 2α on the PS (α in the real space).
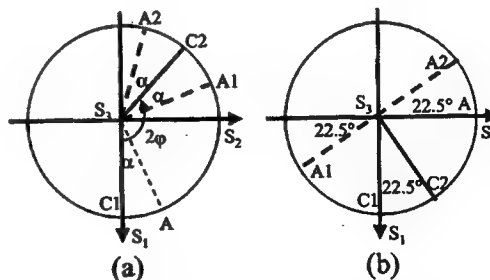

(a)   (b)

FIG. 1. S_1-S_2 projection plane of the Poincaré sphere for the linear SOP output. C1 and C2 are the directions of the entrance and rear directors, respectively. A is the orientation of the front polarizer. A1 and A2 are two cases where the output SOP is linear. (a) General case, (b) mode A in Table I.
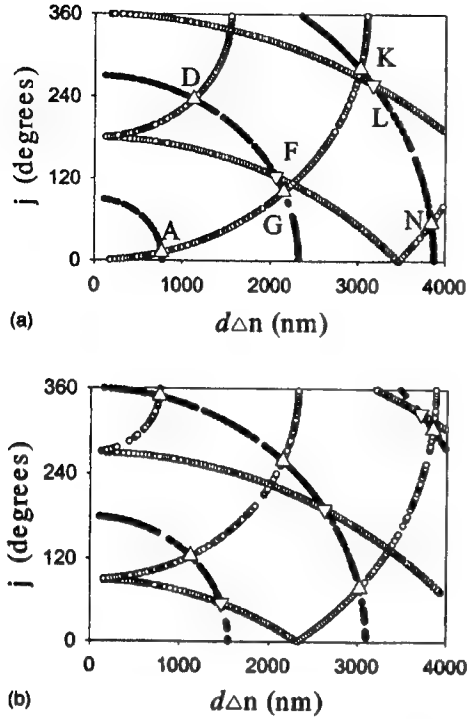
[a]Electronic mail: zxz109@psu.edu

(a)

(b)

FIG. 2. Optimized conditions for a BTN optical switch. (a) ● The φ-twisted states that satisfy Eq. (1b), □ The $(\varphi+2\pi)$-twisted states that satisfy Eq. (1a), and ○ the $(\varphi-2\pi)$-twisted states that satisfy Eq. (1a). (b) ● The φ-twisted states that satisfy Eq. (1a), □ the $(\varphi+2\pi)$-twisted states that satisfy Eq. (1b), and ○ the $(\varphi-2\pi)$-twisted states that satisfy Eq. (1b). △ and ▽ The optimized conditions; the twisted angles for the other states are $\varphi-2\pi$ and $\varphi+2\pi$, respectively. For clarity, only one tenth of the calculated data are shown.

As illustrated in Fig. 1(b), the orthogonality of these two output linear SOP requires that $\alpha=\pm\pi/2$. Therefore the incident light should be linearly polarized at $\pm45°$ with respect to the entrance director. According to the results of our previous work,[4] the conditions for orthogonal linear SOP output can be expressed as follows:

$$\sqrt{(\pi d\Delta n/\lambda)^2+\varphi^2}=m\pi, \tag{1a}$$

or

$$\sqrt{(\pi d\Delta n/\lambda)^2+\varphi^2}=m\pi\pm\pi/2, \tag{1b}$$

where λ is the wavelength, $d\Delta n$ is the birefringence, and m is a positive integer.

The optimized configurations can be obtained by letting the φ-twist state satisfy one of these conditions [Eq. (1a) or (1b)] and the $(\varphi\pm2\pi)$-twist state satisfy the other. For the case of the twisted angle φ in the $0-2\pi$ range, the results are shown in Fig. 2 and summarized in Table I. Each mode listed in Table I gives a set of twisted angles and birefringence that can yield the orthogonal linear SOP output for a specific wavelength if the incident light is linearly polarized at $\pm45°$. In order to complete the optical switching, the rear polarizer should be oriented along one of the output linear polarization directions, i.e., $\beta=\pm45°+\varphi$. According to Eq. (1), if φ and $\varphi-2\pi$ satisfy Eq. (1), then $2\pi-\varphi$ and $-\varphi$ also satisfy Eq. (1) with the same $d\Delta n/\lambda$. This is the reason for several pairs in Table I that have the same $d\Delta n/\lambda$ but opposite twisted angles. For φ and $\varphi+2\pi$ type solutions, the twisted angles

TABLE I. Optimized configurations for the BTN optical switches.

| Mode | Twisted angle (deg) | | $d\Delta n/\lambda$ (nm) |
	1st state	2nd state	
A	11.25	−348.75	0.496
B	348.75	−11.25	0.496
C	123.75	−236.25	0.726
D	236.25	−123.75	0.726
E	56.25	416.25	0.95
F	123.75	483.75	1.333
G	101.25	−258.75	1.39
H	258.75	−101.25	1.39
I	191.25	551.25	1.694
J	78.75	−281.25	1.952
K	281.25	−78.75	1.952
L	258.75	618.75	2.045
M	326.25	686.25	2.39
N	56.25	−303.75	2.48
O	303.75	−56.25	2.48

for their corresponding pairs with the same $d\Delta n/\lambda$ ($-2\pi-\varphi$ and $-\varphi$ twisted states) are all negative and outside the $0-2\pi$ range and, therefore, not listed in Table I.

As stated above, we intend to explore the application of the BTN structure as optical switches in the IR region at 1550 nm wavelength. The operation mode we chose is mode A in Table I, because of its small $d\Delta n$, hence it has a small wavelength dependence and a fast switching speed. In order to have a better understanding of this operation mode, the SOP evolution for these two bistable states was calculated numerically. The calculation principle was described in our previous work.[3,5] The results are shown in Fig. 3. As discussed above, the entrance director is along the S_1 axis (0°), while the front polarizer is along the S_2 axis (45° in real space). For the 11.25°-twisted state, because of the low twist angle, the liquid-crystal cell behaves like a linear birefringence plate, which effectively rotates the SOP from the initial point ($S_1=0$, $S_2=1$, $S_3=0$) to A1. For the −348.75°-twisted state, the high twisted medium behaves like an isotropic medium and the SOP is confined to a small region on the PS. A1 and A2 are both on the equator, so they are linearly polarized states. The Stokes parameters[7] of these two states can be easily calculated from Fig. 1(b) or 3: for A1, $S_1=-0.383$, $S_2=-0.924$, and $S_3=0$; for A2, $S_1=0.383$, $S_2=0.924$, and $S_3=0$. The line connecting these two linear states passes through the center of the PS;
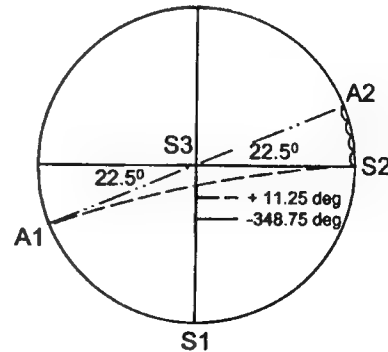

FIG. 3. SOP evolution for the two bistable states of mode A in Table I. The two output SOPs ($A1$ and $A2$) are linear and orthogonal to each other.
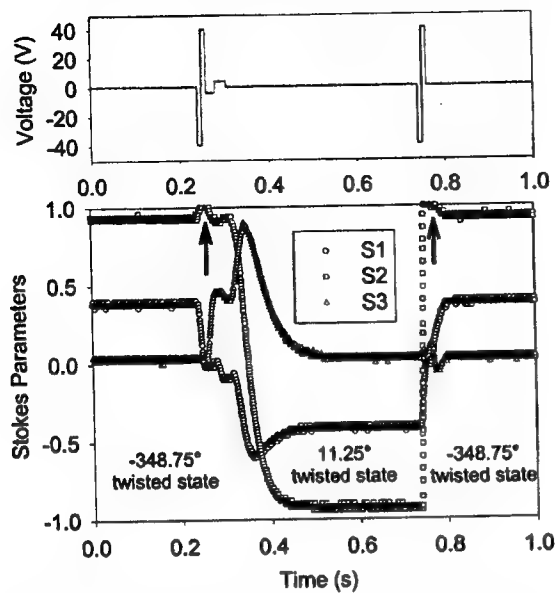
FIG. 4. Driving wave form of the BTN operation (upper part) and the measured Stokes parameters for the emergent light field (lower part).

this indicates that these two states are also orthogonal states. Thus, if the rear polarizer is oriented along A1 ($\beta = -33.75°$) or A2 ($\beta = 56.25°$), the optical switch can be turned on and off by switching between these two bistable states.

It is worth noting that in the optimized structure, when used with polarizers, the polarizer's configuration is neither parallel nor crossed. All the previous studies of the BTN transmissive mode have assumed a parallel-polarizer or a cross-polarizer configuration. Our results show that for a parallel- or cross-polarizer configuration, the SOP may be optimized for one state, but the other state cannot be simultaneously optimized. In order to allow complete extinction and complete transmission, the two polarizers have to be arranged at specific angles, which are neither parallel nor perpendicular. As for mode A, the angle should be 11.25° or $-78.75°$ between the front and rear polarizer to complete the BTN transmissive display or switch.

The validity of the above analysis was tested experimentally by measuring the output SOP for a BTN operated in mode A. The BTN cell was made using indium–tin oxide (ITO) glass substrates coated with polyimide (PI) PI-2555 (Dupont Co.) to promote planar alignment. The upper and lower PI layers were rubbed at angles of 0° and 11.25°, respectively, to produce stable 11.25°-twisted and $-348.75°$-twisted states. The liquid-crystal material we used was ZLI-2293 from E. Merck. The optical anisotropy Δn is about 0.117 at 1550 nm. The chiral dopant (S-811 from E. Merck) was added to the liquid crystal, and the doping concentration was adjusted to give a d/p of around -0.56 (left handed). The cell gap, about 6.6 μm, was maintained by glass spacers. The experiments were conducted with an automatic polarization control and measurement system. The Stokes parameters

of the emergent light field were measured with a Hewlett-Packard HP8509B polarization analyzer using the internal laser source at 1550 nm. A linear polarizer oriented at 45° was placed in front of the BTN cell, and the entrance director of the BTN cell was oriented at 0°. The SOP of the light that emerged from the BTN cell was measured by the polarization analyzer and captured by a Tektronix TDS460A oscilloscope. The driving signal is shown in Fig. 4. The width of the reset and the selection signal are 20 and 40 ms, respectively. The magnitude of the reset voltage was fixed at 40 V. The selection voltages are 4 V for the 11.25°-twisted state and 0 V for the $-348.75°$-twisted state. The dynamics of a similar switching process has been studied by other groups.[10] The SOP measurement results are also shown in Fig. 4. The SOP after the reset pulse is at $S_1 = 0$, $S_2 = 1$, $S_3 = 0$ (indicated by arrows in Fig. 4), which is the same as the incident SOP because the incident light is linearly polarized at 45°. This is because the high reset voltage drove the liquid-crystal director to the homeotropic configuration, thus the SOP remains unchanged as it passes through the cell. After the selection pulse, there are two distinct bistable states: the 11.25°-twisted state, which produced the SOP output A1 (see Figs. 1 and 2) and the $-348.75°$-twisted state, which produced the SOP output A2 (see Figs. 1 and 2). The average Stokes parameters for A1 are $S_1 = -0.39$, $S_2 = -0.92$, and $S_3 = -0.03$, while the average Stokes parameters for A2 are $S_1 = 0.39$, $S_2 = 0.92$, and $S_3 = 0.03$. These two SOPs are the same as those predicated by theory [see Fig. 1(b)]. The extinction ratio was better than 33 dB if the rear polarizer is placed at $-33.75°$ or 56.25°.

In conclusion, we have used the PS method to obtain optimized configurations for the BTN optical switch. Our results indicate that the widely used 0–2π-twisted and cross-polarizer configuration is not an optimal configuration (for BTN operation as optical switches). The analytical forms of the optimization conditions are given, and the specific conditions are obtained. The measurement of the output SOP in the IR region is used to study one of the optimized geometries. The experimental results agree well with the theoretical preditions. These results can be easily extended to the transmissive BTN LCDs.

[1] D. W. Berreman and W. R. Heffner, J. Appl. Phys. **52**, 3032 (1981).
[2] Z. L. Xie and H. S. Kwok, Jpn. J. Appl. Phys., Part 1 **37**, 2572 (1998).
[3] Y. J. Kim, Z. Zhuang, and J. S. Patel, *SID 99 Digest* (Society for Information Display, San Jose, 1999), p. 866.
[4] Z. Zhuang, Y. J. Kim, and J. S. Patel, Opt. Lett. **24**, 1166 (1999).
[5] Z. Zhuang, Y. J. Kim, and J. S. Patel, Appl. Phys. Lett. **75**, 1225 (1999).
[6] H. S. Kwok, T. Z. Qian, Z. L. Xie, and P. Sheng, *SID 97 Digest* (Society for Information Display, San Jose, 1999), p. 89.
[7] E. Collett, *Polarized Light: Fundamentals and Applications* (Dekker, New York, 1992).
[8] J. E. Bieglow and R. A. Kashnow, Appl. Opt. **16**, 2090 (1977).
[9] S. W. Suh, Z. Zhuang, and J. S. Patel, *SID 98 Digest* (Society for Information Display, San Jose, 1999), p. 997.
[10] J. Li, C. D. Hoke, and P. J. Bos, Jpn. J. Appl. Phys., Part 1 **35**, 706 (1996).

Behavior of cholesteric liquid crystals in a Fabry–Perot cavity

Zhizhong Zhuang and J. S. Patel

Departments of Physics and Electrical Engineering, Pennsylvania State University, University Park, Pennsylvania 16802

We investigate the behavior of cholesteric liquid crystals (CLC's) inside a Fabry–Perot (FP) cavity. Although FP cavities filled with various liquid crystals have been extensively studied, to our knowledge the behavior of CLC-based FP cavities has not been reported. In CLC the twisted structure can be changed because the pitch is a function of temperature. In a parallel-rubbed CLC FP cavity the balance between strong surface anchoring and elastic energy yield a steplike resonance spectrum. This corresponds to the quantized effective pitch that the system assumes when both surface alignments are fixed. Experiment results for parallel-rubbed samples are presented and explained theoretically by use of Jones matrix calculations. © 1999 Optical Society of America

OCIS codes: 230.3720, 160.3710, 120.2230, 160.6840.

The Fabry–Perot (FP) interferometer[1] is a powerful yet versatile spectroscopic tool. It consists of two parallel, flat, and partially transparent mirrors that are separated by a small distance. Conceptually, the FP interferometer is a very simple structure, and, in principle, it is a lossless device when it is on resonance. FP cavities filled with liquid-crystal (LC) materials have enormous potential to be used as wavelength-tuning devices in wavelength-division multiplexing systems. These devices offer low driving voltages, compact and easy fabrication, and relatively wide tuning ranges. Various kinds of LC materials, such as nematic LC's[2,3] and ferroelectric LC's,[4] have been used in FP cavities. Each application has interesting and unique properties. However, to our knowledge there has been no study of the behavior of cholesteric liquid crystal (CLC) inside a FP cavity.

For a long time the CLC has been used as a material that is capable of producing selective Bragg diffraction effects.[5] Periodic helical arrangement of the molecules in the CLC leads to a variety of unique properties that can be used in various applications, such as a color filter,[6] a broadband polarizer,[7] a polarized light source,[8] a bistable display,[9] and a grating.[10] In this Letter we provide a detailed study of the behavior of CLC inside a FP cavity as its helical pitch changes with temperature. Experimental results are presented and explained by use of Jones matrix calculations.

For a twisted nematic LC structure the twisted director profile is a product of the surface-anchoring effect. The pitch of the twisted structure is determined by the surface-rubbing direction and the thickness of the cell. For CLC the material has a natural pitch that is determined by the temperature of the material. When the CLC molecules at the surfaces are in the plane of the surface, the planar structure of the CLC is well defined, at least in principle. If we consider the surface to be parallel to the $x-y$ plane, then the director can be represented by $(\sin kz, \cos kz, 0)$, where $k = 2\pi/p$ and p is the helical pitch. The director is rotated linearly along the z axis by an angle kd from one surface to the other, where d is the thickness of the sample. In

general, k is temperature dependent. However, if the CLC is confined to a cell with fixed boundary conditions such that the directors at both surfaces are forced to lie along a fixed direction, then the total amount of twist from one surface to the other is no longer kd but rather $k'd$, where k' satisfies the relation $k'd = m\pi$. The integer m is chosen so that k and k' differ as little as possible. Although k is a continuous function of temperature, k' is quantized. That this is so suggests that a CLC FP cavity subjected to temperature changes would produce cavity-resonance spectra that vary in steplike fashion.

To demonstrate the above considerations we used a material that is readily available from Aldrich Chemical Company and shows a rapid change in helical pitch with temperature: 4-[(S, S)-2,3-expoxyhexyloxy] phenyl4-(decyloxy)benzoate. Figure 1 shows the pitch of this material as a function of the temperature. The measuring technique was described in Ref. 11. The natural pitch of the materials is shown by the dashed curves in Fig. 1. In addition to the change of the helical structure, there exists a critical temperature
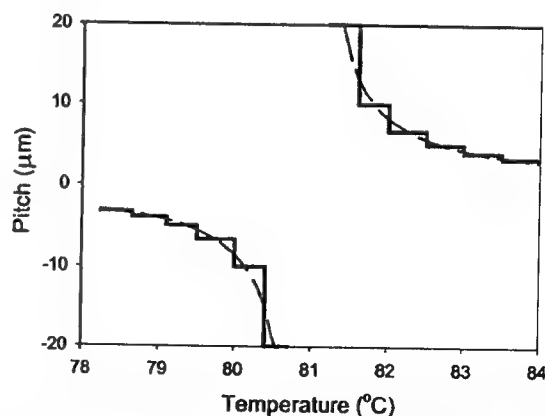

Fig. 1. Pitch of 4-[(S, S)-2,3-expoxyhexyloxy] phenyl4-(decyloxy)benzoate as a function of temperature. Dashed curves, natural pitch of the material. Solid curves, effective pitch.

76

($T_c \approx 81$ °C) at which the helical pitch becomes infinite and the twisting sense of the helix is opposite on either side of T_c. In our experiments the cell surfaces are parallel rubbed. Because of the strong surface-anchoring effect, the total twisted angle can take only integer numbers of π, i.e., $\phi = m\pi$, where m is an integer. This discrete twisted angle makes the effective pitch quantized ($P = d2\pi/\phi = 2d/m$), although the natural pitch can change continuously. A simple model is to assume that the effective pitch takes the quantized value $2d/m$ when the natural twisted angle falls in the range $(m - 1/2)\pi \sim (m + 1/2)\pi$. The quantized effective pitch is also shown in Fig. 1 by steplike solid curves.

The FP cavities were fabricated by use of two indium tin oxide–coated glass plates. The glass plates were first coated with dielectric mirrors with reflectivity of ~98% in the 1400–1600-nm region. We then coated them with a thin layer of polybutylene terepthallate and unidirectionally rubbed them to define the direction of the directors at the surfaces. The glass plates were then cut into two pieces and assembled into a 10-μm-thick cell by use of glass fiber spacers and ultraviolet-curable epoxy. The CLC material was inserted into the cell in its isotropic phase by capillary action.

The transmission spectrum of the CLC FP cavity was obtained as a function of temperature by use of a temperature controller with an accuracy of less than 0.1 °C and an optical spectrum analyzer. The light source was a 1.5-μm light-emitting diode, which we used in conjunction with a multimode optical fiber and graded-index rod lenses to couple the light into and out of the FP cavity. In this setup we made no effort to minimize the coupling losses.

The results of the measurements are shown in Fig. 2, which shows the transmission spectra as a function of temperature for unpolarized light [Fig. 2(a)] and light linearly polarized parallel to the rubbing direction [Fig. 2(b)]. The transmittance of the spectrum is shown in arbitrary units. One interesting observation is that the unpolarized spectrum looks symmetric about T_c. This means that at T_c the material is in the nematic phase. The material behaves as a uniaxial material, with its principal optical axes parallel and perpendicular to the directors. This finding can be verified by comparison of the unpolarized spectrum with the polarized spectrum. In the polarized spectrum one of the transmission peaks, corresponding to the mode that is perpendicular to the polarizer axis, is completely missing at T_c. Therefore the eigenmodes in the cavity at T_c are linearly polarized. Increasing or decreasing the temperature about T_c causes the polarization states of the eigenmodes within the cavity to change to elliptically polarized states. This mode mixing is clearly shown in the polarized spectrum. Furthermore, the spectra change in a steplike fashion that is represented by similar transmission spectra in a small temperature region. This result is expected because, as indicated above, the sample can support only integral numbers of helical turns. Therefore the effective pitch of the material is quantized, as shown in Fig. 1. When the temperature is far away from T_c, the

total twisted angle increases, and the material behaves as an isotropic medium with the average refractive index. As illustrated in Fig. 2, the resonance spectra thus become polarization independent.

The above results can be explained by use of Jones matrix calculations. For a single pass the Jones matrix of a twisted planar structure can be represented as follows[12]:

$$J = \exp(-i\Phi/2)R(\phi)$$

$$\times \begin{bmatrix} \cos\chi - i\dfrac{\Gamma}{2}\dfrac{\sin\chi}{\chi} & \phi\dfrac{\sin\chi}{\chi} \\[2ex] -\phi\dfrac{\sin\chi}{\chi} & \cos\chi + i\dfrac{\Gamma}{2}\dfrac{\sin\chi}{\chi} \end{bmatrix}, \quad (1)$$

where $\Phi = k_0(n_e + n_o)d$, $\Gamma = k_0(n_e - n_o)d$, $\chi = [\phi^2 + (\Gamma/2)^2]^{1/2}$, $k_0 = 2\pi/\lambda$ is the wave vector, λ is the wavelength, d is the cell thickness, and ϕ is the twisted angle. For a round trip the Jones matrix is[13]

$$M = {}^tJJ = \exp(-i\Phi)\begin{bmatrix} \kappa & ih \\ ih & \kappa^* \end{bmatrix},$$

$$\kappa = 1 - 2\left(\frac{\Gamma}{2}\frac{\sin\chi}{\chi}\right)^2 - i\Gamma\cos\chi\frac{\sin\chi}{\chi},$$

$$h = -\phi\Gamma(\sin\chi/\chi)^2. \quad (2)$$

Suppose that the incident light field is $\mathbf{E}_i$ and the reflectance and transmittance of the dielectric mirror are r and t, respectively. The transmission of a CLC FP cavity can be calculated as follows:
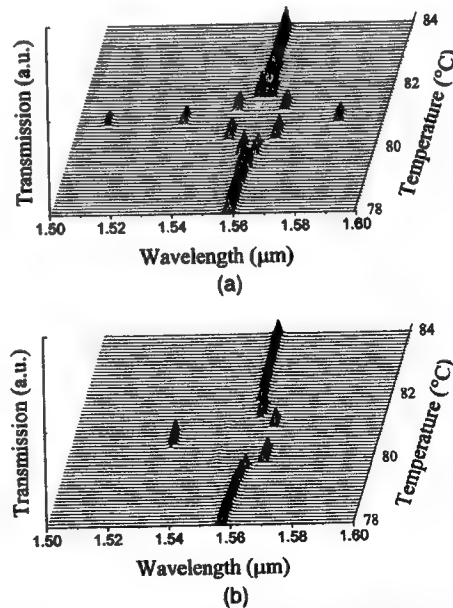

Fig. 2. Experimental results of the resonance spectra as a function of temperature: (a) unpolarized light, (b) light that is linearly polarized parallel to the rubbing direction.
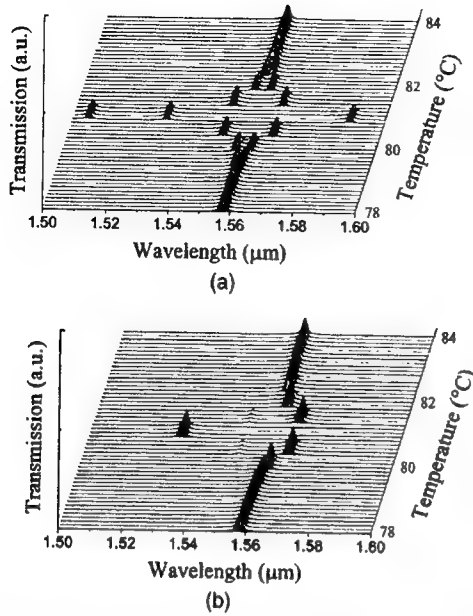
Fig. 3. Theoretically calculated results of the resonance spectra as a function of temperature: (a) unpolarized light, (b) light that is linearly polarized parallel to the rubbing direction.

$$|\mathbf{E}_o|^2 = t^4|(1 + r^2M + r^4M^2 + \ldots) \cdot \mathbf{E}_i|^2$$
$$= \frac{t^4}{|1 - r^2 \exp(i\varphi_+)|^2} |\mathbf{E}_i \cdot \mathbf{e}_+|^2$$
$$+ \frac{t^4}{|1 - r^2 \exp(i\varphi_-)|^2} |\mathbf{E}_i \cdot \mathbf{e}_-|^2, \qquad (3)$$

where $\mathbf{e}_\pm$ are the eignvectors of the matrix M and $\exp(i\varphi_\pm)$ are the corresponding eigenvalues. Each term in Eq. (3) represents the transmission of one eigenmode. From Eq. (2), the eigenvalues of matrix M can be calculated as

$$\varphi_\pm = \Phi \pm 2\sin^{-1}\left(\frac{\Delta nk_0 d}{2\chi}\sin\chi\right). \qquad (4)$$

The two corresponding eigenvectors can also be calculated directly or by the use of the coupled-mode theory[14]:

$$e_\pm = \begin{bmatrix} \exp(i\chi)\sqrt{\dfrac{1 \pm q}{2}} \pm \sqrt{\dfrac{1 \mp q}{2}} \\ -ip\exp(i\chi)\sqrt{\dfrac{1 \pm q}{2}} \pm \dfrac{i}{p}\sqrt{\dfrac{1 \mp q}{2}} \end{bmatrix},$$

$$p = \frac{2\chi - \Gamma}{2\phi}, \qquad q = \frac{\cos\chi}{[(2\phi/\Gamma)^2 + \cos^2\chi]^{1/2}}. \qquad (5)$$

By substitution of Eqs. (4) and (5) into Eq. (3), the transmission spectra for unpolarized light [Fig. 3(a)] and light that is linearly polarized parallel to the rubbing direction [Fig. 3(b)] can be calculated. By use of the effective pitch as shown in Fig. 1, we find that the calculated resonance spectra also show the steplike behaviors that were found in the experimental results. Figures 2 and 3 clearly show that the steplike behavior of the resonance spectrum is due to the quantization of the effective helical pitch of the CLC materials when the temperature changes. The parameters that we used in the calculation are $r = 0.09$, $n_e = 1.53$, $n_o = 1.43$, and $d = 10$ μm, which is consistent with the experimental parameters.

In conclusion, the behaviors of CLC inside a FP cavity as a function of temperature have been studied both experimentally and theoretically. The steplike resonance spectra have been observed experimentally and explained by use of Jones matrix calculations.

References

1. C. Fabry and A. Perot, Ann. Chem. Phys. **16**, 289 (1899).
2. J. S. Patel, M. A. Saifi, D. W. Berreman, C. Lin, N. Andreadakis, and S.-D. Lee, Appl. Phys. Lett. **57**, 1718 (1990).
3. J. S. Patel and S.-D. Lee, Appl. Phys. Lett. **58**, 2491 (1991).
4. J. S. Patel, Opt. Lett. **17**, 456 (1992).
5. S. Chandrasekhar, *Liquid Crystals* (Cambridge U. Press, Cambridge, 1992), pp. 213–300.
6. A. Hochbaum, Y. Jiang, L. Li, S. Vartak, and S. Faris, in *SID 99 Digest* (Society for Information Display, San Jose, Calif., 1999), p. 1063.
7. H. G. Galabova, Y. Jiang, L. Li, S. Vartak, and S. M. Faris, in *SID 99 Digest* (Society for Information Display, San Jose, Calif., 1999), p. 1058.
8. S. V. Belavey, M. Schadt, M. I. Barnik, J. Funfschilling, N. V. Mailmoneko, and S. Schmitt, Jpn. J. Appl. Phys. **29**, L634 (1990).
9. D.-K. Yang, J. L. West, L.-C. Chien, and J. W. Doane, J. Appl. Phys. **76**, 1331 (1994).
10. D. Subačius, S. V. Shiyanovskii, Ph. Bos, and O. D. Lavrentovich, Appl. Phys. Lett. **71**, 3323 (1997).
11. S.-W. Suh, K. Joseph, G. Cohen, and J. S. Patel, Appl. Phys. Lett. **70**, 2547 (1997).
12. P. Yeh, *Optical Waves in Layered Media* (Wiley, New York, 1988), pp. 289–291.
13. H. Yoda, Y. Othera, O. Hanaizumi, and S. Kawakami, Opt. Quantum Electron. **29**, 285 (1997).
14. Y. Ohtera, H. Yoda, and S. Kawakami, "Analysis of twisted nematic liquid crystal Fabry–Perot interferometer (TN-FPI) filter based on the coupled mode theory," Opt. Quantum Electron. (to be published).

78

Behavior of the Cholesteric Liquid-Crystal Fabry-Perot Cavity in the Bragg Reflection Band

Zhizhong Zhuang,* Young Jin Kim, and J. S. Patel

Departments of Physics and Electrical Engineering, Pennsylvania State University, University Park, Pennsylvania 16802
(Received 21 September 1999)

In this Letter, we investigate the behavior of the cholesteric liquid-crystal Fabry-Perot cavity in the spectral range of the Bragg reflection band. We show that in this region the 2×2-Jones-matrix calculation gives a false predication. However, by the use of the 4×4-matrix method, interesting features are revealed in the resonance spectra. The resonance spectra split when $\lambda \sim \bar{n}P$. Our experiments confirm this phenomenon. The experimental results show that the splitting occurs in a steplike fashion. This can be explained by the quantization of the pitch that occurs due to the fixed boundary conditions.

It is well known that a highly twisted cholesteric liquid-crystal (CLC) medium behaves just like an isotropic medium that has an average refractive index of the anisotropic material. Therefore, for a CLC medium inside a Fabry-Perot (FP) etalon, if the pitch is much larger compared to the wavelength, one expects to have two sets of resonance peaks, for the two refractive indices n_e and n_o, respectively. As the pitch of the medium gets shorter, the two sets of peaks converge into one set, which corresponds to the average refractive index. However, if the CLC medium is inside its Bragg reflection band, due to the selective Bragg reflection, one expects that new features will appear in the resonance spectrum. This is the main topic of this Letter.

The CLC materials are chiral nematic materials, which have helical structure results from the uniformly twisted director. The physical properties of the CLC materials are similar to those of the nematics; the only exception is that it has a helical director profile with a finite pitch that is a function of the temperature. Since the optical property is integrally related to the director profile, the helical arrangement of the directors in the CLC materials introduces new optical properties, particularly with respect to the propagation and reflection of light. For example, the selective Bragg reflection of a circularly polarized light having the same sense of twist as that of the CLC medium is observed in these materials. This reflection is centered at the wavelength $\lambda_0 = \bar{n}P$, where P is the pitch and $\bar{n}$ is the mean refractive index of the medium. These optical properties can be worked out by the use of the widely accepted spirally dielectric ellipsoid model proposed by Oseen [1]. In the work on optics in stratified and anisotropic media, Berreman [2] proposed the 4×4-matrix method as a powerful numerical technique to handle complicated reflection and transmission problems. This method was further modified by Abdulhalim et al. [3] and Wöhler et al. [4]; both permit the replacement of the infinite series expansion of Ref. [2] by a sum of four terms for a homogeneous slab. In calculating the optical properties of CLC materials, because the directors lay in a plane that is perpendicular to the light path, the transfer matrix has been worked out in a simple form in Ref. [4]. Therefore, Wöhler's faster 4×4-matrix method was used in this Letter.

Liquid-crystal (LC) materials have been frequently used inside FP etalons because of their unique electro-optical properties. LC FP offers low driving voltages, compact and easy fabrication, and relatively wide tuning ranges. Nematic LC [5,6] and the ferroelectric LC [7] filled FP etalons have been reported and showed interesting and unique properties. However, the study of the behavior of the CLC FP has been limited. There have been studies of an optically active FP etalon [8,9] filled with an isotropic, optically active medium. In a recent work [10], we studied both experimentally and theoretically the behavior of a CLC FP etalon in the long pitch range when the CLC medium is outside the Bragg reflection band. In our study, the CLC FP showed steplike resonance spectra because of the fixed boundary conditions. These resonance peaks quickly converged into a single set of degenerate peaks as the twisted angle increased. In this Letter, we investigate the behavior of the CLC FP in the spectral range of the Bragg reflection band.

The optical properties of the long pitch CLC FP are similar to those of the twisted nematic LC FP. The resonance spectra can be easily calculated by the use of the Jones matrix. The details of this calculation method have been described in our previous work [10]. The two sets of resonance peaks correspond to the two refractive indices converged into one set as the twisted angle increased, and no new feature could be found when $\lambda \sim P\bar{n}$. This is not surprising because the Jones matrix calculation completely omits the multiple reflections inside the CLC medium; thus, no information related to the selective Bragg reflection can be obtained by the use of the Jones 2×2-matrix calculation.

In order to consider the selective Bragg reflection of the CLC medium, the 4×4-matrix calculation was performed. In doing so, we assumed that the entrance director was along the x direction and the linearly polarized light was polarized along the y direction. We also assumed that the CLC medium was in the so-called planar state, which means that the helical axis was perpendicular to the cell surface. From the Maxwell's equations, the following set of four linear differential equations for the tangential components of the electromagnetic field can be derived [2]:

$$\partial\psi/\partial z = -ik_0\Delta\psi, \tag{1}$$

$$\psi = (E_x, H_y, E_y, -H_x)^T, \tag{2}$$

where $k_0 = \omega/c$, ω is the angular velocity, and c is the velocity of light in vacuum. The matrix Δ depends on the dielectric constants, the wave vector, and the orientation of the optic axis. One can relate the electromagnetic field at $z = 0$ to the field at $z = d$ by dividing the CLC medium into N layers, where each layer has a thickness a:

$$\psi(0) = M\psi(d)$$

$$= M(0, a)M(a, 2a), \dots, M((N-1)a, Na)\psi(d). \tag{3}$$

In our calculation, $N = 500$ is used. Other values of N yield the same results if N is chosen in such a way that there are more than ten layers per pitch [4]. M is the transfer matrix. For CLC FP, because the CLC medium is in the planar state, the matrix M can be written out explicitly [4].

To apply this 4×4-matrix method in the FP transmission calculation, the Ψ vector defined in Eq. (2) is not suitable because it is not directly related to the transmission and reflection. It is usually convenient to work with other bases, such as the ordinary and the extraordinary waves that propagate forward and backward in the medium. The transformation between these two bases can be done by the use of the dynamic matrix D defined by Yeh [11]. For a thin birefringence layer oriented at ρ degree and with refractive indices n_e and n_o, the dynamic matrix D is defined as

$$D(\rho) = \begin{pmatrix} \cos\rho & \cos\rho & -\sin\rho & -\sin\rho \\ n_e\cos\rho & -n_e\cos\rho & -n_o\sin\rho & n_o\sin\rho \\ \sin\rho & \sin\rho & \cos\rho & \cos\rho \\ n_e\sin\rho & -n_e\sin\rho & n_o\cos\rho & -n_o\cos\rho \end{pmatrix}. \tag{4}$$

Therefore, as shown in Fig. 1, we can rewrite Eq. (3) as

$$\begin{pmatrix} r_1 E'_x + t_1 E^i_x \\ E'_x \\ r_1 E'_y + t_1 E^i_y \\ E'_y \end{pmatrix} = D^{-1}_{z=0} M D_{z=d} \cdot \begin{pmatrix} E^o_x/t_2 \\ r_2 E^o_x/t_2 \\ E^o_y/t_2 \\ r_2 E^o_y/t_2 \end{pmatrix}, \tag{5}$$
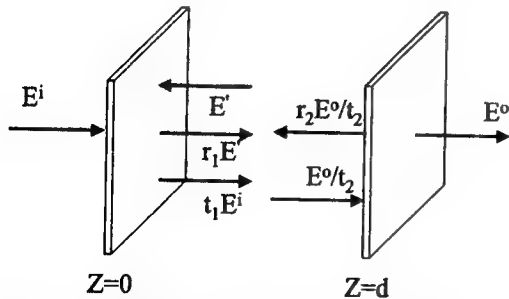

FIG. 1. Electromagnetic wave inside the CLC FP.

where E^i and E^o are the incident and the emergent light fields, respectively, $r_{1,2}$ and $t_{1,2}$ are the reflectance and transmittance of the two mirrors, respectively, E' represents the reflective wave that travels backward inside the medium (see Fig. 1), and matrix M is defined in Eq. (3). By eliminating E' in the above equation, E^o can be solved. The parameters used in the calculation were $n_e = 1.655$, $n_o = 1.565$, $d = 2\ \mu m$, and $r = 95\%$, where d is the thickness of the cell and r is the reflectivity of the mirrors. We omitted the chromatic dispersion of the refractive index and the variation of the refractive index due to the temperature. The calculated resonance spectra by the use of the 4×4-matrix method are shown in Fig. 2. If the CLC medium is outside the reflection band, the resonance spectra are the same as the results obtained by the use of the Jones matrix calculation [10]; thus Fig. 2 shows only the results in the range of $\lambda \sim P\bar{n}$ for (a) unpolarized and (b) linearly polarized incident light. As Fig. 2 illustrates, inside the Bragg reflection band, the resonance spectrum of the CLC FP splits.

To verify these results experimentally, we used a material (TM216 from British Drug House) that shows a rapid change in its helical pitch in the visible range at room temperature. The FP cavity was fabricated by the use of two indium-tin-oxide coated glass plates. First, the glass
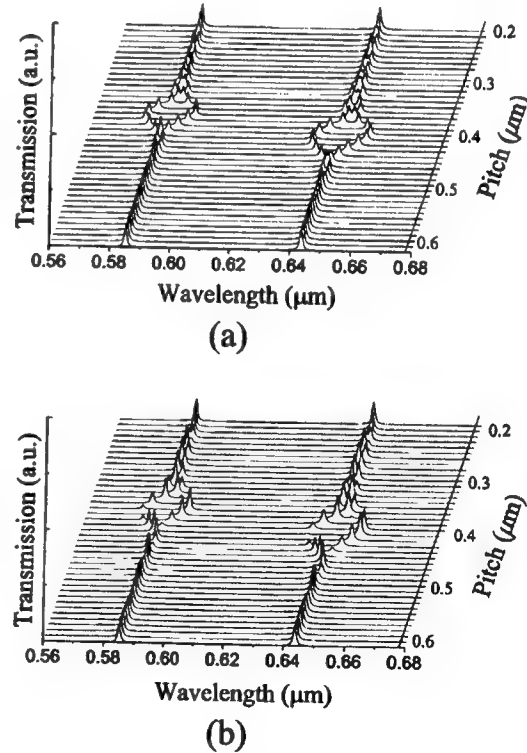

(a)

(b)

FIG. 2. The 4×4-matrix calculation for a $2\ \mu m$ CLC FP. The incident light is (a) nonpolarized and (b) linearly polarized. The resonance spectra splits when $\lambda \sim P\bar{n}$, where $\bar{n} = 1.61$.

plates were custom coated with thin films of the dielectric mirrors with a reflectivity of 90% to 95% in the 550 to 700 nm range. Then the glass plates were coated with a thin layer of Polybutylene-terepthallate as an alignment layer and unidirectional rubbed to define the direction of the directors at the surfaces. The glass plates were then cut into two pieces. Glass fiber spacers and ultraviolet curable epoxy were used to assemble the glass plates into a 2 μm thick cell. The CLC material was inserted into the cell in its isotropic phase by the capillary action. Light from a visible to near infrared fiber light source (300–1000 nm) was coupled into the FP cavity by the fiber-collimating lens and then it was coupled into the detector of a spectrometer. The transmission spectra of the CLC FP cavity were obtained as a function of temperature by the use of a temperature controller (Mettler hot stage) whose accuracy is better than 0.1 °C and an optical spectrometer. The rate of temperature change was set to be linear and was 0.1 °C per minute. The spectra were taken approximately every 0.08 °C. With a scan time of about 50 msec, the temperature variation during the scan time was negligible; therefore, the temperature can be assumed to be fixed during the time that the scan was taken. This slow rate also minimizes the multidomain problem associated with the pitch change. To limit the multidomain problem, a pinhole was put in front of the CLC FP to reduce the beam size.

The experimental results are shown in Fig. 3 for (a) unpolarized and (b) linearly polarized incident light. It clearly shows that when the CLC medium is inside its Bragg reflection band, the resonance spectra split. However, instead of the continuous splitting, as shown in Fig. 2, the splitting occurs in a steplike fashion. This steplike splitting occurs because of the fixed boundary conditions of the CLC FP cell. The total twisted angle of the CLC director inside the FP can only assume integer number of π because the cell surfaces are parallel rubbed. Therefore, the effective pitch of the CLC material adopts a set of quantized values that minimizes the free energy, and at the same time, satisfies the fixed boundary conditions. In order to explain the observed spectra, a simple model is proposed. We assumed that the effective pitch takes the quantized value $2d/m$ when the natural twisted angle falls in the range $(m - 1/2)\pi \sim (m + 1/2)\pi$. This pitch quantization is experimentally confirmed by measuring the transmission spectra of a CLC cell, which has a similar structure as the CLC FP cell but without the dielectric mirror coatings. This CLC cell is expected to show a Bragg reflection band centered at $\lambda_0 = \bar{n}P$. Therefore, the pitch of the material at a certain temperature can be obtained by measuring the position of the Bragg reflection band. As shown in Fig. 4, the Bragg reflection band (represented by the notch of each spectrum) responded to the temperature change in a steplike manner, which is characterized by a set of similar transmission spectra in a small temperature region. Thus the pitch quantization is clearly verified in this experiment. The oscillation of the transmission outside the reflection
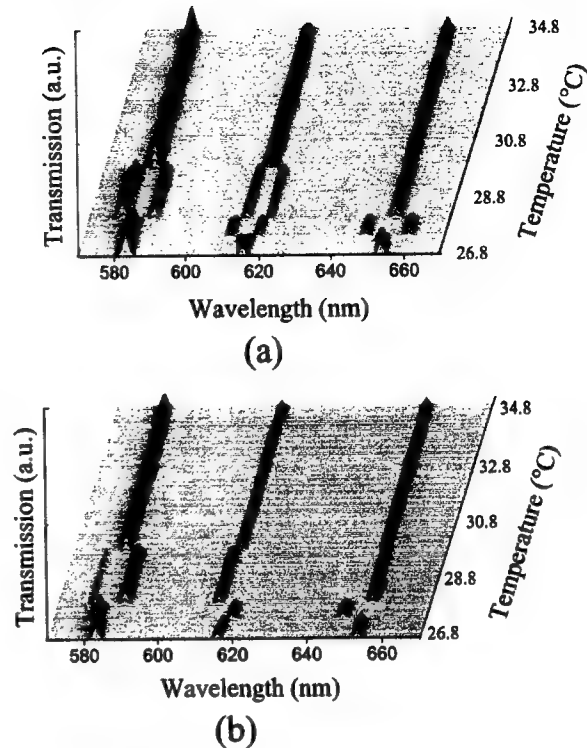

FIG. 3. Experimental results of the resonance spectra for a 2 μm CLC FP. The incident light is (a) nonpolarized and (b) linearly polarized.

band is because of the FP effect due to the reflections from the front and back surfaces of the cell. Based on these results, we proposed a simple model of the effective pitch for a 2 μm CLC FP. The quantization of the pitch is shown in the inset of Fig. 4, which is very similar to the steplike behavior of the reflection band. The small difference is a result of the small variation in the cell thickness. Although both cell thicknesses are maintained by 2 μm spacers, the actual thickness is not exactly the same.
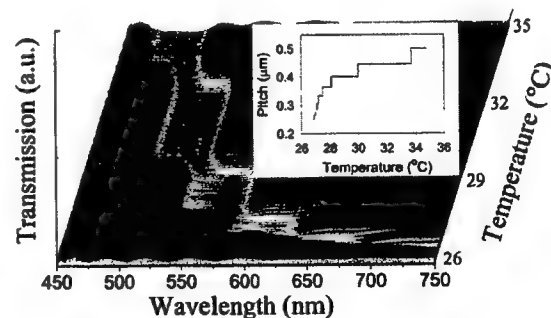

FIG. 4. The steplike behavior of the reflection band for a 2 μm CLC cell as the temperature changes. The reflection band is represented by the notch for each spectrum. The inset is the quantized pitch for a 2 μm CLC FP cell used in the calculations.
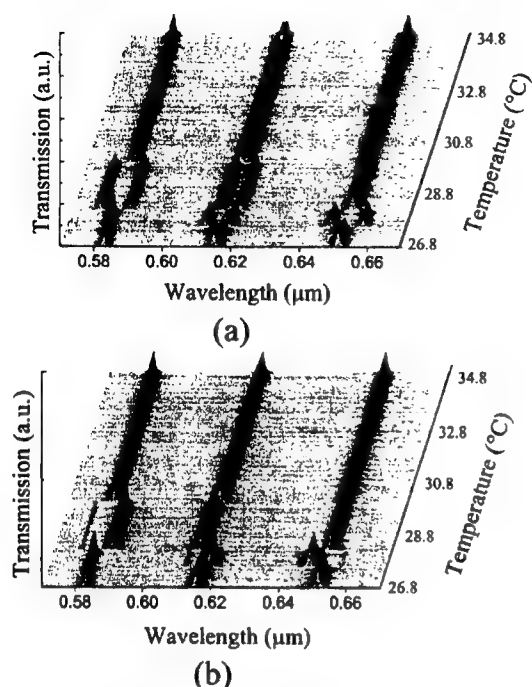
FIG. 5.   Calculated results of the CLC FP. The incident light is (a) nonpolarized and (b) linearly polarized.

By only applying this effective pitch, one cannot obtain the same results as shown in Fig. 3; the penetrating depth of the dielectric mirror coating must also be considered. To account for this additional thickness, we added an isotropic layer at both sides of the CLC medium inside the FP. To avoid the spectrum oscillation due to the multiple FP cavities effect, the refractive index of these two layers was set to equal the average refractive index of the CLC medium. The numerical results are shown in Fig. 5. A comparison of Figs. 5 and 3 shows that the agreement is excellent, even in details. In the calculation, a penetrating depth of 0.72 μm was chosen for both mirror coatings. Because of sample nonuniformity, as the temperature changes, the sample is expected to form the multidomain structure, which has been confirmed under a polarizing microscope. Although a slow rate of temperature change and a pinhole were used in the experiment to minimize this problem, the multidomain structure still caused the broader resonance peaks and the gradual change in the step edge.

In this paper we have examined the spectral response of a Fabry-Perot containing cholesteric liquid crystal in the region of the Bragg reflection band. Theoretical consideration by means of the 4×4-matrix calculation revealed a splitting of the resonance spectrum when $\lambda \sim \bar{n}P$. Experiments were conducted to confirm the theoretical predictions. For a parallel rubbed sample, the splitting occurs in a steplike fashion, which can be explained by the quantization of the effective pitch of the CLC medium. The complexity of the results is due to the spiraling dielectric ellipsoid and the helix quantization. The behavior is similar to a one dimensional photonic band-gap structure. Currently, we are attempting to develop a CLC FP cell structure with a continuously changing pitch.

*Electronic address: zxz109@psu.edu

[1] C. W. Oseen, Trans. Faraday Soc. **29**, 883 (1933).
[2] D. W. Berreman, J. Opt. Soc. Am. **61**, 502 (1972).
[3] I. Abdulhalim, L. Benguigui, and R. Weil, J. Phys. (Paris) **46**, 815 (1985).
[4] H. Wöhler *et al.*, J. Opt. Soc. Am. A **5**, 1554 (1988).
[5] J. S. Patel *et al.*, Appl. Phys. Lett. **57**, 1718 (1990).
[6] J. S. Patel and S.-D. Lee, Appl. Phys. Lett. **58**, 2491 (1991).
[7] J. S. Patel, Opt. Lett. **17**, 456 (1992).
[8] I. J. Lalov and A. I. Miteva, J. Mod. Opt. **38**, 395 (1991).
[9] M. P. Silverman and J. Badoz, J. Opt. Soc. Am. A **11**, 1894 (1994).
[10] Z. Zhuang and J. S. Patel, Opt. Lett. **24**, 1759 (1999).
[11] P. Yeh, J. Opt. Soc. Am. **69**, 742 (1978).

VOLUME 76, NUMBER 17 24 APRIL 2000

Electrically controllable azimuth optical rotator

Zhizhong Zhuang,[a] Young Jin Kim, and J. S. Patel
Departments of Physics and Electrical Engineering, Pennsylvania State University, University Park, Pennsylvania 16802

The transformation of the state of polarization (SOP) of light from one state to another can be graphically illustrated by a trajectory on the Poincaré sphere (PS). We use this method to illustrate the control of the azimuth SOP rotation on the PS. Traditionally, azimuth rotation is achieved by the use of a Faraday rotator or by the mechanical movements of birefringent wave plates. In this letter, an electrically controllable azimuth optical rotator is introduced theoretically and verified experimentally. It consists of two quarter-wave plates and one liquid-crystal variable wave plate and allows polarization rotation of an arbitrary polarized light by an angle determined by the magnitude of the applied field. This electrical approach avoids the errors and inconvenience associated with the magnetic field and the mechanical movements of other methods. © *2000 American Institute of Physics.* [S0003-6951(00)04517-4]

As the polarization effects, such as polarization-mode dispersion and polarization-dependent loss, become important considerations in optical systems, the ability to control the transformation of the state of polarization (SOP) (Refs. 1 and 2) of light is becoming increasingly important. When examining the SOP properties of light, the Stokes parameters[3] and the Poincaré sphere[3] (PS) representation provide a clear visualization of the evolution of the SOP. Thus, these methods are widely used. It is well known that the rotation of the SOP on the PS about an axis that lies on the equatorial plane can be achieved simply by a linear birefringence wave plate, such as a homogeneous aligned liquid-crystal cell. However, to azimuth rotate the SOP on the PS is a challenging task. Traditionally, the azimuth rotation of the SOP on the PS is achieved by the use of a Faraday rotator or by the mechanical rotations of quarter-wave plates and/or half-wave plates.[4] A Faraday rotator requires magnetic field, so it is inconvenient in most applications and difficult to integrate into optical systems. The mechanical movements may cause various kinds of errors. Misalignment and the nonuniformity of wave plates are typical problems associated with the moving parts. Due to the inertia of the moving parts, processes involving mechanical movements are typically time consuming, complicated, and inaccurate. Therefore, it is important to develop an electrically controllable azimuth optical rotator with no moving parts.

It is well known that to electrically azimuth rotate a specific linearly polarized light, one can use a variable wave plate and a quarter-wave plate. These two wave plates are oriented at 45° and 0°, respectively, with respect to the axis of the linearly polarized light. The rotation angle can be controlled by controlling the birefringence of the variable wave plate. But, such a device cannot be used for an arbitrary incident SOP. In a recent paper,[5] Ye and Keranen used a device with a similar configuration in front of an analyzer to examine the light intensity. They concluded that this configuration can effectively simulate an electrically control-

lable azimuth rotation of the analyzer by changing the retardation of the linear retarder. However, this azimuth rotation is only in terms of the light intensity, since the SOP of the emergent light field is not azimuth rotated. Furthermore, the input polarization has a fixed relation with the rotator elements. In this letter, we introduce a device that can azimuth rotate an arbitrary SOP on the PS by an arbitrary angle using electrical control.

As Jones predicted,[6] a variable linear retarder, placed between two orthogonal quarter-wave plates whose slow axes make an angle ±45° with that of the linear retarder, acts as an azimuth optical rotator that can rotate the SOP about the polar axis on the PS. We have fabricated an optical rotator from two quarter-wave plates and a homogeneous aligned nematic liquid-crystal cell. Liquid crystal was chosen because of its unique electro-optical effects, which permit us to use a small electric field to change the retardation of the cell. The amount of the azimuth rotation is determined by the retardation of the liquid-crystal cell, which can be controlled by the applied electric field. In the following discussion, we present a theoretical consideration of this device by the use of the Jones matrix calculations and the Stokes parameters; this is followed by a detailed report of our experimental results.

We can define the structure of the azimuth optical rotator as $Q(45°)B(0°)Q(-45°)$, where Q stands for the quarter-wave plate and B is the birefringence of the middle wave plate. The angles in the brackets are the orientation of the slow axis for the corresponding wave plate. In other words, the first and third wave plates are quarter-wave plates with their slow axes orientated at 45° and −45°, respectively, and the middle wave plate is a liquid-crystal cell with birefringence B and a slow axis oriented at 0°.

Suppose that the incident light field is represented by

$$\begin{pmatrix} E_x^i \\ E_y^i \end{pmatrix} = \begin{pmatrix} \cos\alpha \\ \sin\alpha\,\exp(i\delta) \end{pmatrix}. \tag{1}$$

This light field can also be expressed by the Stokes parameters as follows:
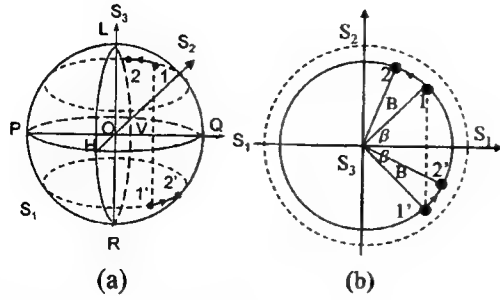
[a]Electronic mail: zxz109@psu.edu

83

Appl. Phys. Lett., Vol. 76, No. 17, 24 April 2000

Zhuang, Kim, and Patel

FIG. 1. Azimuth rotation of the SOP about the polar axis on the PS for the $Q(45°)B(0°)Q(-45°)$ configuration $(1\rightarrow2)$ and the $Q(0°)B(45°)Q(0°)$ structure $(1\rightarrow1'\rightarrow2')$. (a) The initial SOP is represented by point 1. The final SOP for the $Q(45°)B(0°)Q(-45°)$ structure is rotated in a lateral intercept circle that contains point 1 (S_1^i, S_2^i, S_3^i). The final SOP for $Q(0°)B(45°)Q(0°)$ is rotated in a lateral intercept circle that contains the point $1'$ $(S_1^i, -S_2^i, -S_3^i)$. (b) The projection plane on the equator. The dashed circle represents the equatorial plane.

$$S_1^i = E_x^i E_x^{i*} - E_y^i E_y^{i*} = \cos\beta = \cos 2\alpha,$$

$$S_2^i = E_x^i E_y^{i*} + E_y^i E_x^{i*} = \sin\beta = \sin 2\alpha \cos\delta, \qquad (2)$$

$$S_3^i = i(E_x^i E_y^{i*} - E_y^i E_x^{i*}) = \sin 2\alpha \sin\delta,$$

where β is the azimuth angle of the SOP on the PS, as shown in Fig. 1.

The output light field emerging from the stack structure is given by

$$\begin{pmatrix} E_x^o \\ E_y^o \end{pmatrix} = R\left(\frac{\pi}{4}\right)QR\left(-\frac{\pi}{4}\right)J(B)R\left(-\frac{\pi}{4}\right)QR\left(\frac{\pi}{4}\right)\begin{pmatrix} E_x^i \\ E_y^i \end{pmatrix}, \qquad (3)$$

where $J(B)$ is the Jones matrix for a retarder with retardation B and $R(\theta)$ is the rotation matrix with a rotating angle θ. Q is the Jones matrix for the quarter-wave plate. The Stokes parameters of the output light can be calculated as follows:

$$S_1^o = \cos 2\alpha \cos B - \sin 2\alpha \sin B \cos\delta,$$

$$S_2^o = \cos 2\alpha \sin B + \sin 2\alpha \cos B \cos\delta, \qquad (4)$$

$$S_3^o = \sin 2\alpha \sin\delta.$$

If Eq. (2) is substituted into Eq. (4), one can obtain the following results that relate the output SOP with the incident SOP:

$$S_1^o = S_1^i \cos B - S_2^i \sin B,$$

$$S_2^o = S_1^i \sin B + S_2^i \cos B, \qquad (5)$$

$$S_3^o = S_3^i.$$

Therefore, this configuration will rotate the SOP about the polar axis by an angle B.

As we discussed above, the $Q(45°)B(0°)Q(-45°)$ structure will rotate the SOP about the polar axis on the PS by an angle B. With this method, it is easy to show that a $Q(-45°)B(0°)Q(45°)$ structure will rotate the SOP about the polar axis on the PS by an angle $-B$.

To demonstrate the above considerations, a Hewlett-Packard HP8509B polarization analyzer at 1.55 μm was used to measure the Stokes parameters of the emergent light field. The voltage applied to the liquid-crystal cell was con-
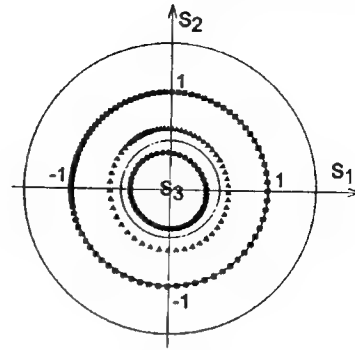

FIG. 2. Experiment results of the electrically controlled optical rotator. The initial SOP are arbitrarily chosen. S_3 for the initial SOP are: 0 for ■, 0.78 for ▲, and 0.92 for ●. The resulting SOP preserves S_3 and forms a circle on the lateral plane, while the retardation of the linear retarder is changed by 2π. For clarity, only one third of the experimental results are shown. The unequal spacing between the experiment points is due to the nonlinear electro-optic response of the liquid crystal.

trolled by a HP33120A function generator. The liquid-crystal cell was made using indium–tin–oxide glass substrates coated with a thin layer of polybutylene–terepthallate and unidirectionally rubbed to define the direction of the directors at the surfaces. The glass plates were then cut into two pieces and assembled into a 10-μm-thick cell using glass fiber spacers and ultraviolet curable epoxy. The liquid-crystal material (E7 from Merck) was inserted into the cell in its isotropic phase by the capillary action. The two quarter-wave plates used in the experiment were also made of liquid-crystal cells. Two cells were filled with liquid crystal (E7) doped with a small amount of cross-link materials, and then polymerized under UV light with the presence of an electric field. The field was adjusted to keep the retardation of the cell to be $\pi/2$ at 1.55 μm. The results of the experiment are shown in Fig. 2 in the S_1-S_2 projection plan. In this experiment, the incident SOP was arbitrary chosen to have different S_3^i (0, 0.78, and 0.92). Clearly, this experiment shows that as the voltage applied to the liquid-crystal cell changes, the emergent SOP preserves S_3 and rotates about the polar axis. As a result, each set of the emergent SOP forms a circle with radius 1, 0.63, and 0.4, respectively. The nonuniform space between the data points is due to the nonlinear electrical response of the liquid-crystal cell.

Because of the mirror symmetry of the above structure, there is an equivalent reflective structure $Q(45°)B(0°)M$, where M represents a mirror. A mirror in the optical path is equivalent to a half-wave plate and a mirror image of all of the optical components in front of the mirror.[7,8] Therefore, the above reflective structure is equivalent to $Q(45°)B(0°)H(0°)B(0°)Q(-45°)$, where H represents a half-wave plate. Since the three middle wave plates have the same orientation, they are equal to a single wave plate with a retardation of $\pi+2B$ at 0°. Therefore, this reflective structure will rotate the SOP about the polar axis on the PS by an angle $\pi+2B$. In the case of a $Q(-45°)B(0°)M$ structure, the SOP will rotate about the polar axis on the PS by an angle $-\pi-2B$.

When the incident light is linearly polarized, this reflective structure can be used to replace a Faraday rotator in a variety of applications. For example, in the Martinelli

effect,[9,10] a mirrored 45° Faraday rotator is needed in order to eliminate the effects of reciprocal birefringence and dichroism fluctuation in the medium on the SOP after the light beam retraces its path. The above reflective structure can replace a Faraday rotator, and in so doing the required magnetic field can be eliminated.

Another interesting configuration of the azimuth optical rotator is the $Q(0°)B(45°)Q(0°)$ structure. By calculating the emergent light field as before, the Stokes parameters of the emergent light field can be calculated as

$$S_1^o = S_1^i \cos B + S_2^i \sin B,$$

$$S_2^o = S_1^i \sin B - S_2^i \cos B, \tag{6}$$

$$S_3^o = - S_3^i.$$

A comparison of Eqs. (5) and (6) shows that in this case, the emergent light field does not preserve S_3. In fact, the sign of S_3 is inverted. According to Eq. (2), as shown in Fig. 1, the emergent light reverses S_2 and S_3 ($1 \rightarrow 1'$ in Fig. 1), and rotates the SOP about the polar axis by an angle B ($1' \rightarrow 2'$ in Fig. 1).

From the above equation, if $B = \pi$ (the middle liquid-crystal cell is a half-wave plate), then $S^o = -S^i$. In other words, the SOP of the emergent light is always the orthogonal state of the incident SOP; this holds true no matter what the incident SOP.

In conclusion, we have theoretically introduced and experimentally verified an electrically controlled optical rotator for an arbitrary incident polarization state. The degree of rotation is controlled only by the retardation of the electrically controllable liquid-crystal cell. Detailed studies of this azimuth optical rotator are provided for different kinds of configurations. The main advantage of this azimuth optical rotator is that the rotation can be controlled electrically; thus, the required magnetic field in a Faraday rotator and the mechanical movements of other methods are avoided. The speed of the rotation is essentially limited by the electro-optic response time of the liquid-crystal material and is typically in the millisecond range. Although the liquid-crystal materials have unique electro-optical properties and, therefore, are chosen to make this optical rotator, the structure itself is not limited to liquid crystal. In cases where high-speed rotation is desired, one can replace the liquid-crystal cell with another material with a high electro-optical speed.

[1] N. G. Walker and G. R. Walker, J. Lightwave Technol. **8**, 438 (1990).
[2] Z. Zhuang, S. Suh, and J. S. Patel, Opt. Lett. **24**, 694 (1999).
[3] E. Collett, *Polarized Light: Fundamentals and Applications* (Marcel Dekker, New York, 1992).
[4] R. Bhandari, Phys. Lett. A **138**, 469 (1989).
[5] C. Ye and E. Keranen, J. Opt. Soc. Am. A **14**, 682 (1997).
[6] R. C. Jones, J. Opt. Soc. Am. **31**, 500 (1941).
[7] R. Bhnadari, Phys. Lett. A **135**, 240 (1989).
[8] R. Bhandari, Physica B **175**, 111 (1991).
[9] M. Martinelli, Opt. Commun. **72**, 341 (1989).
[10] R. Bhandari, Opt. Commun. **88**, 1 (1992).

Defect in the circular-circularly rubbed liquid crystal cell with off-center alignment

Zhizhong Zhuang,[a] Seong-Woo Suh,[b] Young Jin Kim, and J. S. Patel
Departments of Physics and Electrical Engineering, Pennsylvania State University, University Park, Pennsylvania 16802

In this letter, we investigate the behavior of the defects in a circular-circularly rubbed liquid crystal cell with an off-center alignment. We show that the line defect forms a circle that passes through the rubbing centers of the two surfaces. The size and the position of the defect circle depend on the cell gap and the pitch of the materials. We propose a simple model, based on an analysis of the free energy, to explain this interesting phenomenon. This technique of defect making is useful to confine the defect to a particular position by controlling the cell parameters and the material properties. It can also be applied to the pitch measurement, the generation of the space-variant polarized light, and the study of the dynamic properties of the defect. © *2000 American Institute of Physics.* [S0003-6951(00)02321-4]

From a structural point of view, liquid crystals are materials intermediate between ordinary liquids and the solid crystals. The electro-optical effects of liquid crystals are due to the reorientation of the director, when subjected to small external forces, such as an electrical field, a change in the temperature, or the surface anchoring effect. The surface properties can be controlled and can alter the director profile, both in the bulk as well as the surface. It is well known that liquid crystal molecules on a rubbed surface tend to align along the rubbing direction.[1] In this letter, we study a special surface: the circularly rubbed surface. If both surfaces of a liquid crystal cell are rubbed circularly and these two surfaces are aligned off-center, then a circular disclination line appears, separating the two domains. These two domains have the same free energy, but they are twisted in opposite directions. We provide a detailed experimental and theoretical study of this phenomenon.

Liquid crystals are very sensitive to any spatial variation of the surface forces, which may alter their surface alignment. This sensitivity renders the interfacial phenomena of liquid crystals extraordinarily variable and interesting. In most applications, a cell is treated in such a way that the orientation of the director is uniform across its surface. The parallel-rubbed cell, the twisted cell, the homeotropic cell, and the hybrid cell have uniform aligned molecules at their surfaces. Other researchers have studied liquid crystal cells with a circularly rubbed surface, which has a concentric circular molecule arrangement at the surface.[2–4] A liquid crystal cell with one surface rubbed unidirectionally and the other surface rubbed circularly has been used in generating linearly polarized light with axial symmetry[2,3] and in measuring the pitch of the cholesteric liquid crystal.[4]

In this letter, we focus on the situation when the two surfaces used to form a liquid crystal cell are both circularly rubbed and they are off-center aligned, which means that the two circularly rubbed surfaces are not aligned concentrically. First, we describe the fabrication of the circularly aligned cell, followed by a discussion of the experimental results. The observed results are discussed in term of the free energy analysis. We show that the disclination line forms a circle, which passes through the rubbing centers of both surfaces. The size and the position of the circle depend on the cell structure and the pitch of the materials.

To study the defect formation in a circular-circularly rubbed cell, we chose a liquid crystal (ZLI-3488 from Merck) whose pitch continuously changes with the temperature. This material has a cholesteric phase when its temperature is between 66 and 85 °C. Figure 1 shows the nominal pitch of this material as a function of the temperature. The cell was made using indium–tin–oxide (ITO) glass substrates. To promote planar alignment, the ITO glass was coated with a thin layer of polybutylene-terepthallate (PBT). PBT was chosen with no specific reason, and other alignment material, such as polyimide, yields the same results. Then, the PBT layers were rubbed circularly. To have a uniform rubbing pattern, the rubbing strength should be adjusted because of the variation in the linear speed as one moves away from the center of rubbing. The rubbed plates were assembled into a 10 μm thick cell. When assembling the
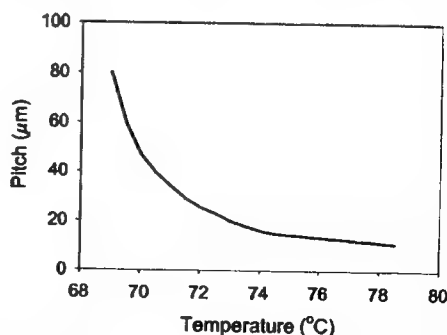

FIG. 1. The nominal pitch of the liquid crystal material (ZLI-3488) as a function of the temperature.

[a]Author to whom correspondence should be addressed; electronic mail: zxz109@psu.edu
[b]Present address: YAFO, Inc. 1340 F Charwood Rd. Hanover, MD 21076.
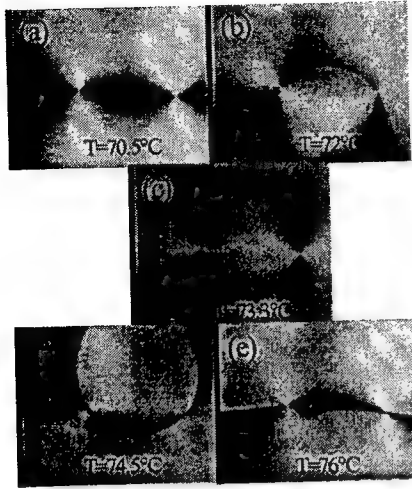
86

FIG. 2. Microphotographs of the disclination line formed in the circular-circularly off center aligned liquid crystal cell at different temperatures. The defect forms a circle that passes through the rubbing centers of the two surfaces.

FIG. 3. Theoretical model for the circular-circularly off-center aligned liquid crystal cell. C_1 and C_2 are the rubbing centers of the two surfaces. Circles α and β represent the rubbing direction at the bottom and the upper surfaces, respectively.

cell, the rubbing centers of the two surfaces were deliberately separated by a small distance. Several cells were made, and the one with a suitable separation (about 1 mm) between the two rubbing centers was chosen to be used in our experiment. The liquid-crystal material was inserted into the cell in its isotropic phase by the capillary action.

Figure 2 is composed of a series of microphotographic images. Each image was taken when the cell was at a different temperature. The angle between the entrant and the emergent polarizers was adjusted to obtain the best contrast. With reference to these images, it is obvious that the line defect forms a smooth curve and that it always passes through the rubbing centers of the two surfaces. As the temperature changes, the shape and the position of the defect curve also change.

In order to obtain a better understanding of this phenomenon, we propose a simple model, which is based on an analysis of the free energy. The details of this model have been thoroughly discussed in our previous letter.[4] We assume that the molecules are in the so-called planar state, which means that the molecules are parallel to the surfaces of the cell. By doing so, the small pretilt angle generated by rubbing was omitted. The influence of the pretilt angle is so small that no sensible effect was observed in our experiment. In this case, the elastic free energy has only one term, the twisted term[5]

$$f = \int_0^d K_2 \left(\frac{\partial \phi}{\partial z} - q \right)^2 dz, \qquad (1)$$

where K_2 is the twist elastic constant, ϕ is the azimuth angle of twist for the director, z is the coordinate in the surface normal, d is the cell gap, $q = 2\pi/p$, and p is the pitch. If the temperature and the pitch are fixed, $(d\phi/dz)$ is a constant and there is no external field, then the free energy can be written in a simple form as

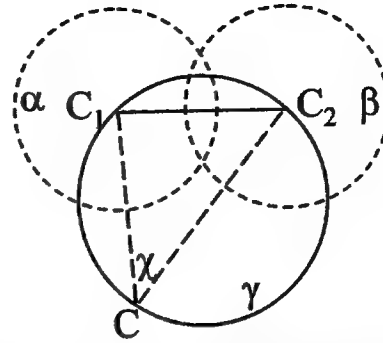$$f = K_2 \left(\frac{\phi_T}{d} - q \right)^2 d, \qquad (2)$$

where ϕ_T is the total twisted angle from one surface to the other.

The nature of the disclination line tells us that the molecules on either side of the disclination line should have the same free energy in equilibrium state. If this were not the case, the disclination line would move to reach a stable, equilibrium configuration. If one assumes that at the two sides of the disclination line, the total twisted angles are $\theta \pm \pi/2$, then, the equilibrium conditions yield the following equation:

$$\left(\frac{\theta + \pi/2}{d} - q \right)^2 = \left(\frac{\theta - \pi/2}{d} - q \right)^2. \qquad (3)$$

Therefore, the deviation angle θ can be easily determined as

$$\theta = \frac{2\pi d}{p}. \qquad (4)$$

The equilibrium between the two domains separated by the disclination line requires that the total twisted angle should be $\theta \pm \pi/2$ on the two sides of the defect. As illustrated in Fig. 3, C_1 and C_2 are the two rubbing centers of the bottom and the upper surfaces, respectively. The two dashed circles (α and β) represent the rubbing direction at the two surfaces. According to the above analysis, if point C is on the defect curve, then the molecules at this point should have a total twisted angle $\theta \pm \pi/2$ on the two sides of the defect. Because, at the surface, the molecules are aligned as a circle that follows the rubbing pattern, the $\theta \pm \pi/2$ total twisted angle along the defect line requires the angle $\chi = \theta \pm \pi/2$. The handedness of the twist determines which sign ($+$ or $-$) should be used. Because the angle χ is a constant, the trajectory of the defect should form a circle (circle γ in Fig. 3).

An immediate result from the above analysis is that if the deviation angle θ is an integer number of π ($\theta = n\pi$), the angle χ equals $\pm \pi/2$. Because $C_1 C$ and $C_2 C$ are perpendicular to each other, $C_1 C_2$ serves as the diameter of the defect circle. In this case the defect circle has the minimum size, and the center of the defect circle is at the midpoint of $C_1 C_2$. This situation is shown in Fig. 2(c). According to Fig. 1, at 73.3 °C the pitch of the material is about 20 μm. Therefore, from Eq. (4), it can be determined that the deviation angle θ equals π. This conclusion can be easily confirmed by inserting nematic liquid crystal into the circular-circularly
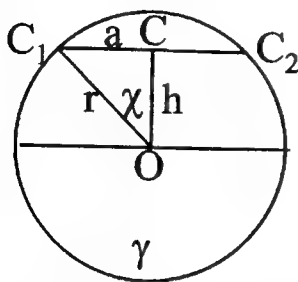
FIG. 4. The theoretical model used to calculate the size and the position of the defect circle.

rubbed cell. The nematic liquid crystal has an infinite pitch, which makes the deviation angle equal to zero. Therefore, by introducing the nematic liquid crystal we should get a circle centered at the midpoint of C_1C_2. This is exactly the case and has been confirmed by the experiment. The result for a nematic liquid crystal filled cell is identical to Fig. 2(c).

Another result that can be easily deduced from the above discussion is that if the deviation angle θ is $n\pi \pm \pi/2$, then angle χ will have the value $\pm\pi$. This means that the defect circle will expand into a straight line, as shown in Figs. 2(a) and 2(e). It is easy to confirm from Fig. 1 that at these two temperatures (70.5 and 76 °C), the pitch is about 40 and 13.3 μm, respectively. Therefore the deviation angles are $\pi/2$ and $3\pi/2$. The other value of the deviation angle θ will move the defect circle away from the center of C_1C_2 along the normal of C_1C_2 [as shown in Figs. 2(b) and 2(d)], but the defect circle will always pass through the rubbing center of the two surfaces.

One may notice that the curves shown in Fig. 2 are not perfect circles. The reason for this is the nonuniformity of the cell, which means that the gap may have a small variation across the cell. This nonuniformity of the cell has been confirmed by measuring the thickness of the empty cell at different positions. The variation of the thickness was found to be around 0.2 μm.

There is a simple way to determine the size and the position of the defect circle. As shown in Fig. 4, the size of the defect circle is represented by its radius r, and the position of the circle is represented by the distance h from its center (point O) to the midpoint of the line C_1C_2 (point C). According to the previous discussion, it is easy to find that

$$r = \frac{a}{\cos\theta}, \quad h = \frac{a}{\cot\theta}, \tag{5}$$

where a is the half length of line C_1C_2. Therefore, from the size or the position of the defect circle and Eqs. (4) and (5), one can obtain information about the deviation angle of the cell, and the pitch of the material.

The previously reported method[4] to measure the pitch used a liquid-crystal cell with one surface rubbed unidirectionally and the other surface rubbed circularly. In this configuration, the defect forms a straight line, and the deviation angle can be measured through the angle between the disclination line and the rubbing direction of the unidirectionally rubbed surface. The current method has several advantages compared to the previous one. According to Eq. (5), the deviation angle can be determined by measuring the radius (or equivalently, the area of the defect circle), which is more convenient than measuring the angle. Moreover, the current method eliminates the need of a reference direction, which the previous method required.

In conclusion, this letter provided a detailed study of the defect in a circular-circularly rubbed cell with an off-center alignment. The disclination line forms a circle that passes through the rubbing centers of the two surfaces. The deviation angle, which is a function of the cell gap and the pitch of the material, controls the size and the position of the defect circle. This technique can confine the defect to a particular position, and can be applied to the pitch measurement, the generation of the space-variant polarized light, and the study of the dynamic properties of the defects.

[1] For a comprehensive discussion of the liquid crystal alignment, see J. Cognard, *Alignment of Nematic Liquid Crystals and their Mixtures* (Gordon and Breach, London, 1982).

[2] R. Yamaguchi, T. Nose, and S. Sato, Jpn. J. Appl. Phys., Part 1 **28**, 1730 (1989).

[3] M. Stalder and M. Schadt, Opt. Lett. **21**, 1948 (1996).

[4] S.-W. Suh, K. Joseph, G. Cohen, and J. S. Patel, Appl. Phys. Lett. **70**, 2547 (1997).

[5] P. G. de Gennes and J. Prost, *Physics of Liquid Crystals* (Clarendon, Oxford, 1993), Chap. 6.

Achromatic linear polarization rotator using twisted nematic liquid crystals

Zhizhong Zhuang,[a] Young Jin Kim, and J. S. Patel
Departments of Physics and Electrical Engineering, Pennsylvania State University, University Park, Pennsylvania 16802

In this letter, we propose a simple configuration that is capable of rotating a linear polarization state of light by a certain angle for a wide range of wavelengths. The device consists of three liquid-crystal cells: two homogeneous cells and one twisted nematic (TN) cell. It is well known that a thick TN cell can rotate the linear polarization state of light by following the twisted structure. However, for a thin TN cell, achromatic polarization rotation is not possible. By the use of the Poincaré sphere model of the TN structure, we demonstrate that if one thin homogeneous cell is placed before and another one is placed after a thin TN structure, then a linear polarization state can be transformed close to the eigenmodes of TN. Therefore, this structure can be used to achieve the achromatic polarization rotation. This letter provides a detailed discussion of the theoretical analysis and a demonstration of the achromatic linear polarization rotator by the use of a 1.9 μm TN cell for the wavelength range 450–700 nm. © *2000 American Institute of Physics.*
[S0003-6951(00)01526-6]

Liquid-crystal (LC) materials, in various configurations, may be used in information displays and optical communication applications. Most of these devices involve the use of the twisted nematic (TN) LC structure.[1] The Jones matrix calculation has been widely used to study the optical properties of the TN LC structure. Recently, these studies were summarized by Yeh and Gu.[2] The operation of a device with a TN structure is generally described in terms of the rotation of the linear input polarization of the light following the twisted structure. This explanation, however, holds true only for specific cases. The exact rotation of the linear polarization in the TN structure can be achieved when the structure satisfies either one of the following two criterions: the Mauguin limit ($\lambda \ll \Delta nd$)[3] or the "Gooch-Tarry" relation.[4] Both criterions result in limitations on the practical applications: the Mauguin limit requires a thick sample, and the "Gooch-Tarry" relation works optimally only for a single wavelength. In this letter, we propose a simple structure that can achieve the achromatic linear polarization rotation by adding two homogeneous nematic LC cells to a thin TN structure.

As we mentioned earlier, the Jones matrix calculation has been used to study the optical properties of the TN structure. Although the Jones matrix calculation can be used to effectively study the TN structure, it offers little insight about the polarization evolution of the light. Moreover, when the Jones matrix is used to study the optical properties of the TN structure, complex numerical calculations are usually required. Recently, we introduced a Poincaré sphere (PS) model[5] to represent the TN structure on the PS. The PS model represents the evolution of the state of polarization (SOP) inside a TN structure as a curve on the PS. Because of its geometrical nature, the PS model offers a clear visualization of the evolution of the SOP and eliminates the need for complex numerical calculations. The PS model used in this letter also has been applied to the simultaneously optimiza-

tion of the reflective bistable nematic liquid crystal structure.[6–8] In the discussion later, we first use the PS model to examine the eigenmodes of the TN structure. After that, we discuss the configuration of the achromatic linear polarization rotator and the theoretical and experimental results. These results show that, compared to a single thin TN cell, our device can greatly reduce the wavelength dependence of the emergent polarization state.

A TN LC has an intriguing structure. The optical properties of a TN LC are a combination of the linear birefringence and the optical rotation. Consider a structure, which has a total phase retardation that can be expressed as $2\pi d\Delta n/\lambda$, where d is the thickness of the cell and Δn is the optical anisotropy. The total twisted angle is ϕ. As it passes through the TN structure, the evolution of the initial SOP can be visualized by tracing the trajectory of a point on a cone, where the cone is rolled on the equatorial plane at a rate that is twice that of the twist of the directors. As Fig. 1 shows, the cone's axis is represented by OC, and the half-angle of the cone ω is defined as[5]

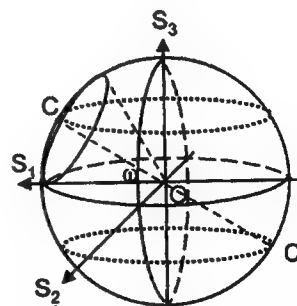$$\tan \omega = \frac{2\lambda}{\Delta np},\qquad(1)$$

FIG. 1. PS representation for a TN LC cell. ω is the half angle of the cone; OC is the cone axis; and C and C' are two orthogonal eigenmodes of the structure.

[a]Electronic mail: zxz109@psu.edu

Appl. Phys. Lett., Vol. 76, No. 26, 26 June 2000

Zhuang, Kim, and Patel

where $p = 2\pi d/\phi$ is the pitch.

It is obvious from Fig. 1 that if the incident polarization is at point C, while it moves with the cone, the ellipticity does not change. The only effect of this movement is the azimuth rotation of the polarization direction. This polarization state is called the "rotated eigenmode" of the TN structure. In the following discussion, we refer to this state as the eigenmode. It should be noted that, for the TN structure, there are two orthogonal eigenmodes (points C and C' in Fig. 1). The azimuth angle of eigenmode (C) is parallel to the entrance director and the polar angle is defined by Eq. (1). The same results have been achieved with the use of the Jones matrix formalism.[9,10]

Based on the earlier discussion, one can easily conclude that if the incident polarization state is the eigenmode, then the only effect is the exact rotation of the polarization state by the total twisted angle without a change in its ellipticity. On the other hand, as described in Eq. (1), the eigenmode for the TN structure is wavelength dependent; therefore, this pure polarization azimuth rotation can only be achieved for a specific wavelength. There are two ways to accomplish the achromatic polarization azimuth rotation. The first method requires that the Mauguin limit ($\lambda \ll \Delta nd$) be satisfied. From Eq. (1), it is clear that, at the Mauguin limit, the cone will be reduced to a line that lies along the equatorial plane; therefore the wavelength dependence is eliminated. However, the Mauguin limit requires a thick sample, which is not practical in most applications and results in a slow response. The other method is to transform the incident polarization state of different wavelengths close to their corresponding eigenmodes. This method can be applied to a thin TN cell, and it is the method used in this letter.

As Eq. (1) illustrates, the half-angle of the cone (ω) increases as the wavelength increases. In effect, this causes the polar angle of the eigenmode to increase as the wavelength increases. On the other hand, the phase retardation of a homogeneous nematic LC cell decreases as the wavelength increases. It is well known that the effect of a homogeneous waveplate on the incident polarization state of light is to rotate the polarization state by an angle equal to the phase retardation of the waveplate. Therefore, if one can design a suitable structure, which can transform the linear polarization state close to the eigenmodes of different wavelengths, the achromatic azimuth linear polarization rotation can be achieved.

Figure 2(a) shows the configuration of the achromatic azimuth linear polarization rotator. The incident polarization is assumed to be linear at angle α. The TN cell (B) has a twisted angle ϕ, and the entrance director is parallel to the incident polarization direction (α). Cell A and cell C are homogeneous LC cells which are oriented at (α-45°) and ($\alpha + \phi + 45°$), respectively. The purpose of cells A and C is to transform the polarization state of all wavelengths between the linear polarization state and their corresponding eigenmodes.

Figure 2(b) illustrates the operating principle of this device. The discussion later is limited to the case with a single wavelength (600 nm). Here we assume that the incident light is linearly polarized at 0°($\alpha = 0$), and that the TN cell has a twisted angle of $\pi/2$($\phi = \pi/2$). The phase retardation of cells

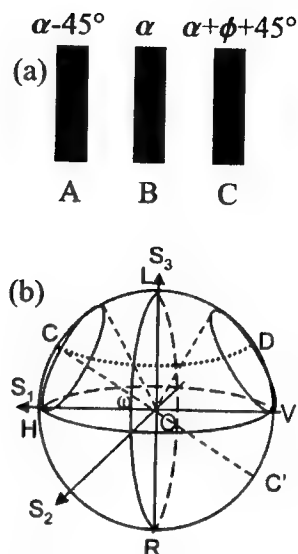FIG. 2. (a) Structure of the achromatic polarization rotator. Cell B is a TN cell with a twisted angle ϕ. Cells A and C are homogeneous waveplates with their slow axes oriented at specific angles; both orientations depend on the incident polarization angle α and the twisted angle ϕ. This configuration is capable of rotating the linear polarization at α by angle ϕ for a wide range of wavelengths. (b) Operation principle of the achromatic polarization rotator.

A and C is set at $\omega_{600}600/\lambda$, where λ is the wavelength in nanometers, and ω_{600} is the half angle of the cone calculated when $\lambda = 600$ nm. The incident polarization is at point H. If the wavelength is 600 nm, then the incident polarization is transformed to point C through the arc path HC by passing through cell A. The phase retardation of cell A equal the arc length of the Point C is the eigenmode of the TN structure, therefore, it is rotated by the TN structure to point D without changing its ellipticity. By passing through cell C, point D is further transformed to point V through the arc path DV, which has the same length as arc HC. In the following sections, the effect of the wavelength variation is discussed.

If the wavelength increases (decreases), according to Eq. (1), the polar angle of the eigenmode (ω) will increase (decrease). Therefore, for the device to work, the arc lengths HC and DV (or in other words, the phase retardation of cells A and C) should increase (decrease). However, if one considers the definition of retardation ($2\pi d\Delta n/\lambda$), the phase retardation is inverse proportional to the wavelength, which changes in the opposite direction as ω does. If one selects phase retardations for cells A and C, which are equal to the half angle of the cone using a middle wavelength, then this problem can be minimized. In our experiments, we set this middle wavelength at 600 nm. By doing this, even if the phase retardation and ω changes with the wavelength in opposite direction, because the change in the phase retardation is small, the emergent polarization states will assume points near the eigenmodes for corresponding wavelengths. Therefore, the linear polarization state can be transformed close to the corresponding eigenmodes for a wide range of the wavelengths.

In order to test the validity of our device, we performed numerical calculations and experiments on the transmission spectrum for our device and a single thin TN cell placed between cross polarizers. Figure 3 shows the results of our
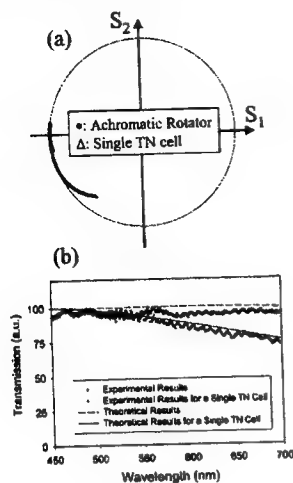
Zhuang, Kim, and Patel

FIG. 3. Theoretical and experimental results for the achromatic polarization rotator and a single TN cell. (a) The calculated emergent polarization states in the S_1–S_2 projection plane. (b) The calculated and experimental results for transmission spectra between cross polarizers.

experiments. Figure 3(a) shows the calculated results of the emergent SOP for the achromatic polarization rotator and for a single TN cell, in the wavelength range 450–700 nm. In our calculations, the twisted angle is 90°; the cell gap is 1.9 μm; and $\Delta n = 0.2$. The retardations of the two homogeneous cells are identical and equal to ω, where ω is calculated with the use of Eq. (1) for a wavelength equal to 600 nm. From the results of our calculations, it is obvious that a single TN cell cannot rotate the polarization for all wavelengths; this is especially evident when the cell gap is small and when the wavelength is large. However, the achromatic polarization rotator is capable of achieving the polarization rotation for a wide range of wavelengths. The transmission results for the achromatic polarization rotator and a single TN cell between cross polarizers are shown in Fig. 3(b). The polarizers are arranged in such a way that the entrant and the emergent polarizers are parallel to the entrant and emergent directors of the TN cell (B). For the achromatic polarization rotator, the emergent light has almost the same polarization state for all wavelengths. This emergent polarization state [point V in Fig. 2(b)] is rotated by 90° compares to the incident linear polarization state [point H in Fig. 2(b)]. Therefore, the transmission is almost 100% in the wavelength range from 450 to 700 nm. For a single TN cell, the transmission approaches 100% for short wavelengths. This is because for short wavelengths, the system is closer to the Mauguin limit. For longer wavelengths, the transmission decreases due to the difference in the emergent polarization state for different wavelengths.

The LC cells used in the earlier experiments were fabricated in our laboratory. Glass plate was first coated with a thin layer of polybutylene-terepthallate as an alignment layer

and rubbed unidirectionally to define the direction of the directors at the surfaces. The glass plates were then cut into two pieces. Glass fiber spacers and ultraviolet curable epoxy were used to assemble the glass plates into a TN cell. When assembled, the thickness of the TN cell is maintained at 1.9 μm. The LC material was inserted into the cell in its isotropic phase by the capillary action. The retardations of the two homogeneous cells can be adjusted by applying a square wave voltage (1 kHz) across the samples. Light from a visible to near-infrared light source (400–750 nm) was polarized by a broadband linear polarizer. The light was passed through the device and the analyzer before it was coupled into the detector of a spectrometer. As Fig. 3(b) shows, the transmission is similar to our calculated results. The small wiggles in the transmission spectra are due to the Fabry–Perot effects results from the index mismatch. The overall intensity is lower than the calculated results, since our calculations did not consider losses in the device due to the reflection and the scattering of light. The results clearly show that although a single TN cell can rotate the linear polarization state of light for short wavelengths, the polarization state of light cannot maintain as linear for longer wavelengths. On the other hand, if we use the configuration shown in Fig. 2(a), then the linear polarization state will be rotated by an angle close to the twisted angle of the TN cell for a wide range of wavelengths.

In conclusions, by using the Poincaré sphere method, we have proposed a simple structure that is capable of rotating the linear polarization state by a certain angle for a wide range of wavelengths. The device utilizes the eigenmode of the TN structure. Theoretical and experimental results show that a single thin TN cell can only rotate the linear polarization state for short wavelengths. However, by adding two compensating homogeneous waveplates, a thin TN cell is capable of achieving the achromatic linear polarization rotation for a wide range of wavelengths.

[1] M. Schadt and W. Helfrich, Appl. Phys. Lett. 18, 127 (1971).
[2] P. Yeh and C. Gu, Optics of Liquid Crystal Displays (Wiley, New York, 1999), pp. 161–213.
[3] M. C. Mauguin, Bull. Soc. Fr. Mineral 34, 71 (1911).
[4] C. H. Gooch and H. A. Tarry, J. Phys. D 8, 1575 (1975).
[5] S. W. Suh, Z. Zhuang, and J. S. Patel, in Proceedings of SID'98 (Society of Information Display, San Jose, CA, 1998), p. 997.
[6] Z. Zhuang, Y. J. Kim, and J. S. Patel, Opt. Lett. 24, 1166 (1999).
[7] Z. Zhuang, Y. J. Kim, and J. S. Patel, Appl. Phys. Lett. 75, 1225 (1999).
[8] Z. Zhuang, Y. J. Kim, and J. S. Patel, Appl. Phys. Lett. 75, 3008 (1999).
[9] J. A. Davis, I. Moreno, and P. Tsai, Appl. Opt. 37, 937 (1998).
[10] I. Moreno, J. A. Davis, K. G. D'Nelly, and D. B. Allison, Opt. Eng. 37, 3048 (1998).

Effect of multidirection rubbing on the alignment of nematic liquid crystal

Young Jin Kim,[a] Zhizhong Zhuang, and Jay S. Patel
*Department of Physics and Department of Electrical Engineering, Pennsylvania State University,
University Park, Pennsylvania 16802*

We have investigated the alignment properties of liquid crystals induced by multiple rubbing of the surfaces in different directions. Experiments were carried out using homeotropic and hybrid-aligned samples. It is experimentally found that the alignment of the liquid crystals is along neither of the rubbing directions, but instead lies along an axis intermediate between these two directions, and that the direction depended on the relative strength of rubbing along the two axes. A model that assumed the grooves along two rubbing directions is proposed, and the relation between the orientation of the liquid crystal and the relative rubbing strength is analyzed. We found that this model can explain the observed experimental results. © *2000 American Institute of Physics.* [S0003-6951(00)02330-5]

It is well known that unidirectional rubbing of surfaces produces well-aligned samples for nematic[1] as well as smectic liquid crystal (LC). Much research has been devoted to developing methods of alignment and understanding of the alignment process itself.[2,3] Most generally, the alignment is produced by unidirectional rubbing of the surfaces that causes the director to orient along the rubbing direction at the surface and through elastic forces causing the bulk to align as well.

Our focus is to investigate the effect of multiple rubbing on the alignment of liquid crystals. In particular, to investigate the correlation between the strength of the different rubbing axes and the orientation angle of the LC. Conventional knowledge suggests that the last rubbing determines the alignment of the LC, and that the LC molecules will be aligned along the direction of the last rubbing. However, as shown in this letter, this is true in the case when the second rubbing is much stronger than the first rubbing along different directions. In order to carry out this investigation systematically, we have limited the rubbing to only two directions while changing the rubbing strengths for each of these two directions. Based on a simple intuitive model, we expect that the alignment of the director should be at some angle that lies between the two rubbing axes, which is found to be the case in our investigation.

In general, there are two mechanisms to explain the planar alignment on the rubbed surface: the groove model[2] and the orientation of the polymer chains.[3] In previous studies, it was reported that the grooves alone are insufficient to provide planar alignment.[4] Nevertheless, it appears that grooves do play an important role in explaining the alignment of the rubbed surface. In a study of tilted homeotropic alignment, it was reported that microgrooves were formed along the rubbing direction.[5] Recently, it was found that the groove profile produced by a rubbing process is closely related to the surface profile of the fiber of the rubbing cloth.[6]

In the present study, we first focus on the alignment of the LC on a rubbed homeotropic surface. Instead of a unidirectional rubbing, we attempted a multidirectional rubbing of

the homeotropic surface. The homeotropic surface was sequentially rubbed in two different directions. The sample was examined by using a polarizing microscope. It is found that the alignment of the liquid crystals is not along either of the rubbing directions but instead lies along an axis intermediate between these two directions, and that the orientation of the LC depends on the ratio of the rubbing strengths of the two rubbing directions. In the latter part of the letter, we propose a theoretical model that assumes sinusoidal grooves that are created along two rubbing directions. Using this analysis, we obtained a relation between the orientation of the LC and the strengths of the two rubbing axes, which showed good agreement with the experimental results.

To promote vertical alignment, JALS-204 (Japan Synthetic Rubber Co.) was coated on indium–tin–oxide (ITO)-coated glass plates. The LC cell was constructed using two substrates: one substrate was rubbed in multidirections while the other one was not rubbed. To control the rubbing strength, we used a rubbing machine equipped with a rotating roller and a glass-holding stage that moves below the roller. Rubbing pressure, the revolutions per minute of the roller, and the speed of the stage, were fixed as constants throughout the experiments. The rubbing strength was increased by increasing the cumulative number of rubs. One can expect that the rubbing strength should be proportional to the cumulative number of rubs as demonstrated in a previous study.[7]

In our experiments, the following process was used to rub the substrate in multiple directions. First, the substrate was placed on the moving stage, and it was rubbed in one direction (along the y axis) by m times. After this was completed, the substrate was rotated by 90°, and it was rubbed along the x axis by n times. Then, the LC cell was constructed by assembling this substrate and another substrate that was not rubbed. The cell thickness was measured to be 10 μm. The cell was filled by a capillary action with LC material, ZLI-4302 from E. Merck, which has a negative dielectric anisotropy. A square-wave voltage was applied to the sample, and the texture of the sample was observed with the use of a polarizing microscope.

In the absence of a field, the cell showed a vertical align-

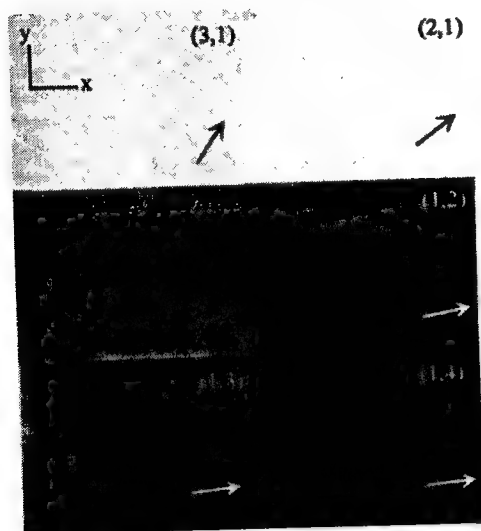[a]Electronic mail: jimk@phys.psu.edu

513

FIG. 1. Photographs of the homeotropic samples. A square-wave voltage (10 V, 100 Hz) was applied to the samples. (m,n) represents the cumulative numbers of rubs along the y and x axes. The samples were placed between cross polarizers with one of the polarizers parallel to the x axis. A change in the brightness of the texture is an indication of the change of the orientation of the LC molecules with (m,n). The arrows indicate the orientation of the LC.

FIG. 2. Dependence of the deviation angle on the ratio of the cumulative number of rubs n/m in homeotropic samples. A square-wave voltage (10 V, 100 Hz) was applied to the samples. The inset shows the relation of $1/\tan \alpha$ to n/m. This relation is obtained from the model that assumes sinusoidal grooves that are created along the x and y axes. The open circles and the solid line represent the experimental and fitted results. The fitted results are $1/\tan \alpha = 2.93(n/m)$.

ment. As the voltage was increased above the Frederick transition voltage, the LC directors gradually moved from a vertical to a planar alignment. If the LC directors aligned along one of the rubbing directions, the sample would show a dark state that was independent of the applied voltage when placed between cross polarizers with one polarizer parallel to one of the rubbing axes. However, the dark state was not observed. Instead, the sample showed a light transmission, which indicated either that the sample was twisted or that the optical axis of the sample was at an angle that deviated from the rubbing direction. However, extinction was observed when the sample was rotated by an angle, which suggested that the director axis lay in between the two rubbing axes. Both the rubbing directions (the x and y axes) had an effect on the alignment of the LC molecules. To control the rubbing strength, the cumulative number of rubs was varied from 1 to 4. One substrate was rubbed with various combinations of the cumulative number of rubs (m,n), where m and n were the cumulative numbers of rubs along y and x axes, respectively. Figure 1 shows the textures of the samples with a sequence of (m,n). The voltage applied to the samples was 10 V with a frequency of 100 Hz.

By rotating the sample in the presence of a field, we were able to measure the extinction angle at which the sample became a dark state with respect to the x or y axis. The deviation angle was found to be invariant to the magnitude of the applied voltage of as much as 40 V. Figure 2 shows the deviation angles for the samples of various combinations of (m,n) as a function of the ratio n/m. The deviation angle decreases as the n/m increases, and the angle converges to 0° as n/m approaches infinity.

The results show that for a finite cumulative number of rubs, the aligning effect of the first rubbing direction cannot be ignored. The results also show that in order to align the LC molecules along the last rubbing direction, one has to
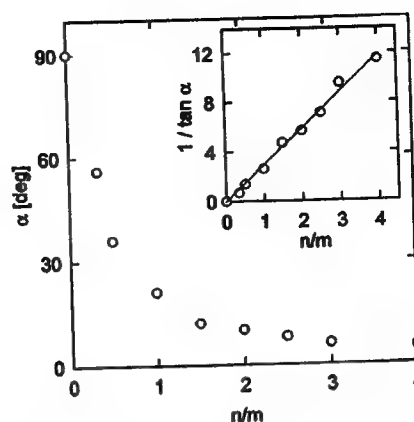
apply several rubs in the direction of the last rubbing. This fact can be critical to the alignment of the tilted homeotropic surface, especially when it is used in domain-dividing technology.

Thus far, this letter has focused on the alignment of the LC in the sample with the rubbed homeotropic surface. We now explore the planar surface. In this study, we have chosen to use one homogeneous substrate that was rubbed in multiple directions and a homeotropic substrate that was not rubbed. For this experiment, poly(1,4-butylene terephthalate) was coated onto the ITO glass plate to promote a planar alignment. The substrate was rubbed using the same method as described above. To promote vertical alignment, an unrubbed JALS-204 surface was used as another substrate. The cell gap was measured to be 10 μm. The LC material ZLI-4302 was filled into the cell as before. Figure 3 shows the textures of the hybrid-aligned nematic (HAN) samples in the absence of a field for various combinations of (m,n). As in the case of the homeotropic samples, the direction of the alignment continuously changes with the ratio n/m. The texture becomes dark at a larger value of n/m. The deviation
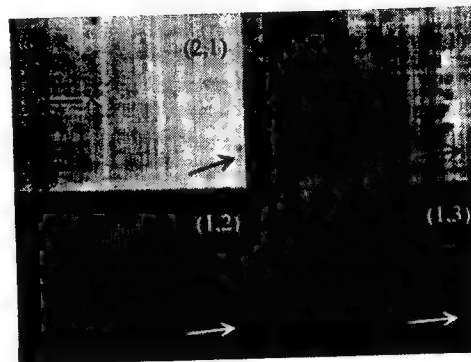

FIG. 3. Photographs of the HAN samples in the absence of a field. (m,n) represents the cumulative numbers of rubs along the y and the x axes. The samples were placed between cross polarizers with one of the polarizers parallel to the x axis. The arrows represent the orientations of the LC.

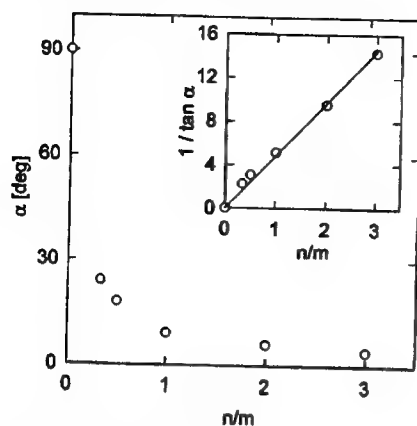Appl. Phys. Lett., Vol. 77, No. 4, 24 July 2000

Kim, Zhuang, and Patel

FIG. 4. Dependence of the deviation angle on the ratio of the cumulative numbers of rubs n/m in the HAN samples. The inset shows the relation of $1/\tan \alpha$ to n/m. The open circles and the solid line represent the experimental and fitted results. The fitted results are $1/\tan \alpha = 4.82(n/m)$.

angles of the samples were measured in the absence of a field as a function of n/m. As shown in Fig. 4, the angle decreases as n/m increases. These results are similar to those for the homeotropic samples.

In the following, we attempted to analyze the relation between the rubbing strengths of two rubbing axes and the orientation of the LC molecules. Our approach is based on the supposition that there are two forces that will determine the overall direction of the alignment of the LC. In 1972, Berreman suggested that the planar alignment relies on the grooves or scratches on the substrate created by rubbing.[2] In his work, the energy needed to align the LC molecules perpendicular to the groove is calculated with the use of a sinusoidal-wave groove on the surface. It has been assumed that in a finite cumulative number of rubs, the grooves created by the first rubbing cannot be completely destroyed. Our model assumes sinusoidal boundary conditions. This is a simple consequence of analysis of the surface using Fourier series. The grooves on the surface can be represented as a series of sinusoidal functions. To the first approximation we have chosen only one term due to the reason of simplicity. Thus, in the framework of this oversimplified model, although the degree of rubbing does not exactly correspond to the spatial frequency, this is a reasonable assumption indicative of the strength of rubbing. Therefore, we suppose that there exist microgrooves along the x and y axes on the surface, which is described as

$$z = A_x \sin q_x x + A_y \sin q_y y. \tag{1}$$

The director of the LC is represented as $(\cos \theta \cos \phi, \cos \theta \sin \phi, \sin \theta)$, where θ is a tilt angle measured from the xy plane, and ϕ is an azimuth angle measured from the x axis. We assumed that θ is a function of x, y, and z, and ϕ a constant independent of the coordinates.

In an approximation of a one elastic constant, the free-energy density of the nematic LC is described as $f = K\{(\cos \phi \theta_x + \sin \phi \theta_y)^2 + \theta_z^2\}$, where K is an elastic constant. The subscripts denote the partial derivative with respect to the coordinates. Using the Euler–Lagrange equation, the equation of motion is obtained as

$$\cos^2 \phi \theta_{xx} + \sin^2 \phi \theta_{yy} + \sin 2\phi \theta_{xy} + \theta_{zz} = 0. \tag{2}$$

The LC molecules on the grating-like boundary align along the tangential or perpendicular direction of the surface in a planar or homeotropic alignment, respectively. A solution to this differential equation that matches the boundary condition Eq. (1) is obtained as $\theta(x,y,z) = A \sin(q_x x + q_y y) \times \exp(-\beta z)$, where $\beta = q_x \cos \phi + q_y \sin \phi$ and A is a constant. Using the solution obtained above, the total free energy per unit area was calculated as $F = \int_0^\infty f dz = KA^2 \beta/2$. By minimizing this free energy with respect to ϕ, the azimuth angle was obtained, satisfying the relation $1/\tan \phi = q_x/q_y$. This relation shows that the orientation of the LC on the surface that is rubbed in multiple directions depends on the density of the grooves in different directions created by the rubbing process.

Based on this model, we attempted to numerically fit the experimental data using the relation $\tan \phi = q_y/q_x$. By increasing the cumulative number of rubs, it is possible to make more scratches or grooves on the surface, which increases the density of the grooves. The increase of grooves can be represented by adding more sinusoidal functions with different spatial frequencies to Eq. (1). In the first-order approximation, we assumed that the density of the groove is represented by a spatial frequency of a single sinusoidal boundary. As the insets of Figs. 2 and 4 show, the value of $1/\tan \alpha$ is indeed linearly proportional to n/m. Thus, the simple model appears to be a fairly good representation of the multiple rubbing of the surface. From the experimental results, we can conclude that the effect of two rubbings depends on the order in which the rubbing was carried out. For $(m,n) = (1,1)$, the direction is not along the bisector of the two rubbing directions, but is biased towards the second rubbing direction. The order of rubbing seems to introduce a bias of a factor of 3 in the homeotropic sample and 5 in the HAN sample shown in the insets of Figs. 2 and 4. This is because some of the grooves created by the first rubbing are erased by the second rubbing.

In conclusion, we have investigated the alignment of LC molecules in homeotropic and HAN samples, which have one substrate that is rubbed in multiple directions. We investigated the orientation of the LC in the samples which were rubbed at various rubbing strengths. Our experiments show that after the multidirection rubbing, both of the rubbing directions have an effect on the alignment of the LC. The observed results are adequately explained with the use of the model that assumes the grooves that are created along two rubbing axes.

[1] J. Cognard, Mol. Cryst. Liq. Cryst. Suppl. Ser. 1, 1 (1982).
[2] D. W. Berreman, Phys. Rev. Lett. 28, 1683 (1972).
[3] J. M. Geary, J. W. Goodby, A. R. Kmetz, and J. S. Patel, J. Appl. Phys. 62, 4100 (1987).
[4] A. J. Pidduck, G. P. Bryan-Brown, S. D. Haslam, and R. Bannister, Liq. Cryst. 21, 759 (1996).
[5] H. Seki, Y. Itoh, T. Uchida, and Y. Masuda, Mol. Cryst. Liq. Cryst. 223, 93 (1992).
[6] M. P. Mahajan and C. Rosenblatt, J. Appl. Phys. 83, 7649 (1998).
[7] Y. Sato, K. Sato, and T. Uchida, Jpn. J. Appl. Phys., Part 2 31, L579 (1992).

Polarization States of Ferroelectric Liquid-Crystal in a Twisted Structure

Young Jin KIM*, Zhizhong ZHUANG and Jay S. PATEL

Departments of Physics and Electrical Engineering, The Pennsylvania State University, University Park, Pennsylvania 16802, U.S.A.

The twisted ferroelectric liquid-crystal structure is investigated using a smectic liquid-crystal that has a low tilt angle of about 25° in the smectic C* phase and has a smectic A phase. The twisted ferroelectric alignment is achieved in a cell that has non-parallel rubbed boundary conditions. Using a polarimeter the structure is investigated by using polarized light. The change of the polarization of the light, as the sample is rotated in the absence and in the presence of an applied field, is compared with the expected behavior based on a theoretical model. By measuring and by calculating Stokes parameters, we are able to demonstrate an agreement between the theory and the experiment, and verify that the twisted structure is produced in this material. This twisted structure shows analog switching in a low field regime.

KEYWORDS: twisted ferroelectric, polarization state, Stokes parameter, rubbing, low tilt angle

Twisted ferroelectric liquid-crystal (TFLC) has attracted much interest, because it combines the fast switching capabilities of a ferroelectric structure and the analog switching of a conventional twisted nematic (TN). The TFLC structure has no threshold field and is capable of intrinsic gray scale. Since its first suggestion in the early 1990s,[1] its electro-optical property and switching mechanism have been extensively studied.[2–4] Gray scale spatial light modulators using a TFLC structure have been investigated.[5,6] However, most of these studies were performed with the use of high tilt angle (about 45°) materials, which generally have a cholesteric to smectic C* (SmC*) phase transition and have no intervening SmA phase. Moreover, the switching property has been investigated with the use of a transmitted light intensity passing through a sample placed between crossed polarizers. In such experiments, the twisted structure was verified by observing the texture of a sample using a polarizing microscope.

In this paper, we construct and provide a detailed analysis of a TFLC structure using smectic liquid-crystal that has a low tilt angle of about 25° in SmC* phase and also has a SmA phase. The polarization property of light passing through the TFLC sample is studied using a polarimeter, as the sample is rotated in the absence and the presence of the field. With the use of a simple model of the TFLC structure, the Stokes parameters of the light passing through a TFLC cell were calculated and compared with the experimental results. Using this method, we verified that the twisted structure could be produced in these materials.

The liquid-crystal cells used in this study were made from indium-tin-oxide coated glass. The glass was coated with polyimide, RN-1155 from Nissan Chemical, and rubbed in one direction. To produce a twisted structure using the low tilt angle material, the two glass substrates were assembled into a cell such that the angle between two rubbing axes was 50°, which is approximately twice of the tilt angle of smectic liquid-crystal at room temperature. The measured sample thickness was 1.8 μm. The cell was filled with a commercial liquid-crystal, CS1015 obtained from Chisso Corp., which has a tilt angle of 26° at room temperature.

To examine the twisted ferroelectric alignment, we observed the texture of the sample as a function of the temperature. The sample was heated to the isotropic state, and

cooled to the cholesteric phase. At the onset of the cholesteric phase, domains that showed different twisted structures were observed. This is because the pitch of the cholesteric at the transition temperature is long compared to the sample thickness at this temperature, which results in right-handed and left-handed twisted domains. However, near the phase transition temperature to the SmA phase (68°C), one domain began to dominate and a single domain is eventually obtained. When such a sample was slowly cooled to the SmA phase, a uniform SmA alignment was obtained. By measuring the extinction angle of the sample which was rotated between crossed polarizers, we found that the smectic layers were aligned parallel to bisector of the two rubbing axes. By slowly cooling the sample to the SmC* phase, the twisted ferroelectric alignment was observed. However, the sample had the residual defects showing non-uniform alignment. We applied a square wave field to the sample (10 V, 100 Hz), and slowly cycled the temperature between room temperature and 50°, while the sample was in SmC* phase. This process helped in removing most of the defects in the sample to produce a well-aligned sample.

Figure 1 shows the textures of the SmA and the twisted SmC* phases at 60°C and 25°C, respectively. The alignment process outlined above depends on the liquid-crystal materials and the material of the alignment layers. When the same method was used to investigate other liquid-crystal materials, CS1011 and CS1013 from Chisso Corporation, which have the same phase sequence as CS1015, a similar twisted alignment was achieved. We have also examined the effect of the alignment materials.

Using poly(1,4-butylene terephthalate) as the alignment layer, however, the sample showed no evidence of the twisted structure. In this case a homogeneous alignment with smectic layer tilted perpendicular to one of the rubbing direction was observed. When this sample was cooled to SmA phase from the cholesteric phase, the smectic layers were observed to be tilted perpendicular to one of the rubbing direction. The direction of the smectic layer did not changed when the sample was cooled to the SmC* phase. Although these experiments were performed on a limited number of samples and only two alignment layers were examined, it was found that the direction of the smectic layer in the SmA phase determine whether twisted structure is obtained or not.

The primary focus of this investigation is to attempt to provide evidence of the twisted ferroelectric structure. We developed a method using the polarization of the light as a

*Present address: YAFO Networks, Inc., 1340 F Charwood Road, Hanover, MD 21076, USA.

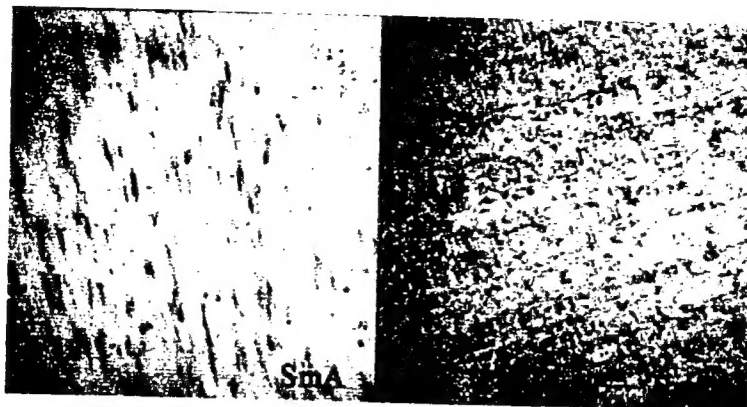Jpn. J. Appl. Phys. Vol. 39 (2000) Pt. 1, No. 10

Y. J. Kim *et al.*

Fig. 1. Photograph of the SmA and the twisted SmC* phase at the temperature of 60°C and 25°C, respectively. The SmC* phase shows a twisted structure.

probe. For linearly polarized light impinging on the sample, the sample is rotated about the wave vector of the incident light. Stokes parameters of the light passing through the sample are measured as a function of the rotation angle of the sample. From this measurement, we can estimate the twist angle and the birefringence of the sample.

The following discussion outlines the basic principle of this method. The Stokes parameter of the linear input light is represented as (1, 1, 0, 0) on a Poincare sphere.[7, 8] If the sample is homogeneously aligned, then the condition for the output polarization which is identical to the input polarization requires that the liquid-crystal is aligned parallel or perpendicular to the input polarization. This requirement means that the linear output polarization is also represented as (1, 1, 0, 0). However, if the sample has a twisted structure, then the output polarization can also be linear, but rotated with the input polarization of light. On a Poincare sphere this point of linear output polarization is located on the equator of the sphere ($S_3 = 0$) and shifted from the input polarization state located at (1, 1, 0, 0) by an angle of ξ ($\tan\xi = S_2/S_1$). The actual output polarization state depends on the birefringence and the twist angle of the sample. In the case of TN, the condition for a linear output polarization was analytically obtained.[9]

In this section, we numerically obtain the general solution of the linear output polarization as a function of the tilt angle of SmC* and the birefringence of the sample. For the calculations, we assumed a bookshelf structure, in which the smectic layer is perpendicular to a substrate and the axis of the smectic cone is parallel to a substrate. Using the assumption of uniform twist, we calculated the angle ξ as a function of the tilt angle of SmC* for various values of the birefringence of the sample. As Fig. 2 shows, ξ has a finite value for a finite tilt angle, and it strongly depends on the birefringence of the sample. However, as the tilt angle is decreased, ξ converges to zero, which means that ξ becomes zero for an untwisted structure as expected.

To model an effect of electric field on the TFLC sample, we introduced a simple model for the twisted structure, instead of numerical calculation of the director profile using minimization of the free energy of the twisted SmC* for various applied voltages. We assumed that the rotation angle (ψ) of director on the cone is proportional to $(z/d)^k$, where k is a real number, z is a coordinate along the cell thickness, and d
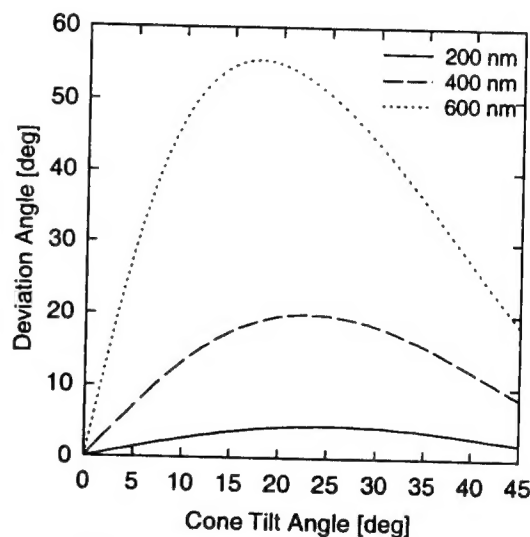

Fig. 2. Numerical results of the deviation angle (ξ) of output linear polarization from (1, 1, 0, 0) as a function of the tilt angle. Uniform twist is assumed and birefringence of the sample is changed from 200 nm to 600 nm.

is a cell gap. Using hard surface anchoring, the distortion of director in the SmC* phase can be approximated by changing the value of k. Quantitatively, the director profile obtained using this method is similar to the exact model which is obtained by minimizing the free energy of SmC* liquid-crystal in one elastic constant approximation. The results are shown in Fig. 3. To examine the effect of a field on the sample of TFLC, the value of k was changed from 1 to 100, and the angle ξ was calculated as a function of the tilt angle of SmC*. The birefringence of the sample was chosen as 250 nm. Fig. 4 shows that as k is increased, the deviation angle ξ is drastically decreased. Although the solution for the linear output polarization is obtained numerically, this study suggested that by measuring the deviation angle ξ of the TFLC sample, we could verify the existence of twisted structure and estimate the distortion of the twist in the presence of a field.

For a TFLC sample using CS1015, the Stokes parameters at each rotation angle of the sample were measured using a
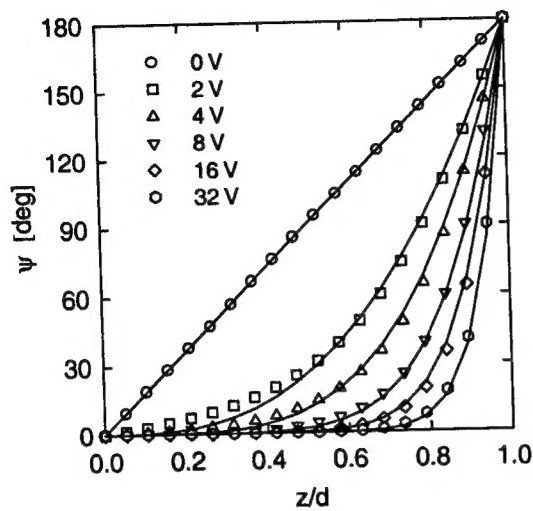
Fig. 3. An example of director profiles of TFLC structure as a function of a field. Symbols represent the director profiles obtained by minimizing the free energy of the twisted SmC* for various applied voltages. For these calculations, we assumed that elastic constant is 20×10^{-11} N (one elastic constant approximation), tilt angle is 26°, spontaneous polarization is 6.6×10^{-5} C/m², and cell thickness is 5.5 μm. Solid lines represent the numerical results of the approximate model, $\psi = \pi(z/d)^k$. The corresponding values of k are 1.0, 2.5, 4.1, 6.5, 9.0, and 14.0 for the applied voltages of 0 V, 2 V, 4 V, 8 V, 16 V and 32 V, respectively.
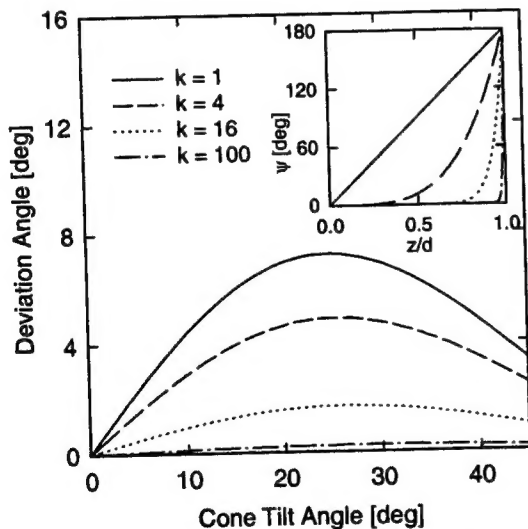

Fig. 4. Numerical results of the deviation angle (ξ) of output linear polarization from (1, 1, 0, 0) as a function of the tilt angle. The value of k is changed from 1 to 100 to examine the effect of field on the TFLC sample. $K = 1$ means a uniform twist and a homogeneous state is achieved at large value of k. The inset shows the director profile ψ as a function of z at the various values of k.

Hewlett-Packard HP8509B lightwave polarization analyzer. The wavelength used for this measurement was 1547 nm. Figure 5(a) (open circle) shows the measurement results in the absence of a field. Stokes parameters are drawn on a Poincare sphere as a function of a rotation angle of the sam-

ple, and in doing so they form an eight-shaped curve. The point at which the eight-shaped curve meets the equator is shifted from (1, 1, 0, 0), which indicates that the sample has a twisted structure in the absence of a field.

To examine the Stokes parameters during the switching of the TFLC, we applied an electric field to the sample. Open circles in Figs. 5(b), 5(c), and 5(d) show the measured results for 2 V, 5 V, and 20 V, respectively. The results show two clear trends: (i) the size of the eight-shaped curve get larger with field, and (ii) the point at which the eight-shaped curve meets the equator moves toward (1, 1, 0, 0) with field. At the voltage of 20 V, the curve meets the equator nearly at (1, 1, 0, 0), which indicates that the liquid-crystal directors are almost aligned in one direction without a twist.

In the following, we compared the observed results with the expected behavior of the calculated results. Since there is no analytic solutions in the TFLC geometry, we attempted numerical calculations. We expected that the birefringence and twist of the sample could be estimated from the comparison between the numerical calculations and the observed experimental results.

In a twisted structure, since the director is confined on a cone, the tilt angle (θ) and the twist angle (ϕ) change simultaneously as the director rotates along the cone. Let α is the tilt angle, and ψ is the rotation angle of the director on a cone from the plane parallel to the substrate. Then, the tilt and twist angles are given by the relationship of $\sin \theta = \sin \alpha \sin \psi$ and $\tan \phi = \tan \alpha \cos \psi$. For numerical calculations the sample is divided into several layers, and ψ is assumed to be a constant for each layer. The output polarization of light passing through the sample was calculated by using the Jones matrix of the sample, which is the same method that is used to calculate the optical property of TN. The incident polarized light was assumed to be linear, and Stokes parameters were calculated as a sample rotation angle which was varied between 0 and π. In the absence of a field, we assumed a uniform twist ($k = 1$ in an approximate model). Table I summarizes the parameters used for the calculation and compared with the cell parameters used for experiment. The solid line in Fig. 5(a) shows the results of the numerical calculations. The excellent agreement between the experimentally obtained results and the calculated results using a twisted smectic structure provide strong evidence that the sample exhibits a twisted smectic structure.

We also performed numerical calculations to fit the experimental results in the presence of a field using the approximate model, $\psi = \pi(z/d)^k$, to calculate the director profile. The same cell parameters shown in Table I were used, and the value of k was changed to give an effect of field on the TFLC sample. The parameter k determines the curvature of the twist distortion. At large value of k, the structure is nearly the same as the homogeneous alignment. The solid lines in Figs. 5(b),

Table I. The parameters used for experiment and calculation.

Parameter	Experiment	Calculation
LC	CS1015	—
Tilt angle	26°	25°
Δn (1547 nm)	0.133	0.133
Cell gap (μm)	1.8	1.85

Jpn. J. Appl. Phys. Vol. 39 (2000) Pt. 1, No. 10

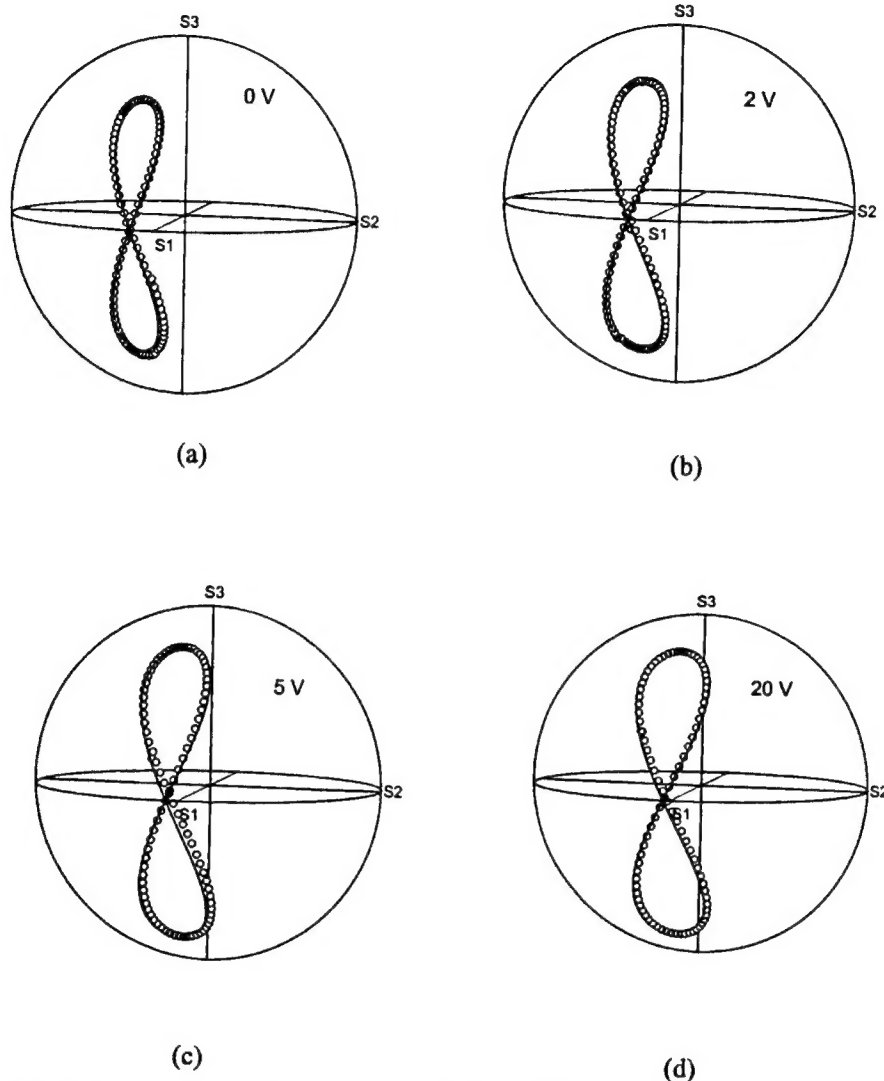Y. J. KIM et al.

(a)

(b)

(c)

(d)

Fig. 5. Stokes parameters of light passing through a TFLC cell. The sample is rotated from 0 to π about the wave vector of the incident light. The open circles and solid lines represent the measured and the calculated results, respectively. The applied voltage to the sample is (a) 0 V, (b) 2 V, (c) 5 V, (d) 20 V. The deviation angle measured between the point at which the curve meets the equator and $(1, 1, 0, 0)$ is (a) 6.57°, (b) 5.59°, (c) 3.03°, and (d) 1.93°.

5(c), and 5(d) show the numerical results. The fitted k values were 2.8, 5.5, and 11.0 for applied voltage of 2 V, 5 V, and 20 V, respectively. Although we used an approximate model, the numerical results are well fitted to the measured results. The twist distortion of TFLC in the presence of a field is estimated from the fitted value of k. From these studies, it was found that at a low field regime, the twist distortion is proportional to the field strength, which shows the possibility of a gray scale.

In conclusion, we have investigated the TFLC structure using a ferroelectric liquid-crystal that has a low tilt angle and a SmA phase. The twisted ferroelectric alignment was achieved in a cell of twisted structure. We have provided conclusive evidence for the twisted ferroelectric structure by measuring Stokes parameters passing through the sample. By using a simple model and numerical calculations, we determined that the TFLC sample has a twisted structure, and that the twist is

gradually distorted with an external field showing an analog switching.

1) J. S. Patel: Appl. Phys. Lett. **60** (1992) 280.
2) V. Pertuis and J. S. Patel: Ferroelectrics **149** (1993) 193.
3) S.-W. Suh, Y. J. Kim, S.-S. Park, S.-D. Lee and J. S. Patel: Mol. Cryst. Liq. Cryst. **263** (1995) 37.
4) S.-W. Suh, J.-H. Lee, Y. J. Kim, S.-S. Park and S.-D. Lee: Ferroelectrics **179** (1996) 181.
5) L. Le Bourhis, J. Angeke and L. Dupont: Ferroelectrics **181** (1996) 161.
6) L. W. K. Yim, A. B. Davey and A. R. L. Travis: Ferroelectrics **181** (1996) 147.
7) H. Poincare: *Theorie Mathematique de la Lumiere II*, ed. G. Carre (Gauthier-Villars, Paris, 1892) p. 275 [in French].
8) E. Collett: *Polarized Light* (Marcel Dekker, New York, 1993) p. 33.
9) Z. Zhuang, Y. J. Kim and J. S. Patel: Opt. Lett. **24** (1999) 1166.

☆U.S. GOVERNMENT PRINTING OFFICE: 2001-710-038-10176

MISSION
OF
AFRL/INFORMATION DIRECTORATE (IF)

The advancement and application of Information Systems Science

and Technology to meet Air Force unique requirements for

Information Dominance and its transition to aerospace systems to

meet Air Force needs.